ABSTRACT

Modulation of experimental autoimmune myocarditis with cytokine-myosin fusion proteins and novel cardiac peptides

By

Shaun Patrick Reece

1/6/2016

Director of Dissertation: Dr. Robert Lust

Major Department: Physiology

Infectious agents that induce cross-reactive myocarditic T cell responses may cause autoimmune inflammation of the heart, dilated cardiomyopathy (DCM), and heart failure. The purpose of this study was to evaluate the efficacy of GMCSF-Myosin fusion proteins as tolerogenic vaccines capable of inhibiting experimental autoimmune myocarditis (EAM). The fusion proteins were comprised of an N-terminal granulocyte macrophage-colony stimulating factor (GM-CSF) domain and a C-terminal cardiac myosin antigen domain. The antigenic domains Myosin 1052-1076 and Myosin 614-643 were chosen based on epitopes known to cause EAM in Lewis rats and BALB/c mice, respectively. Bioactivity of the cytokine domains for GMCSF-Myo1052 and GMCSF-Myo614 were confirmed with bone marrow proliferation assays. Enhanced antigen presentation was confirmed for GMCSF-Myo1052. Both fusion proteins were found to inhibit disease progression when given as a pretreatment before EAM induction. When administered after disease induction, GMCSF-Myo614 reduced the incidence of EAM. To investigate the mechanisms of these tolerogenic vaccines, a model of EAM was developed in C57BL/6 mice by evaluating a peptide (myosin 718-736) derived from the murine cardiac alpha myosin heavy chain and theorized to bind to H2-I-A^b. EAM was successfully induced in Interferon gamma

receptor knockout (*Ifgr1*$^{-/-}$) mice on the C57BL/6 background. Defining the mechanisms by which Interferon-gamma (IFN-γ) inhibits EAM on the C57BL/6 background is beyond the scope of this project, but it is hypothesized that T cell apoptosis or induction of T regulatory cells is involved. In conclusion, this study demonstrated the feasibility of using GMCSF-Myosin fusion proteins to inhibit EAM, and provides a new model of EAM on C57BL/6 background to explore the mechanisms by which GMCSF-Myosin fusion proteins mediate tolerance.

Modulation of experimental autoimmune myocarditis with cytokine-myosin fusion proteins and novel cardiac peptides

A Dissertation Presented to

The Faculty of the Department of Physiology

Brody School of Medicine at East Carolina University

In Partial Fulfillment of the Requirements for the Degree

Doctor of Philosophy in Physiology

by

Shaun Patrick Reece

January 6, 2016

Modulation of experimental autoimmune myocarditis with cytokine-myosin fusion proteins and novel cardiac peptides

by

Shaun Reece

APPROVED BY:

DIRECTOR OF DISSERTATION: _____
Robert Lust, Ph.D.

COMMITTEE MEMBER: _____
Mark D. Mannie, Ph.D.

COMMITTEE MEMBER: _____
Michael Van Scott, Ph.D

COMMITTEE MEMBER: _____
Jitka Virag, Ph.D.

CHAIR OF THE DEPARTMENT OF PHYSIOLOGY: _____
Robert Lust, Ph.D.

DEAN OF THE GRADUATE SCHOOL: _____
Paul J. Gemperline, Ph.D.

Acknowledgements

I would like to acknowledge my wife, Sky Reece, who has given me unwavering support and encouragement. Thank you dear for listening to me and my ideas. I would also like to thank my committee members: Dr. Van Scott, Dr. Mannie, Dr. Lust and Dr. Virag. Thank you, Dr. Van Scott, for bringing me into your lab and seeing something in me that I could not find in myself. Without the opportunity you provided me with my life would be on a much different track. Thank you Dr. Mannie for providing guidance and listening to my ideas. Your experience and suggestions made the difference between a failed experiment and a successful one. You taught me how to be a better scientist. Thank you, Dr. Lust, for providing assistance as I navigated the Physiology PhD program. Our late night talks rekindled my enthusiasm and provided me with energy to keep going. Thank you, Dr. Virag, for always being there when I needed to talk, and introducing me to the world of histology. Finally I would to thank my brother, Steven Reece. I will always cherish the mutual support we provide one another. You mean more to me than you know.

TABLE OF CONTENTS

LIST OF TABLES

LIST OF FIGURES

LIST OF ABBREVIATIONS

APC	Antigen presenting cells
CFA	complete Freund's adjuvant
DCM	dilated cardiomyopathy
EAE	experimental autoimmune encephalomyelitis
EAM	experimental autoimmune myocarditis
FBS	fetal bovine serum
GFP	green fluorescent protein
GMCSF	granulocyte macrophage-colony stimulating factor
HLA	human leukocyte antigen
IDC	idiopathic dilated cardiomyopathy
IFN-gamma	interferon gamma
IL	interleukin
MHC	major histocompatibility complex
MI	myocardial infarction
MTS	tetrazolium salt / phenazine methosulfate
PCR	polymerase chain reaction
PKA	protein kinase A
PLP	proteolipid protein

CHAPTER 1

Introduction

1.1 A PRIMER ON MYOCARDITIS

Myocarditis is defined as inflammation of cardiac tissue including the walls of the ventricles, valves, chordae tendineae and papillary muscle. The severity of the disease can range from subclinical to life threatening. Multiple viruses are known to directly infect the heart causing acute myocarditis. Often the immune system can resolve viral cardiac infection. However, it is also possible an acute infection can lead to auto-reactive lymphocytes if the infection is not resolved by the innate immune system. Cardiac auto-reactive lymphocytes can also be generated during infections that do not directly infect the heart through molecular mimicry. In either event, cardiac auto-reactive lymphocytes can lead to a specific type of myocarditis defined as autoimmune myocarditis. This subtype of myocarditis is of significant concern because the heart itself provides a constant supply of cardiac antigens that keep the adaptive immune system in a perpetual cycle of inflammation.

Identifying and stopping autoimmune myocarditis is of the upmost importance to prevent dilated cardiomyopathy. Chronic as well severely acute cardiac inflammation can lead to myocyte death and subsequent scarring in place of the dead tissue. Scarring of the ventricles can lead to decreased diastolic and systolic function. If the impairment is severe enough, the heart may enlarge in attempt to compensate for the decreased cardiac output. This enlargement of the heart is an inefficient solution that ultimate results in dilated cardiomyopathy where the walls of the ventricles become progressively thinner reducing cardiac output and function. To prevent

autoimmune myocarditis from evolving into dilated cardiomyopathy and heart failure, diagnosis and novel treatments are needed.

Diagnosis of myocarditis has been difficult due to the focal nature of the disease. Certain sections of the heart can become infected and/or inflamed while the rest of the heart tissue remains normal. This focal characteristic of myocarditis creates problems when endomyocardial biopsies are performed because it is possible that a biopsy may miss an inflamed or infected region resulting in a false negative diagnosis. To gain a better understanding of the true prevalence of the disease, several post mortem studies have been conducted where the entire heart can be removed and analyzed to minimize false negatives. A review several post mortem studies found incidence rates from 1% to 10% [1]. However, 3 of these post mortem studies, in which 10,000 or more subjects were used, found incidence rates for myocarditis between 3.5% and 0.11%. Furthermore, Japan had a lower incidence rate comparted to the United States, indicating environment and/or ethnicity may be contributing factors. Histological analysis of endomyocardial biopsies has revealed that lymphocytic, eosinophilic, and giant cell myocarditis are the three main forms of myocarditis found in patients [2]. Lymphocytic myocarditis is the most common form of myocarditis with the most favorable prognosis [2]. Eosinophilic and giant cell myocarditis may progress rapidly, and both have a poor prognosis and high mortality rates [2].

1.2 CAUSES OF MYOCARDITIS

Pathogenic origins of myocarditis

While the cause of myocarditis in most cases is unconfirmed, known origins for myocarditis include pathogenic infection, autoimmune disease, genetic predisposition, and other factors. Pathogenic infections are the most commonly diagnosed known causes of myocarditis. Practically every class of pathogen from viruses to parasites is known as a potential cause of myocarditis. In North America and Europe, viral agents are the most common cause with adenoviruses and enteroviruses commonly implicated. A 2010 study using endomyocardial biopsy found 38% of 624 patients with myocarditis had viral genomes present in their heart tissue [3]. Viruses can cause direct necrosis of cardiomyocytes and activate the adaptive immune system which can cause collateral damage during viral eradication.

One of the most-well-studied bacteria capable of inducing myocarditis is beta hemolytic streptococcus. Infection with this pathogen is aggressively treated with antibiotics to prevent the development of myocarditis. Myocarditis following beta hemolytic strep is a well-documented condition called Rheumatic fever. Molecular mimicry is implicated as antibodies against the coat protein of beta hemolytic strep also cross react with cardiac myosin [4]. A single cross reactive antibody in theory could opsonize heart tissue leading to the presentation of more cardiac epitopes which may activate naïve cardiac auto-reactive T cells leading to further cardiac damage and autoimmune myocarditis. Antibiotics are commonly prescribed to help the innate immune system quickly clear the invading bacterial pathogen and abrogate the need for adaptive immunity to select and colonially expand lymphocytes, including B cells.

At the protozoan level *Trypanosoma cruzi* is the most common cause of myocarditis. The parasite is responsible for 1-7 million current infections in North America alone and 30% of these patients will develop myocarditis [5]. While some researchers believe *Trypanosoma cruzi* causes myocarditis by direct infection of cardiac tissue, other researchers argue that an autoimmune etiology better explains the current clinical literature. Aspects that support an autoimmune etiology include: parasite load not correlating with severity of myocarditis, multiple target organs are known to be infected by the parasite yet only the heart seems to display chronic inflammation, and *Trypanosoma cruzi* patients maybe asymptomatic for years before displaying signs of myocarditis [5]. Research has also identified antibodies that react to the P0 ribosomal antigen of *Trypanosoma cruzi* and cross-react with the second loop of the beta 1 adrenergic receptor [6]. The beta 1 adrenergic receptor is expressed in cardiac tissue, and antibodies with agonist activity can easily overstimulate the heart and lead to cardiomyopathy. In addition to molecular mimicry at the B cell level, researchers have also discovered T cells that react to the B13 antigen of *Trypanosoma cruzi* and cardiac myosin [7].

HLA associations with myocarditis

Because $CD4^+$ T cells are the pivotal leukocyte that drives EAM and have been implicated in human autoimmune myocarditis, understanding which cardiac epitopes drive $CD4^+$ T cell expansion is critical for managing autoimmune myocarditis [8-11]. $CD4^+$ T cells recognize peptide antigens when presented on MHC II surface molecules by antigen presenting cells (APCs). Genes encoding the major histocompatibility complex, including HLA-DP, HLA-DQ, and HLA-DR, are some of the most polymorphic genes in the human genome. Each allele has the potential to bind a different peptide antigen derived from a protein. Many T cells that bind too strongly to self-peptides in the context of MHC are eliminated during negative thymic

selection [12]. However, thymic elimination of T cells with substantial affinity for self-antigens is not perfect [13]. Evidence also shows the alpha myosin cardiac heavy chain is weakly expressed in the thymus of mice and possibly weakly expressed in the thymus of humans as well [14]. Therefore, it is possible cardiac auto-reactive T cells are commonly found in the periphery. Auto-reactive myosin specific T cells in the periphery are most likely controlled through antigen specific T regulatory cells. Certain allelic versions of MHC II may have a higher affinity for peptides derived from the cardiac myosin heavy chain. In theory, certain MHC II alleles, auto-reactive $CD4^+$ T cells, as well as other unknown genetic factors could contribute to autoimmune myocarditis.

Multiple research studies have been conducted to explore the possible link between certain MHC II alleles and myocarditis as well as inflammatory idiopathic dilated cardiomyopathy (IDC). A study in China found HLA-DQA1*0501 and HLA-DQB1*0303 were statistically associated with higher odds ratios for idiopathic dilated cardiomyopathy [15]. The same study also reported HLA-DQA1*0201 and DQB1*0502 were significantly lower in patients with IDC suggesting that these alleles may offer protection against IDC. A subsequent study showed HLA-DQB1*0303 was associated with myocarditis, and HLA DQB1*02-DQB1*03 was correlated with inflammatory infiltrates in patients with IDC [16]. While the previous two studies used specific patient groups with $n<100$, a meta-analysis was conducted using 1,378 cases of IDC and 10,383 controls. This larger survey found HLA-DR4 and HLA-DR5 had higher associations in patients with IDC [17]. Given the statistical associations between IDC, myocarditis, and certain MHC II alleles, these MHC II alleles may have higher affinities for epitopes derived the cardiac myosin heavy chain. Presentation of cardiac epitopes by antigen presenting cells with these alleles could theoretically activate and clonally expand

$CD4^+$ T cells culminating in myocarditis. Antigen presentation, however, is only one facet of $CD4^+$ T cell clonal expansion. For $CD4^+$ T cell activation, antigen presenting cells must display co-stimulatory molecules, which often require an inflammatory event such as infection or cellular damage.

Evidence for myocardial infarction causing myocarditis

Mounting evidence suggests myocardial infarction (MI) has the potential to lead to autoimmune myocarditis. The uncontrolled release of cardiac epitopes through necrosis and the presence of pro-inflammatory cytokines following a myocardial infarction, provide an optimal environment for the activation and expansion of cardiac reactive lymphocytes [18]. It has been documented in animal models that during the first 3 days following a MI, pro-inflammatory macrophages are present in high numbers and therefore are capable of presenting antigens with costimulatory molecules [19]. Neutrophils are present during an MI and have been documented to cause significant necrosis [18, 19]. High levels of necrosis post MI allow for cardiac antigens to be presented in high quantities on APCs. The potential to activate cardiac specific $CD4^+$ T cells increases with the duration of an inflammatory environment in cardiac tissue. Experiments in mice and rats provide evidence that cardiac autoimmunity can occur following an MI. In Lewis rats, splenocytes harvested from animals following a myocardial infarction were transferred to naïve recipients who subsequently developed myocarditis [20]. Non-obese diabetic mice containing human CD4 and human HLA-DQ8 in place of their murine counterparts were developed to study type-1 diabetes. Although these mice failed to become a suitable model for type 1 diabetes, their propensity to spontaneously develop myocarditis made this strain optimal for studying autoimmune cardiac inflammation and dilated cardiomyopathy [21, 22]. Type 1 diabetic patients commonly possess the HLA-DQ8 allele and are at risk for

developing coronary artery disease [23, 24]. The authors hypothesized CD4 HLA-DQ8 NOD mice might be at a greater risk of developing myocarditis following MI. Indeed the authors demonstrated after MI, CD4 HLA-DQ8 NOD mice developed myocarditis with lymphocytic infiltration and increased IgG antibody production against myocardial antigens [25]. Furthermore, the authors found auto-antibodies against cardiac myosin in type 1 diabetic patients post MI that shared epitope recognition with antibodies from patients with confirmed myocarditis.

1.3 CURRENT THERAPIES AND PROGNOSIS FOR AUTOIMMUNE MYOCARDITIS

Current therapies for myocarditis mainly consist of immunosuppressive medications to inhibit the immune system and pharmacotherapy to minimize blood pressure and workload on the heart. Beta blockers, angiotensin converting enzyme inhibitors, and diuretics are often prescribed to patients with myocarditis experiencing symptomatic heart failure [26]. While these medications reduce the workload on the heart by reducing systemic blood pressure and catecholamine stimulation, they merely treat symptoms caused by the underlying inflammation. Steroids and immunoglobulin have had limited success treating myocarditis [27]. Immunosuppressive treatment is indicated for giant cell myocarditis and eosinophilic myocarditis [11, 28]. However, these two types of myocarditis have extremely poor prognoses with death often occurring without organ transplant. The mortality rate for giant cell and eosinophilic myocarditis highlight an urgent need for more effective therapies for autoimmune myocarditis. Due to their action of mechanisms, steroidal anti-inflammatory treatment and IVIG do not offer a permanent solution as they merely temporarily suppress the immune system and do nothing to permanently address cardiac auto-reactive lymphocytes. Immunosuppressive therapies also inhibit the entire immune system and leave patients vulnerable to opportunistic pathogens. Any permanent solution to autoimmune myocarditis will have to specifically address lymphocytes that recognize cardiac antigens as they are likely the pivotal immune cells perpetuating myocardial inflammation and damage.

Etiology of myocarditis and immunosuppressive therapy

Antigen-specific therapy such as GMCSF-antigen fusion proteins would most likely be of use in instances of myocarditis where immunosuppressive therapy has been beneficial. The decision to use immunosuppressive therapy in myocarditis is often dictated by the etiology. Therefore a review of the etiologies of myocarditis and their benefit from immunosuppressive therapy will be reviewed. Etiologies of myocarditis include systemic autoimmune diseases, viral infection of the heart, cardiovascular disease, and etiologies of unknown origin. When myocarditis has a more autoimmune etiology, such as lupus erythematosus, sarcoidosis, and hypersensitivity myocarditis, immunosuppression is indicated [29].

There is extensive literature on the association of viral genomes with myocarditis and inflammatory dilated cardiomyopathy [3, 30-32]. In myocarditis of viral etiology, effectiveness of immunosuppressive therapy depends on the phase of the disease [33]. If the myocardial viral infection is in the initial stage, anti-viral therapy and not immunosuppression is indicated [33]. Patients with myocarditis due to enteroviral infections respond well to treatment with Interferon-α or Interferon-β, with clinical improvement lasting 12 months in two thirds of the patients [34]. However, myocarditic viruses with specific adaptations to inhibit Interferon-β that evade the innate immune system have been identified [35]. It is more likely viruses with adaptations to avoid the innate immune system will result in more lytic death of cardiomyocytes and have an increased chance of activating the adaptive immune system and creating cardiac specific lymphocytes. Perhaps if future research identified more viral subtypes that can evade the innate immune system and lead to cardiac auto-reactive lymphocytes, then specific viral etiology could be of some clinical diagnostic value when choosing immunosuppression for myocarditis.

When the etiology of myocarditis is unknown, as is often the case, characterizing the subtype of myocarditis can be of great clinical value when choosing the appropriate treatment. Severe acute myocarditis develops in less than 2 weeks and is characterized by progressive symptoms of heart failure. If severe acute myocarditis is caused by necrotizing eosinophilic myocarditis or giant cell myocarditis, then immunosuppressive treatment is immediately recommended [29, 36, 37]. A small percentage of patients can present with fulminant myocarditis where severe symptoms of heart failure are even more sudden and require ventricular assist. However, if patients with fulminant myocarditis survive the initial bout of symptoms, there is a very good chance of survival and complete recovery [29].

Multiple clinical studies have been conducted to assess the therapeutic potential of immunosuppressive therapy in patients with inflammatory dilated cardiomyopathy and myocarditis. A major study published in 1995 investigated the use of azathioprine/cyclosporine with prednisone in 111 patients with histological confirmed myocarditis. The study found no significant difference in left ventricular ejection fraction or survival in the group receiving immunosuppressive therapy compared to the placebo group [38]. Three subsequent studies found significant therapeutic benefit from immunosuppressive therapy, when patients had cardiac autoantibodies, increased HLA expression in myocardial biopsies, or $CD45^{+}CD3^{+}$ lymphocytes in myocardial biopsies [27, 39, 40]. In summary these clinical studies highlight the need for immunosuppressive therapy for myocarditis when there is evidence of an adaptive immune response to cardiac antigens.

1.4 MYOCARDITIS AND DILATED CARDIOMYOPATHY

Accumulating evidence suggests myocarditis can lead to cardiomyopathy, a serious heart condition where the walls of the heart become progressively thinner and less efficient at pumping blood. Dilated cardiomyopathy (DCM) is the leading cause of heart transplant in children [41]. Because myocarditis is pivotal to the etiology of cardiomyopathy, it is imperative to understand the molecular mechanisms underlying myocarditis. Several lines of evidence indicate that an autoimmune etiology may contribute to idiopathic dilated cardiomyopathy. Because infections that cause myocarditis are often subclinical, it is possible a significant percentage of the population possess cardiac-specific, auto-reactive lymphocytes that were activated and expanded during a previous infection. These cardiac-specific, auto-reactive T cells could lay dormant for years until a new cardiac infection or insult occurs. Because viral infection is the most common known cause of myocarditis in developed countries, one might expect a correlation between evidence of past myocardial viral infection(s) and DCM. A 2005 study designed to address this hypothesis found viral genomes in 67% of 245 patients with DCM and 32% of 80 control patients [30]. If the adaptive immune system had previously expanded cardiac specific lymphocytes, one would also expect to see an increased antibody titer to cardiac proteins. Antibodies to the alpha and beta cardiac myosin heavy chains, the beta 1 adrenergic receptor, muscarinic receptors, and mitochondrial proteins have been found in patients with myocarditis as well as DCM [42]. The adrenergic and muscarinic antibodies have obvious implications for cardiac function by binding in an agonist or antagonist manner to their respective receptors. Studies have explored this possibility and found that sera from DCM patients could increase the heart rate of isolated myocytes *in vitro* [43]. While antibodies to intracellular cardiac proteins

may seem insignificant in a non-inflammatory state, their presence suggests a previous event occurred with significant MHC II antigen presentation that could also generate Th1 and/or Th17 $CD4^+$ memory T cells. Given the proper conditions these memory cells could reactivate and exacerbate DCM. In addition to evidence of viral myocarditis leading to DCM, Rheumatic fever and Chagas disease also have a history of DCM. The abundant number of pathogens with documented post infectious myocarditis indicates numerous opportunities for the generation of cardiac auto-reactive lymphocytes through multiple pathways.

1.5 ANIMAL MODELS OF AUTOIMMUNE MYOCARDITIS

Animal models of myocarditis provide an invaluable resource to explore the pathogenesis of autoimmune myocarditis and allow for testing of novel therapeutics. A search of the current literature revealed the most widely used rodent models of experimental autoimmune myocarditis (EAM) are Lewis rats, BALB/c mice, and A/J mice. Lewis rats provide the highest evolutionary model of EAM in the rodent family. The Lewis rat model requires one immunization with complete Freund's adjuvant (CFA) and a myocarditic peptide followed by a booster with incomplete Freund's adjuvant (IFA) and a myocarditic peptide. In contrast, murine models require two CFA/ myosin peptide immunizations. Although the rat model is probably closer to human pathology, murine strains enable mechanistic studies due to the large number of gene knockouts in mice that are not available in rats. Echocardiography provides a noninvasive method to characterize the disease progression of EAM.

A Th1 phenotype is observed in the Lewis rat model of EAM, with high IFN-γ and IL-12 in the myocardium at onset of disease [8]. This is expected given that CFA is used and heat killed mycobacterium normally activates the Th1 pathway. The disease becomes maximal on day 21 with pericardial effusions often present in rats with severe infiltration. The disease is T cell-mediated as studies have shown T cells expanded and activated with myosin 1052-1076 and IL-12 are fully capable of inducing severe myocarditis upon transfer to naïve recipients [8]. Experiments have also shown myosin 1052-1076 can directly bind to toll like receptor 2 and provoke pro-inflammatory cytokines from APCs such as monocytes [44]. By stimulating toll like receptor 2, myosin 1052-1076 may play a dual role in activating T cells by acting as an adjuvant and a stimulatory epitope in the context of MHC II. T cells harvested from the spleens

of Lewis rats immunized with Myosin 1052-1076 can be expanded and maintained *in vitro*, making the model attractive for long term *in vitro* experiments. In addition to T cell responses, Lewis rats immunized with myosin 1052-1076 have also been shown to develop antibodies against the beta adrenergic receptor that are capable of binding with agonist activity [45]. These beta adrenergic antibodies with agonist activity can physiologically produce the same effects as high levels of epinephrine and contribute to heart failure. Lewis rats immunized once with myosin 1052-1076 in IFA induce IL-10 producing T cells with a more tolerogenic phenotype. These myosin 1052-1076 specific T cells can provide protection against EAM when adoptively transferred [46]. These data suggest the Lewis rat model is a suitable choice to explore therapeutics with a possible T regulatory cell mechanism. In summary the Lewis rat model is an excellent choice to simulate autoimmune myocarditis due to a known myocarditic epitope capable of inducing EAM and because rats are easily monitored via echocardiography.

Autoimmune myocarditis can be elicited in BALB/c and A/J mice. In both strains of mice, myocarditic peptides derived from the alpha cardiac myosin heavy chain have been identified that are capable of inducing myocarditis when emulsified in CFA. The myocarditic myosin peptide 614-629 in BALB/c mice appears to be more potent as 100 μg per mouse per injection is sufficient [9]. A minimum of 200 μg of myosin 334-352 is required for EAM in A/J mice [47]. In most rodent models of EAM inflammation is reported to peak at day 21 and then gradually wane over time [48]. At day 21 for BALB/c mice hearts with internal leukocyte infiltration appear fairly normally upon removal with no major external lesions or pericardial effusion present. This is in stark contrast to Lewis rats where external lesions covering more than 50% of heart surface and pericardial effusions containing as much as 5 ml of fluid are commonly observed.

One of the major drawbacks of studying EAM in mice is the lack of models in the C57BL/6 strain. A majority of genetic knockouts are maintained on the C57BL/6 background. To study a gene of interest in EAM, mice containing the knocked out gene of interest are commonly back crossed for multiple generation on to strain that is susceptible. This process is expensive and time consuming. Previous attempts to induce EAM in C57BL/6 mice using whole cardiac myosin heavy chain emulsified in CFA have failed [49]. Using a single antigen in the form of a peptide has advantages for inducing EAM. Peptides are easy to synthesize/ order and can be more effective due to the same antigen being present in extremely high quantities. One could argue whole proteins offer more epitopes, but if a significant amount of the protein mass does not contribute to antigen recognition, then this mass is effectively wasted. When purified peptides are used to induce experimental autoimmune disease, the recognized epitope is present in much higher molar quantities compared to a given epitope in whole protein extracts. When choosing a peptide antigen to induce autoimmune disease in mice, an understanding of the H2 haplotype is crucial. Protein derived antigens are presented in the context of MHC II on APC to $CD4^+$ T cells. Each allelic version of murine MHC II has an affinity for different peptide antigens derived from a protein. This is why myosin 614-629 induces EAM in BALB/c mice with H2-I-A^d but this same peptide does not induce EAM in A/J mice which possess H2-I-A^a.

Hypothesis for EAM in C57BL/6 mice

Algorithms have been developed to attempt to predict which peptide sequences from a protein are likely to bind to a given MHC II allele. Given that all previous known epitopes capable of inducing EAM in mice and rats are derived from the cardiac myosin heavy chain, the murine cardiac alpha myosin heavy chain protein was selected to search for peptide antigens capable of inducing EAM in mice with the H2-I-A^b allele including C57BL/6 mice. The website:

http://tools.immuneepitope.org/mhcii/ identified 6 different peptide antigens between residues 718-737 from murine cardiac alpha myosin heavy chain with predicted high affinity to H2-I-A^b. It was therefore hypothesized that myosin 718-736 would be capable of inducing EAM in mice on the C57BL/6 background possessing the H2-I-A^b haplotype.

1.6 CYTOKINE ANTIGEN FUSION PROTEINS AND AUTOIMMUNE DISEASE

Cytokine-peptide fusion proteins have demonstrated efficacy in the treatment of experimental autoimmune encephalomyelitis (EAE) in rats and mice [50-59]. Specifically the cytokine neuroantigen fusion proteins have been able to inhibit disease when EAE is induced by the same antigen used in the fusion protein. Studies have explored linking an encephalitic antigen to various cytokines. Of the cytokines tested in neuroantigen fusion proteins, some were more potent than others at inhibiting EAE. From most inhibitory to least inhibitory GM-CSF, IL-16, IL-2, M-CSF, IL-4, IL-13, and IL1RA were found to attenuate EAE when covalently linked to a neuroantigen [53]. The most potent cytokine found to inhibit EAE was GM-CSF. GM-CSF neuroantigen fusion proteins have successfully inhibited EAE when delivered in pretreatment and treatment regimens for Lewis rats, SJL mice and C57BL/6 mice [50, 53-55]. *In vitro* experiments confirmed GMCSF-antigen fusion proteins were able to activate T cell lines specific for the covalently attached antigen [55]. The fusion proteins were 10 to 1,000 fold more potent at stimulating antigen specific T cells compared to free antigen, suggesting the GM-CSF fusion proteins were targeting antigen presenting cells [55]. Indeed competitive inhibition experiments in which free unconjugated GM-CSF was added in increasing concentrations to GMCSF-NAg confirmed the cytokine portion of the fusion protein was targeting myeloid APCs and enhancing uptake of the fusion protein via GM-CSF binding to its cognate receptor [55]. To confirm that the covalent bond between GM-CSF and the neuroantigen was necessary for inhibition of EAE, experiments were conducted in which an equal molar mix of MOG35-55 + GM-CSF or GP69-88 + GM-CSF was compared to the same number of moles of fusion protein

[54]. The investigators found the covalent bond between GM-CSF and the neuroantigen was absolutely necessary for the inhibition of EAE in Lewis rats and C57BL/6 mice in pretreatment and treatment experiments [54, 55]. In addition to inhibiting actively-induced EAE, GMCSF-MOG was also tested against EAE induced by adoptive transfer of activated MOG 35-55 T cells [54]. Mice treated with GMCSF-MOG on days 9, 11, and 14 post adoptive transfer had a significantly milder course of EAE compared to control animals. In summary, GMCSF-NAg fusion proteins are potent tolerogenic vaccines against EAE that operate through antigenic targeting and most likely alter the phenotype of APCs due to signaling from the cytokine portion of the fusion protein. Given their potent ability to inhibit EAE, GMCSF-antigen fusion proteins may well be effective against other models of autoimmune disease including experimental autoimmune myocarditis.

Hypothesis for GMCSF-Myosin fusion proteins treating EAM

Given the previous success of antigen specific inhibition of EAE using GMCSF-NAg fusion proteins, it is hypothesized that GMCSF-Myosin fusion proteins will be able to inhibit myocarditis in experimental autoimmune myocarditis in Lewis rats and BALB/c mice. These models were chosen because myosin derived epitopes capable of inducing myocarditis have been identified. It is hypothesized that GMCSF-Myosin fusion proteins will at minimum provide protection against myocardial inflammation when EAM is induced by the same antigen present in the fusion protein.

Chapter 2

Materials and Methods

2.1 CREATING VECTORS CODING FOR GMCSF-MYO614 AND GMCSF-MYO334

GMCSF-Myo614 and GMCSF-Myo334 were created by expanding primers to yield a double stranded DNA segment with the following order: 5'-GM-CSF overlap-Myosin peptide-histidine tag-vector overlap-3'. These expanded primer segments were then extended against a pIRES2 vector already containing GMCSF-PLP178. The product containing pIRES2 with the new fusion proteins was used to transfect HEK 293F cells which were sorted for isolation of cells producing high quantities of the transfected proteins.

GMCSF-Myo614

For GMCSF-Myo614, primer 4 and primer 5 were expanded to create a 90 bp segment, GMCSF-Myo614 fragment 1. This 90 bp sequence was then expanded with primers 3 and 7 to produce a 144 bp segment, GMCSF-Myo614 fragment 2. The 144 bp segment was expanded with primers 1 and 11 to yield a 178 bp fragment, GMCSF-Myo614 fragment 3. The 178 bp has the following order: 5'-GMCSF overlap-Myosin 614-643 peptide-histidine tag-vector overlap-3'. This 178 bp fragment was extended against GMCSF-PLP178 in a pIRES2 vector to produce full length pIRES2 vector containing GMCSF-Myo614 with a size of 5805 bp. The product from the extension reaction was digested with Afel I and Dpn I to eliminate residual GMCSF-PLP178 template and methylated DNA respectively.

GMCSF-Myo334

To create GMCSF-Myo334 primers were expanded via two PCR reactions. The first reaction with primers 2 and 6 created a 111 bp segment, GMCSF-Myo334 fragment 1. The 111 bp fragment was further expanded using primers 1 and 10 to create a 145 bp fragment, GMCSF-Myo334 fragment 2, with 5'-GM-CSF overlap-Myo 334-352 peptide-histidine tag-vector specific overlap-3'. The 145 bp fragment was used with GMCSF-PLP178 in pIRES2 to create a full length GMCSF-Myo334 inside the pIRES2 vector with a size of 5297 bp. This product was then digested with Afel I and Dpn I to remove residual GMCSF-PLP178 template and methylated DNA respectively.

The pIRES2 vector containing GMCSF-Myo614 or GMCSF-Myo334 was added to top10 E. coli for transformation via electroporation. The electroporated E. coli were cultured on agar plates containing (50 µg/ml) kanamycin. After 15 hours of growth single colonies were selected and grown for one hour in 100 µl of LB containing 50 µg/ml kanamycin in preparation for whole cell polymerase chain reaction (PCR). Whole cell PCR was setup using 1 µl from each colony with primers 12 and 13 to produce a fragment containing 5'-GMCSF overlap-peptide sequence-histidine tag-vector overlap-3'. Because the PLP 178-192 peptide contains a recognition site for the Afel I restriction endonuclease, PCR product from colonies transfected with GMCSF-PLP178 should digest into two fragments with the larger fragment equaling 535 bp. PCR amplification using the vector specific primers 12 and 13 should yield a 676 bp for GMCSF-Myo614 and a 643 bp fragment for GMCSF-Myo334. Therefore all whole cell PCR products were digested with Afel I and run on an agarose gel to identify colonies containing GMCSF-Myo614 or GMCSF-Myo334. Positively identified colonies were used to create glycerol stocks.

Table 2.1 Primers for GMCSF-Myo614 and GMCSF-Myo334

Primer number	Primer sequence
1	ACTGATATCCCCTTTGAATGCAAAAAACCAGGCCAAAAA
2	TTTGAATGCAAAAAACCAGGCCAAAAAGATAGTGCCTTTGATGTGCTGAGCTTCACGGCAGAGGAGAAGGCT
3	TTTGAATGCAAAAAACCAGGCCAAAAATCCCTCAAGCTCATGGCTACACTCTTC
4	TCCCTCAAGCTCATGGCTACACTCTTCTCTACCTATGCTTCTGCTGATACCGGTGACAGT
5	GCCTTTCTTCTTGCCTCCTTTGCCTTTACCACTGTCACCGGTATCAGCAGAAGCATA
6	TCAGTGATGGTGATGGTGATGGTGATGCTTGTAGACACCAGCCTTCTCCTCTGCCGTGAAGCTCAG
7	TCAGTGATGGTGATGGTGATGGTGATGGCCTTTCTTCTTGCCTCCTTTGCCTTTACC
8	ACTTCTCGACAAGCTTGGTACCTCAGTGATGGTGATGGTGATGGTGATGCTTGTAGACACC
9	ACTTCTCGACAAGCTTGGTACCTCAGTGATGGTGATGGTGATGGTGATGGCCTTTCTTCTT
10	GGGCAGGCCTAGTACTCCCGGGTCAGTGATGGTGATGGTGATGGTGATGCTTGTAGACACC
11	GGGCAGGCCTAGTACTCCCGGGTCAGTGATGGTGATGGTGATGGTGATGGCCTTTCTTCTT
12	GTACGGTGGGAGGTCTATATAAGCAG
13	ATTCCAAGCGGCTTCGGCCAGTAACG

Table 2.2 DNA sequences for GMCSF-Myo614 and GMCSF-Myo334

Name	Size (bp)	Sequence 5' to 3'
GMCSF-Myo614 fragment 1	90	TCCCTCAAGCTCATGGCTACACTCTTCTCTACCTATGCTTCTGCTGATACCGGTGACAGTGGTAAAGGCAAAGGAGGCAAGAAGAAAGGC
GMCSF-Myo614 fragment 2	144	TTTGAATGCAAAAAACCAGGCCAAAAATCCCTCAAGCTCATGGCTACACTCTTCTCTACCTATGCTTCTGCTGATACCGGTGACAGTGGTAA AGGCAAAGGAGGCAAGAAGAAAGGCCATCACCATCACCATCACCATCACTGA
GMCSF-Myo614 fragment 3	178	ACTGATATCCCCTTTGAATGCAAAAAACCAGGCCAAAAATCCCTCAAGCTCATGGCTACACTCTTCTCTACCTATGCTTCTGCTGATACCGGT GACAGTGGTAAAGGCAAAGGAGGCAAGAAGAAAGGCCATCACCATCACCATCACCATCACTGACCCGGGAGTACTAGGCCTGCCC
Full GMCSF-Myo614-643	5805	ATGGCCTGGCTGCAGAATTTACTTTTCCTGGGCATTGTGGTCTACAGCCTCTCAGCACCCACCCGCTCACCCATCACTGTCACCCGGCCTTGG AAGCATGTAGAGGCCATCAAAGAAGCCCTGAACCTCCTGGATGACATGCCTGTCACGTTGAATGAAGAGGTAGAAGTCGTCTCTAACGAG TTCTCCTTCAAGAAGCTAACATGTGTGCAGACCCGCCTGAAGATATTCGAGCAGGGTCTACGGGGCAATTTCACCAAACTCAAGGGCGCCT TGAACATGACAGCCAGCTACTACCAGACATACTGCCCCCCAACTCCGGAAACGGACTGTGAAACACAAGTTACCACCTATGCGGATTTCAT AGACAGCCTTAAAACCTTTCTGACTGATATCCCCTTTGAATGCAAAAAACCAGGCCAAAAATCCCTCAAGCTCATGGCTACACTCTTCTCTA CCTATGCTTCTGCTGATACCGGTGACAGTGGTAAAGGCAAAGGAGGCAAGAAGAAAGGCCATCACCATCACCATCACCATCACTGA
GMCSF-Myo334 fragment 1	111	TTTGAATGCAAAAAACCAGGCCAAAAAGATAGTGCCTTTGATGTGCTGAGCTTCACGGCAGAGGAGAAGGCTGGTGTCTACAAGCATCAC CATCACCATCACCATCACTGA
GMCSF-Myo334 fragment 2	145	ACTGATATCCCCTTTGAATGCAAAAAACCAGGCCAAAAAGATAGTGCCTTTGATGTGCTGAGCTTCACGGCAGAGGAGAAGGCTGGTGTCT ACAAGCATCACCATCACCATCACCATCACTGACCCGGGAGTACTAGGCCTGCCC
Full GMCSF-Myo334-352	5297	ATGGCCTGGCTGCAGAATTTACTTTTCCTGGGCATTGTGGTCTACAGCCTCTCAGCACCCACCCGCTCACCCATCACTGTCACCCGGCCTTGG AAGCATGTAGAGGCCATCAAAGAAGCCCTGAACCTCCTGGATGACATGCCTGTCACGTTGAATGAAGAGGTAGAAGTCGTCTCTAACGAG TTCTCCTTCAAGAAGCTAACATGTGTGCAGACCCGCCTGAAGATATTCGAGCAGGGTCTACGGGGCAATTTCACCAAACTCAAGGGCGCCT TGAACATGACAGCCAGCTACTACCAGACATACTGCCCCCCAACTCCGGAAACGGACTGTGAAACACAAGTTACCACCTATGCGGATTTCAT AGACAGCCTTAAAACCTTTCTGACTGATATCCCCTTTGAATGCAAAAAACCAGGCCAAAAAGATAGTGCCTTTGATGTGCTGAGCTTCACGG CAGAGGAGAAGGCTGGTGTCTACAAGCATCACCATCACCATCACCATCACTGA

Vector sequencing and eukaryotic transfection

Glycerol stocks containing GMCSF-Myo614 or GMCSF-Myo334 were streaked for isolation and individual colonies were expanded in LB containing kanamycin (50 µg/ml) for 15 hours at 37^0C. Approximately 5 ml of expanded clones for GMCSF-Myo614 or GMCSF-Myo334 was used to isolate DNA plasmid using the Qiagen Plasmid Mini Prep kit. Purified plasmid with primers 12 and 13 were sent to GeneWiz.com for sequencing. Multiple clones from each fusion protein were identified with perfect sequences, however only one clone for each fusion protein was selected for eukaryotic transfection. Clone 2 for GMCSF-Myo614 and clone 1 for GMCSF-Myo334 were chosen for expansion and transfection. Glycerol stocks for each clone were streaked for isolation on agar plates containing kanamycin (50 µg/ml). An isolated colony for each fusion protein was expanded in 50 ml of LB containing kanamycin (50 µg/ml) for 15 hours. The bacteria were then harvested and used in Midi preps (Qiagen) to isolate vector plasmid. 37.5 µg of plasmid for each fusion protein was used with lipofectamine (Life Technologies) to transfect HEK 293F cells. Transfected HEK 293F cells were cultured with Geneticin to positively select pIRES2 transfected cells. Transfected cells were then sorted for green fluorescent protein (GFP) production using a 488 nm laser on a Becton Dickinson FACSVantage SE high speed cell sorter. Approximately 100,000 high GFP cells for each fusion protein were sorted and expanded in culture using cRPMI (1640 media with 10% heat inactivated fetal bovine serum) with Geneticin. Freezer stocks were made by adding 10 million cells to cRPMI in 10% DMSO. The cells were frozen at -80^0C for 24 hours and then transferred to liquid nitrogen for permanent storage.

2.2 GMCSF-MYO1052 EXPRESSION

Baculovirus stock coding for GMCSF-Myo1052 or GM-CSF was removed from liquid nitrogen and scraped with an 18 gauge needle to remove a very small amount of virus. This ice scraping was used to expand the virus by infecting approximately 20 million cells plated on 150 mm diameter polystyrene dish with 20 ml of SF9 expression media. The cells were cultured at standard atmospheric conditions with no light for approximately 8 days and upon visual confirmation of viral infection the supernatant was harvested and used for protein expression. 1 ml of the expanded virus stock and 19 ml of serum free media was added to a 150 mm diameter plate with 10 million naïve insect cells and cultured at standard atmospheric conditions with no light for approximately 4 days. The supernatant was then collected and spun at 4000 G for 12 minutes to remove cellular debris and stored at -20^{0}C until approximately 1 liter was accrued.

2.3 GMCSF-MYO614 AND GMCSF-MYO334 EXPRESSION

Before HEK 293 F cells were used for fusion protein expression, production of GFP was assessed as an indirect measure of GMCSF-Myo614 expression. Naïve HEK cells were compared against GMCSF-Myosin transfected cells on a flow cytometer using a 488 nm laser with detection set at 505 nm. If fluorescence of the transfected cells at 505 nm was at least two orders of magnitude higher than naïve HEK cells, the transfected cells were used for protein production. HEK 293 F cells containing pIRES2 coding for GMCSF-Myo614 or GMCSF-Myo334 were seeded at 20 million cells in 30 ml of Serum Free 293 Expression Medium (Life Technologies) containing 0.4 mg/ml of Geneticin (G418, Life Technologies) in a 125 ml plain bottom vented shaker flask (Fisher Scientific). Culture conditions consisted of 5% CO^2, 80% humidity, and constant circular shaking in the dark. The cells were allowed to double twice over 48 hours at which time all supernatant was collected, spun at 4000 G for 12 minutes and stored at -20^0C. The cells were diluted back to 20 million per flask using the same culture conditions. This process was repeated until 1 to 2 liters of supernatant was accumulated, at which point the concentration and purification protocols listed below were initiated.

2.4 PROTEIN CONCENTRATION AND PURIFICATION

For GM-CSF, GMCSF-Myo1052, GMCSF-Myo614, and GMCSF-Myo334 frozen supernatant was thawed and centrifuged at 4000 G for 12 minutes followed by sterile filtration to remove debris. The filtered supernatant was added to a pressurized Amicon Stir cell system (Millipore, Billerica, MA) with a YM10 ultrafiltration Membrane (Millipore) to concentrate all protein from approximately one liter to about 25 ml. For protein expressed in the insect cell system an extra diafiltration procedure was conducted where the 25 ml was expanded to 300 ml with wash buffer and concentrated again to 25 ml. This diafiltration step was not necessary for protein produced in the HEK 293 F system.

The 25 ml of concentrated protein was further concentrated and purified using two passes over a Ni-NTA column. The nickel column was first equilibrated with 10.0 ml of wash buffer (50 mM NaH_2PO_4 (monobasic and anhydrous), 500 mM NaCl, pH 8.0) containing 10 mM imidazole. After equilibrating the column the 25 ml containing the protein was added in 1 ml increments. The column was then washed with 10 ml of wash buffer containing 10 mM imidazole and then eluted with 6 ml of wash buffer containing 250 mM imidazole. The eluted protein was washed with approximately 13 ml of wash buffer 3 times using an Amicon ultra 15 tube (Millipore, Billerica, MA). The nickel column was again equilibrated with wash buffer containing 10 mM imidazole and the retentate from the Amicon ultra 15 was added. The column was washed with 10 ml of wash buffer containing 10 mM imidazole. Next 2 ml fractions containing increasing concentrations of imidazole (20 mM, 40 mM, 60 mM and 100 mM) were added. 2 ml from each concentration was collected in a separate tube. Finally any remaining protein was eluted using 3 x 2ml fractions of wash buffer containing 250 mM imidazole.

SDS PAGE was performed to determine which elution fractions contained the fusion protein. The fractions were diluted 1:2 using loading buffer (100 mM Tris-HCl, 4% SDS, 0.2% bromophenol blue, 20% glycerol, 200 mM beta-mercaptothethanol) and heated for 10 minutes at 90^0C prior to loading. The gels contained a 5% stacking layer and a 12% resolving layer containing 30% bisacrylamide, Tris-HCl (pH 6.8 or 8.8), 10% SDS, 10% ammonium persulfate, TEMED, and MilliQ water. The samples were run at 60 milliamps through the stacking layer and 90 milliamps through the resolving layer until the leading edge of the loading dye reached the end of the gel. The gels were then fixed using 50% methanol, and 8% acetic acid for 15 minutes before being stained overnight with a Coomassie-based dye. The next morning the gel was washed repeatedly in MilliQ water and pictures were acquired using a BioRad Gel doc system.

Fractions identified from SDS PAGE containing the protein were combined in an Amicon ultra 15 tube and washed three times with wash buffer containing no imidazole. The final 400 µl fraction containing the protein was expanded to 1 ml with sterile PBS and analyzed at 280 nm on a nanodrop 1000 to determine the final protein concentration. The protein was then aliquoted and stored at -80^0C.

2.5 FUSION PROTEIN VALIDATION

Cytokine domain validation

The GM-CSF cytokine domain of GMCSF-Myo1052, GMCSF-Myo614 and GMCSF-Myo334 was validated using bone marrow proliferation assays with [3H]thymidine. A 96 well flat bottom plate was used to serially dilute GMCSF-Myo1052 or GM-CSF in triplicate using cRPMI supplemented with FBS from one micromolar to one picomolar in full log steps. All wells had 100 µl of volume after the serial dilution. For GMCSF-Myo1052, bone marrow was harvested from the femurs of Lewis rats. For GMCSF-Myo614 and GMCSF-Myo334, bone marrow was harvested from the femurs of BALB/c mice. The bone marrow cells were washed twice in HBSS and counted using a hemocytometer. 55,000 bone marrow cells were added to each well in 100 µl of cRPMI, leaving 200 µl per well final volume. The cells were incubated at 37^0C with 5% CO^2 and 80% relative humidity. After 48 hours of total incubation, 20 µl of [3H]thymidine (1 µCi / well, Perkin Elmer, Waltham, MA.) was added to each well. After 72 hours of total culture the cells were harvested onto a filter for 96 well plates using a Tomtec Mach III harvester. The filters were screened for [3H]thymidine incorporation using a Wallac 1450 Microbeta Plus liquid scintillation counter.

Antigen domain validation

Antigen presentation of Myosin 1052-1076 from GMCSF-Myo1052 was assessed using irradiated splenocytes and a Lewis rat derived, stable T cell line specific for myosin 1052-1076. GMCSF-Myo1052 or myosin 1052-1076 was titrated in triplicate in a 96 well plate using cRPMI supplemented with 10% FBS from one micromolar to 10 femtomolar in full log dilutions.

Myo1052 T cells were counted, washed twice with HBSS to remove any residual IL-2, and plated at 25,000 cells per well in cRPMI. A spleen was harvested from a Lewis rat, irradiated, and processed into a single cell suspension. The splenocytes were washed twice with HBSS counted and plated at 250,000 cells per well in cRPMI. The final volume for each well was 200 µl of cRPMI. The cells were incubated at 37^0C, 5% CO^2, 80% relative humidity in complete darkness. After 24 hours of incubation, 100 µl of supernatant was removed for IL-2 analysis and 100 µl of fresh cRPMI was added back to each well. After 48 hours of total incubation, 20 µl of [3H]thymidine (1 µCi / well, Perkin Elmer, Waltham, MA.) was added to each well. After 72 hours of total culture the cells were harvested onto a filter for 96 well plates using a Tomtec Mach III harvester. The filters were screened for [3H]thymidine incorporation using a Wallac 1450 Microbeta Plus liquid scintillation counter.

Twenty four hours after Myosin 1052 T cells were activated, supernatants were collected and assayed for IL-2 production by culturing CTLL cells in the presence of MTS/PMS (Promega, Madison, WI). CTLL cells require IL-2 for growth, and are therefore suitable for assaying IL-2. CTLL cells were washed twice with HBSS to remove any residual IL-2. The cells were suspended in cRPMI at 100,000 cells/ml, and 100 µl was added to each well giving 10,000 CTLL cells per well with total volume of 200 µl per well. After 48 hours of culture, the CTLL cells were pulsed with 10 µl of 1% PMS in MTS. After 72 hours of culture, optical density was measured at 490 nm.

To confirm GMCSF-Myo1052 was presented via MHC II to $CD4^+$ T cells, two antibody inhibition experiments were conducted. For both experiments, GMCSF-Myo1052 was added to six columns of a 96 well plate, while myosin 1052-1076 was added to the remaining six columns. For both experiments, GMCSF-Myo1052 and myosin 1052-1076 were titrated in full

log dilutions from one micromolar to 1 picomolar. For one experiment 2.0% of W3/25 (a monoclonal antibody specific for CD4 in rats) was added to each well. For the other experiment 2.0% of OX6 (monoclonal antibody against MHC II) was added to three columns with GMCSF-Myo1052 and three columns with myosin 1052-1076. An isotype control antibody against IL-4 was added to the remaining wells for the second experiment. For both experiments, 25,000 myosin 1052-1076 specific T cells were rested and washed prior to being added to each well. For both experiments, 250,000 irradiated splenocytes from a naïve Lewis rat were added to each well. All cells and proteins were added using cRPMI and each well contained a final volume of 200 µl of cRPMI. Cells were pulsed with [3H]thymidine at 48 hours and harvested at 72 hours as previously described [60].

2.6 EAM INDUCTION, MONITORING, AND SCORING

Lewis rat Active EAM

Experimental autoimmune myocarditis was induced in Lewis rats using two injections of myosin 1052-1076 (KRKLEGDLKLTQESIMDLENDKQQL). On day 0, each rat received two 100 µl subcutaneous injections containing 500 µg of myosin 1052-1076 emulsified in 100 µl of PBS, 50 µl of Complete Freund's Adjuvant (200 µg Mycobacterium tuberculosis in Incomplete Freund's Adjuvant (Difco, Detroit, MI)), and 50 µl of IFA delivered at the base of the tail . On days 0 and 3, each rat received an intraperitoneal injection containing 0.2 µg of Pertussis toxin (Millipore) in 0.5 ml of PBS. On day 7, each rat received two 100 µl subcutaneous booster injections containing 500 µg of myosin 1052-1076 emulsified in 100 µl of PBS and 100 µl of IFA delivered at the base of the tail. For active EAM induction animals were euthanized on day 21 using 90:10 mg/ml Ketamine/Xylazine (0.05 ml/10 g body weight). The only exception of euthanasia on day 21 for active EAM was the longitudinal experiment, where rats were euthanized with Ketamine/Xylazine on days 14, 21, 28, and 50. The hearts were removed, the atria were cut off and the ventricles were flushed with cold PBS and placed in approximately 10 ml of zinc fix (100 mM Tris buffer, 3.16 mM Calcium Acetate, 22.78 mM Zinc Acetate, 36.68 mM Zinc Chloride) for one week at 4^0C. The hearts were cut three times from apex to base generating four separate pieces which were placed in a tissue cassette and dehydrated using ethanol and xylene in preparation for paraffin embedding. The paraffin blocks were sliced to create 0.5 µm sections which were stained with hematoxylin and eosin. The hearts were then scored to assess infiltration using the following scale: 0 = normal myocardium, 1 = mild myocarditis (<5% cross section infiltrated), 2 = moderate myocarditis (5-10% cross section

infiltrated), 3 = marked myocarditis (10-25% cross section infiltrated), 4 = severe myocarditis (>25% cross section infiltrated).

Lewis rat Passive EAM

Passive EAM was induced in Lewis rats using adoptive transfer. Two donor rats were injected with 500 µg of myosin 1052-1076 emulsified in 0.05 ml of PBS and 0.05 ml of CFA. 0.2 µg of pertussis toxin in 0.5 ml of saline was administered via intraperitoneal injection to donor rats on days 1 and 3. On day 14, the donor rats were euthanized and their spleens were collected and homogenized into a single cell suspension. The cells were cultured at 2.7 million cells per ml in cRPMI with 0.4% IL-12 (from SF-9 expression) and 1 µM myosin 1052-1076. After 3 days of culture, six recipient rats each received 22 million activated donor cells via intraperitoneal injection. Four of the recipient rats were euthanized on day 14 post injection while the remaining 2 rats were euthanized on day 19 post injection. The hearts were fixed in zinc fix, paraffin embedding, stained with H&E and scored as previously described for active EAM in Lewis rats.

BALB/c and C57BL/6 Mice

Experimental Autoimmune myocarditis was induced in BALB/c mice and C57BL/6 mice using myosin 614-629 (SLKLMATLFSTYASAD) and myosin 718-736 (GDFRQRYRILNPAAIPEGQ) respectively. For BALB/c mice, 100 µg of myosin 614-629 was emulsified in 0.05 ml of PBS and 0.05 ml of CFA and delivered via two 0.05 ml subcutaneous injections at the base of the tail on day 0 and day 7. Interferon gamma receptor 1 deficient mice (*Ifngr1* $^{-/-}$)(B6.129S7-Ifngr1tm1Agt/J; stock No. 003288), B cell–deficient mice (*Ighm* $^{-/-}$*)*(B6.129S2-Ighmtm1Cgn/J; stock No.002288) mice, inducible nitric oxide synthase 2 deficient

mice (*Nos2* $^{-/-}$) (B6.129P2-Nos2tm1Lau/J, stock 002609), and wildtype C57BL/6 mice received 200 µg of myosin 718-736 emulsified in 0.05 ml of PBS and 0.05 ml of CFA via two 0.05 ml subcutaneous injections at the base of the tail on day 0 and day 7. For both strains of mice 0.2 µg of pertussis toxin (Millipore) in 0.5 ml of PBS was administered via intraperitoneal injection on day 0. All mice were euthanized on day 21 using 18:2 mg/ml Ketamine/Xylazine (0.05 ml/10 g body weight). The hearts were placed in zinc fix (100mM Tris buffer pH=7.4, calcium acetate 3.16mM, zinc acetate 27.25mM, zinc chloride 36.68mM), dehydrated, paraffin embedded, stained with H&E, and scored as previously described for Lewis rats.

Activation of Myosin 718 splenocytes

Two female *Ifngr1* $^{-/-}$ mice on the C57BL/6 background were injected with 200 µg of myosin 718-736 emulsified in 0.05 ml of saline and 0.05 ml of CFA on day 0 and day 7. One of the two female mice also received 0.2 µg of pertussis toxin in 0.5 ml of saline via intraperitoneal injection on day 0. On day 14 both mice were euthanized and their spleens were harvested and homogenized into a single cell suspension. The splenocytes were washed twice with HBSS and suspended in cRPMI at 2.5 million cells per ml. 250,000 splenocytes in 100 µl of cRPMI were added to each well of a 96 well plate. The plate already contained 100 µl of myosin 718-736, myosin 721-735, myosin 614-629, or myosin 1052-1076 in triplicate full log dilutions from 10 micromolar to 10 picomolar. After 48 hours of total incubation, 20 µl of [3H]thymidine (1 µCi / well, Perkin Elmer, Waltham, MA.) was added to each well. After 72 hours of total culture the cells were harvested onto a filter for 96 well plates using a Tomtec Mach III harvester. The filters were screened for [3H]thymidine incorporation using a Wallac 1450 Microbeta Plus liquid scintillation counter.

Echocardiography

Echocardiography was performed in both rats and mice using a Vevo 2100 (Visual Sonics, Toronto, Canada) imager to noninvasively assess myocarditis. Isoflurane was used for anesthesia. Rats were maintained at approximately 2% isoflurane with 100% O^2 while mice were maintained at approximately 1% isoflurane with 100% O^2. In all rodents, Nair was used in a depilatory manner to remove hair. Images were captured in rats using a MS250 transducer at 13-24 MHz. In mice a MS400 transducer at 18-38 MHz was used. Images were acquired in M mode using parasternal long axis and short axis views. Images were subsequently marked to measure left ventricular inner diameter and left ventricular posterior wall thickness in both systole and diastole. Heart rate was also measured to ensure the animals were not overly anesthetized. The images were also examined for the presence of pericardial effusion by confirming separation of the pericardial membrane from the myocardial surface.

2.7 FUSION PROTEIN PRETREATMENT AND TREATMENT REGIMENS

Pretreatment experiments were conducted in Lewis rats and BALB/c mice to determine if GMCSF-Myo1052 and GMCSF-Myo614 could inhibit EAM in their respective models. A PBS group was included to control for the vehicle. A myosin 1052-1076 group and a myosin 614-629 group were included to control for immune tolerance in Lewis rats and BALB/c mice respectively. In Lewis rats all fusion protein batches used in animal experiments were previously tested for cytokine bioactivity and antigen presentation. In BALB/c mice all fusion proteins used for animal experiments were previously tested for cytokine bioactivity. On days -21, -14 and -7 Lewis rats or BALB/c mice were subcutaneously injected on both sides at the base of the tail with vehicle (PBS for Lewis rats and saline for BALB/c mice), 2.5 nanomoles of peptide (myosin 1052-1076 for Lewis rats or myosin 614-629 for BALB/c mice), or 2.5 nanomoles of fusion protein (GMCSF-Myo1052 for Lewis rats or GMCSF-Myo614 for BALB/c mice). EAM induction began on day 0 as previously described. Hearts were harvested for histology on day 21 and scored as previously described.

Treatment experiments were conducted in BALB/c mice to evaluate the ability of GMCSF-Myo614 to inhibit or attenuate actively developing disease in EAM. A saline group was present to control for vehicle. A myosin 614-629 group was included to control for immune tolerance to the myosin antigen. GMCSF-Myo334 was included to control for any effects due to the presence of GM-CSF. The 334 epitope of GMCSF-Myo334 should not be presented on MHC II glycoproteins in BALB/c mice due to the absence of the H2-I-A^a allele and therefore GMCSF-Myo344 can effectively serve as cytokine control in BALB/c mice. EAM induction

started on day 0 as previously described. Mice were injected on days 10, 12, 14, and 16 with saline, myosin 614-629, GMCSF-Myo334, or GMCSF-Myo614. For peptide or fusion protein injections each mouse received 2 nanomoles of their respective molecule each injection day. Upon euthanasia on day 21, hearts were collected for histology while whole blood was collected for serum cytokine analysis. Hearts were processed and scored as previously described.

Chapter 3

Results

3.1 EXPRESSION AND VALIDATION OF GMCSF-MYO1052 FOR THE LEWIS RAT MODEL OF EAM

GMCSF-Myo1052 was expressed using the SF-9 insect cell system, concentrated by use of Millipore filters, and finally purified with a nickel column. Baculovirus encoding GMCSF-Myo1052 was expanded by two passages and then used to infect naïve insect cells. Supernatant was harvested after approximately 7 days of culture and concentrated using filters that allowed proteins 10 kilodaltons and smaller to pass through. Because GMCSF-Myo1052 has a weight of 18,484 daltons, the protein was retained above the membrane. GMCSF-Myo1052 was purified by two passes over a nickel column. Because GMCSF-Myo1052 contains an 8 residue histidine tag on the C terminus, the protein readily binds nickel. The first pass over the nickel consisted of a 10 mM wash with imidazole followed by elution with 250 mM imidazole. This first pass is designed to remove any proteins with low affinity to the nickel column. The second pass consists of increasing concentrations of imidazole designed to elute proteins produced by the insect cells with weak to moderate affinity to the nickel column. In Figure 3.1 nonspecific proteins are shown eluting from the nickel column using 40 mM to 100 mM concentrations of imidazole. The 250 mM elution resulted in relatively pure GMSF-Myo1052 which was washed to remove imidazole prior to *in vivo* use. Assays were conducted to validate the bioactivity of the cytokine domain prior to use in Lewis rats. To validate the cytokine domain bone marrow cells harvested from the femurs of Lewis rats were cultured with increasing concentrations of GMCSF-Myo1052 or GM-CSF. Figure 3.2 shows an equal increase in cellular proliferation

between GMSF-Myo1052 and GM-CSF. These data indicate covalent attachment of myosin 1052-1076 to the C terminus of GM-CSF does not impair cytokine bioactivity.

To assess bioactivity of the antigen domain myosin, 1052-1076 specific T cells were cultured with irradiated splenocytes and increasing concentrations of GMCSF-Myo1052 or myosin 1052-1076. Figure 3.3 (A) shows enhanced T cell proliferation as measured by [^{3}H]thymidine with GMCSF-Myo1052 versus myosin 1052-1076 peptide. GMCSF-Myo1052 displays high proliferation at lower concentrations compared to myosin 1052-1076 and indicates receptor mediated uptake with subsequent antigen presentation is likely occurring. In addition to [^{3}H]thymidine incorporation, 100 µl of supernatant was removed from each well after 24 hours of growth to measure IL-2 production. Expanding/activated $CD4^+$ T cells produce high levels of IL-2 for autocrine use as a growth factor. Therefore IL-2 levels can be used as a surrogate marker of $CD4^+$ T cell activation. The supernatant was transferred to a blank 96 well plate which was used to culture CTLL cells. CTLL proliferation, in the presence of the supernatant, was assessed using MTS/PMS and measured at 492 nm. Figure 3.3 (B) represents CTLL growth which can be used as a surrogate for IL-2 production. Figure 3.4 shows enhanced IL-2 production from GMCSF-Myo1052 compared to myosin 1052-1076. Data from a single experiment in figure 3.3 confirm enhanced bioactivity of the antigen domain of GMSCF-Myo1052 in the presence of splenocytes as APCs.

To confirm the antigen domain of GMCSF-Myo1052 was being presented via MHC II to $CD4^+$ T cells, antibody inhibition assays were conducted. Myosin specific 1052-1076 T cells were cultured with irradiated splenocytes and increasing concentrations of GMCSF-Myo1052 or myosin 1052-1076. In Figure 3.4 (A) cultures contained either OX6 (anti MHC II) or an isotype control/OX81 (anti IL-4). OX6 completely inhibited growth in the presence of GMSF-Myo1052

or myosin 1052-1076. In Figure 3.4 (B) W3/25 (anti CD4) reduced T cell growth in the presence of GMCSF-Myo1052 or myosin 1052-1076. This reduced response from W3/25 is expected as CD4 stabilizes and enhances MHC II antigen/T cell receptor binding but is not absolutely required.

Figure 3.1 Expression of GMCSF-Myo1052

SDS PAGE was performed to identify which fractions eluted from the nickel column contained GMCSF-Myo1052. Significant quantities of nonspecific proteins are seen eluting at lower imidazole concentrations (40 mM to 100 mM) while relatively pure GMCSF-Myo1052 is seen eluting at 250 mM of imidazole.

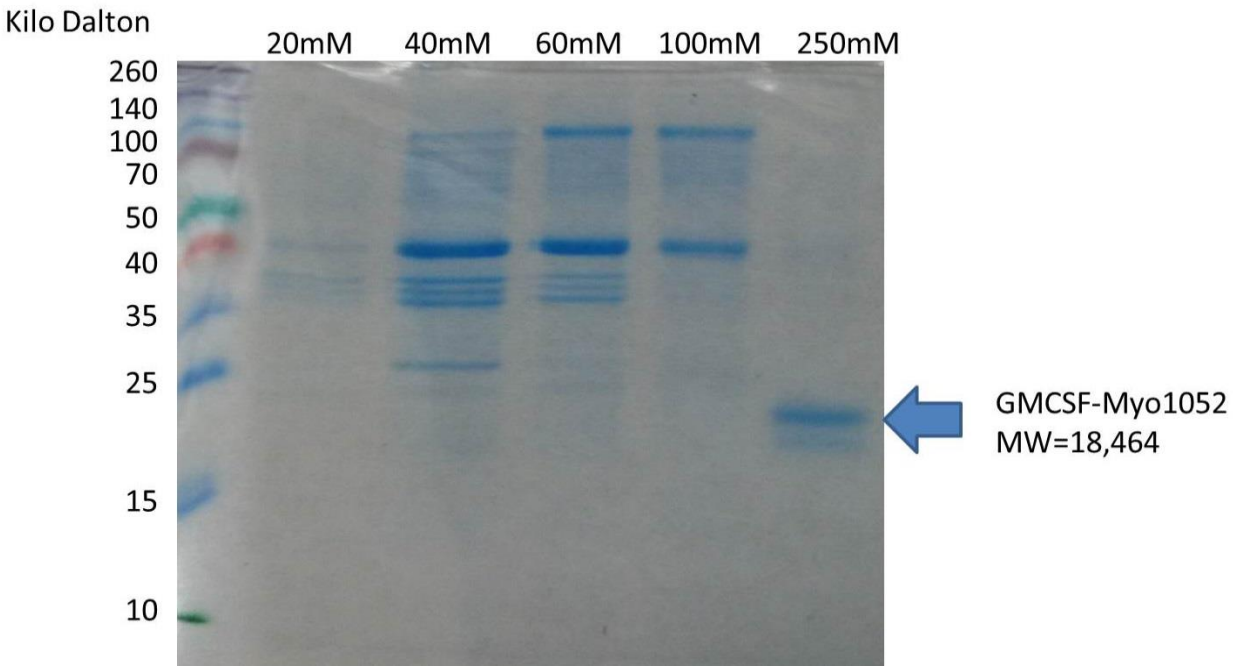
Kilo Dalton
20mM
40mM
60mM
100mM
250mM
260
140
100
70
50
40
35
25
15
10
GMCSF-Myo1052
MW=18,464

Figure 3.2 Validation of the cytokine domain of GMCSF-Myo1052

To validate the cytokine domain of GMCSF-Myo1052, two preparations of GMCSF-Myo1052 were tested in a bone marrow proliferation bioassay. The GMCSF-Myo1052 and GM-CSF preparations had essentially equipotent cytokine activity. The EC50 values for GMCSF-Myo1052 preparation 1, GMCSF-Myo1052 preparation 2, and GM-CSF were respectively 893 fM, 1.19 pM, and 3.4 pM.

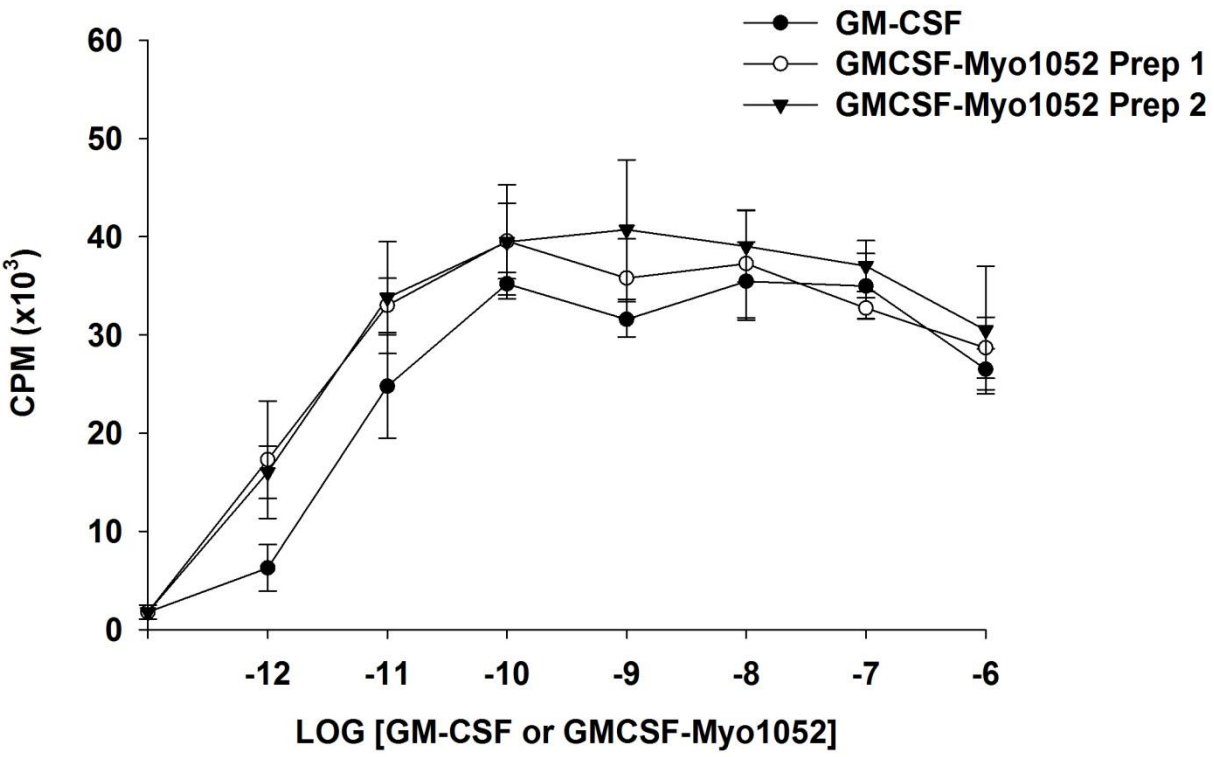
GM-CSF
GMCSF-Myo1052 Prep 1
GMCSF-Myo1052 Prep 2
CPM (x10^3)
60
50
40
30
20
10
0
-12
-11
-10
-9
-8
-7
-6
LOG [GM-CSF or GMCSF-Myo1052]

Figure 3.3 Validation of the antigen domain of GMCSF-Myo1052

The antigenicity of the peptide domain of GMCSF-Myo1052 was assessed by measuring the activation of Myosin 1052 specific T cells in the presence of irradiated splenocytes with increasing concentrations GMCSF-Myo1052 or myosin 1052-1076. After 48 hours all cells were pulsed with [3H]thymidine and at 72 hours all cells were harvested for [3H]thymidine counts. [3H]thymidine counts in (A) show the antigenic response to GMCSF-Myo1052 was approximately 1000-fold more potent than the response to myosin 1052-1076.

Activation of the myosin specific T cells was also assessed by measuring IL-2 production from 100 µl of supernatant collected 24 hours after activation. IL-2 was measured with CTLL cells and MTS/PMS. Figure 3.3 (B) shows a consistent pattern of activation where an increase in IL-2 from T cells cultured with GMCSF-Myo1052 started at 10 nM while an increase in IL-2 from T cells cultured with Myosin 1052-1076 is not present until 100 µM.

A

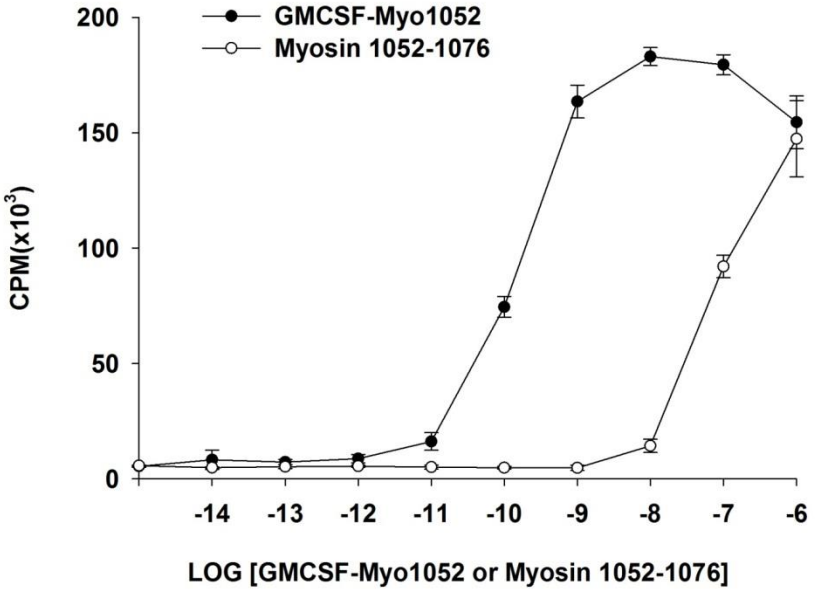
GMCSF-Myo1052
Myosin 1052-1076
CPM(x10^3)
200
150
100
50
0
-14
-13
-12
-11
-10
-9
-8
-7
-6
LOG [GMCSF-Myo1052 or Myosin 1052-1076]

B

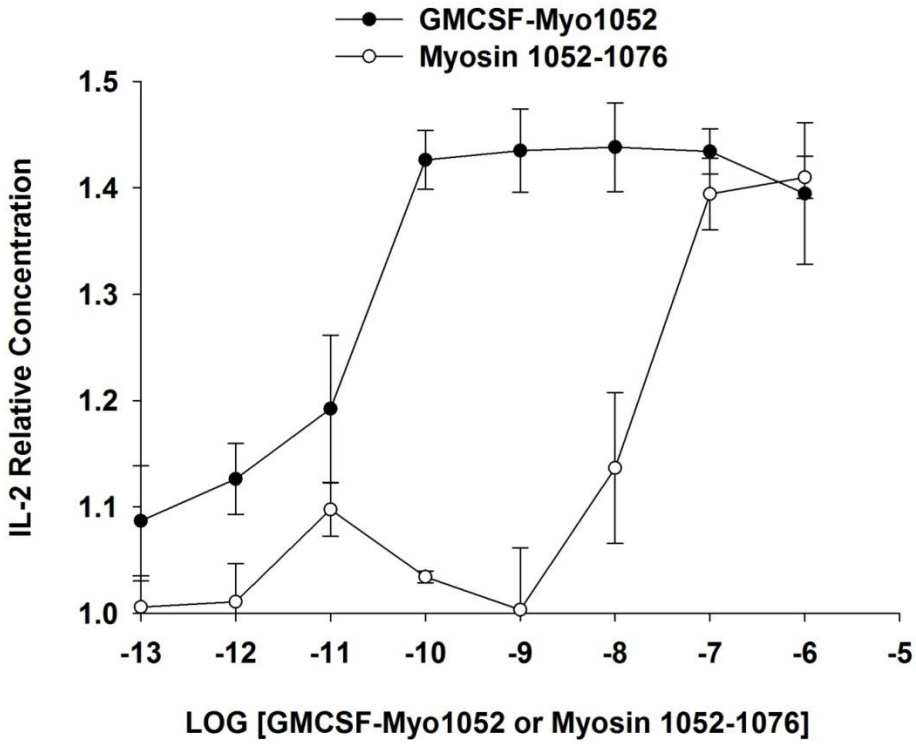
GMCSF-Myo1052
Myosin 1052-1076
IL-2 Relative Concentration
1.5
1.4
1.3
1.2
1.1
1.0
-13
-12
-11
-10
-9
-8
-7
-6
-5
LOG [GMCSF-Myo1052 or Myosin 1052-1076]

Figure 3.4 The Antigenic domain of GMCSF-Myo1052 is presented via MHC II to CD4+T cells

To verify that GMCSF-Myo1052 stimulated the expansion of $CD4^+$ T cells via cells displaying myosin 1052-1076 on MHC II, assays were performed in the presence or absence of neutralizing anti-MHC II or anti-CD4 monoclonal antibodies (mAb). Proliferation of myosin 1052-1076 specific T cells in the presence of irradiated splenocytes and GMCSF-Myo1052 or myosin 1052-1076 was completely blocked by anti-I-A MHCII-RT1B (OX6) and was inhibited by anti-CD4 (W3/25).

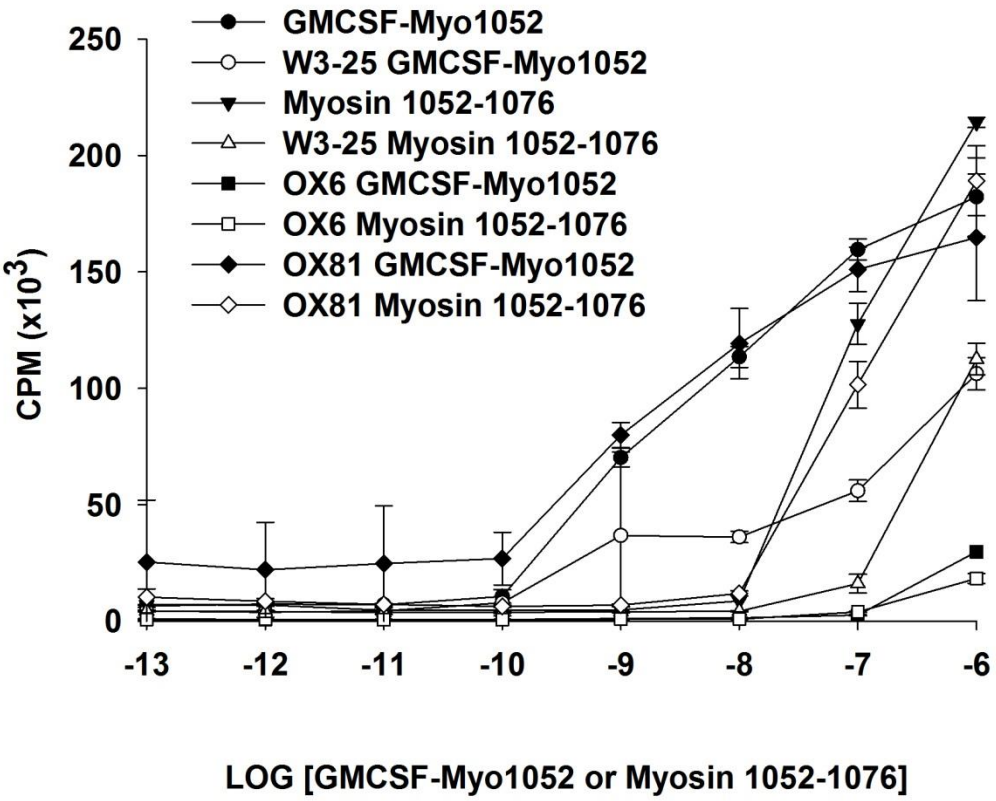
GMCSF-Myo1052
W3-25 GMCSF-Myo1052
Myosin 1052-1076
W3-25 Myosin 1052-1076
OX6 GMCSF-Myo1052
OX6 Myosin 1052-1076
OX81 GMCSF-Myo1052
OX81 Myosin 1052-1076
CPM (x10^3)
250
200
150
100
50
0
-13
-12
-11
-10
-9
-8
-7
-6
LOG [GMCSF-Myo1052 or Myosin 1052-1076]

3.2 EFFICACY OF GMCSF-MYO1052 IN THE LEWIS RAT MODEL OF EAM

After validating both domains of GMCSF-Myo1052 and demonstrating evidence suggesting that the antigen domain of GMCSF-Myo1052 is presented by MHC II to $CD4^+$ T cells, experiments were designed to test the efficacy of GMCSF-Myo1052 in the Lewis rat model of EAM. Because GMCSF-Myo1052 was hypothesized to attenuate EAM in Lewis rats by modulating the T cell repertoire, it was deemed prudent to insure and validate that myosin 1052-1076 induced EAM was a T cell mediated disease. Limited data has been published demonstrating EAM induced with myosin 1052-1076 in Lewis rats is T cell mediated. Therefore an adoptive transfer experiment was conducted to validate previous findings that myosin 1052-1076 induced EAM in Lewis rats is T cell mediated. Adoptive transfer was performed by injecting rats once with myosin 1052-1076 in CFA. Fourteen days after this injection, splenocytes were harvested and expanded and activated *in vitro* using myosin 1052-1076 and IL-12. These activated T cells were then injected in naïve recipients and euthanized at days 14 and 19. Figure 3.5 demonstrates T cells activated with myosin 1052-1076 and IL-12 are sufficient to induce severe EAM. Figure 3.6 shows myosin 1052-1076 induced EAM in the Lewis rat is a T cell mediated disease.

True autoimmune myocarditis is a self-perpetuating disease that can cycle in severity over time and is not limited to one acute occurrence. To better define the potential for chronic disease in the Lewis rat model of EAM, a longitudinal study was conducted. Instead of euthanizing all subjects at day 21, rats were divided into 4 four groups and euthanized on days 14, 21, 28 or 50. Figure 3.6 shows severe myocarditis at day 50. These data indicate actively induced EAM with myosin 1052-1076 has the potential to manifest as a chronic disease that can

persist well past the published 3 week typical maximum reported in the literature. The chronic inflammation in Figure 3.6 parallels data reported on autoimmune myocarditis in clinical literature.

To test the hypothesis that GMCSF-Myo1052 could inhibit myosin 1052-1076 induced EAM in Lewis rats, a pretreatment experiment was performed. GMCSF-Myo1052 was given once a week for three weeks prior to active EAM induction. Figure 3.7 shows animals receiving GMCSF-Myo1052 generally had minimal inflammation or no inflammation while animals receiving the myosin peptide control or PBS vehicle control had significantly higher levels of myocardial infiltration. These data indicate pretreatment with GMCSF-Myo1052 provides significant protection against myocarditis in Lewis rats when EAM is induced with the same antigen present in the fusion protein. Figure 3.8 shows histological cross sections of a (A) normal rat heart and (B) rat heart experiencing level 4 infiltration (>25% cross section infiltration). In (C) and (D), a normal heart and a heart with level 4 infiltration, respectively, are shown in parasternal long axis M mode during echocardiography. These data from echocardiography and histological analysis show pretreatment with GMCSF-Myo1052 significantly reduces the incidence of pericardial effusion and myocardial infiltration during EAM induction with myosin 1052-1076.

Figure 3.5 EAM induced by Myosin 1052-1076 in Lewis rats is a T cell mediated disease

Passive EAM was induced in Lewis rats by activating myosin primed splenocytes *in vitro* with IL-12 and myosin 1052-1076. These activated and expanded T cells were injected into naïve rats and euthanized on days 14 and 19. Figure 3.6 shows 4 recipient rats euthanized at day 14 had a maximum histology score of 4 meaning, greater than 25% of myocardium contained infiltration. At day 19, one animal had a score of 3 (10-25% infiltration), while another had a score of 2 (5-10% infiltration).

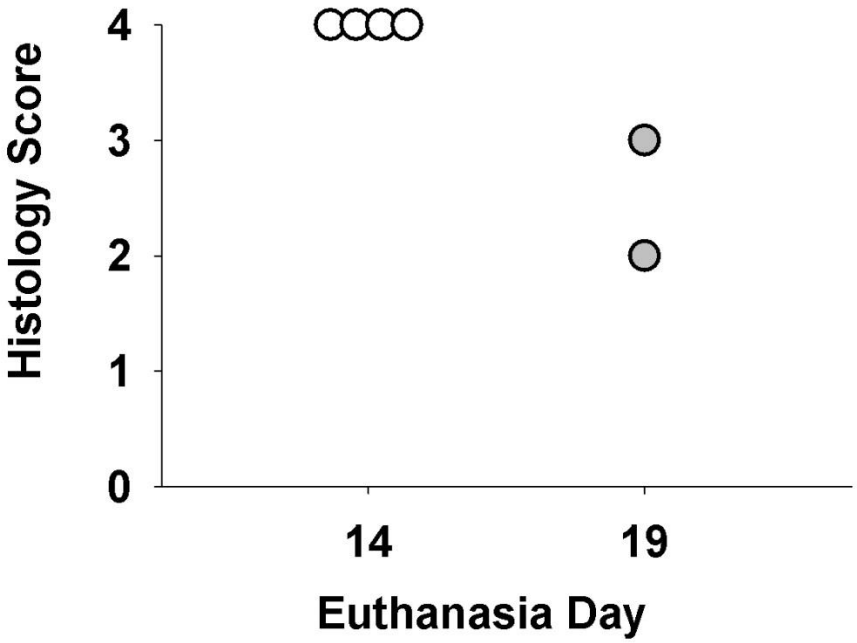
Histology Score
4
3
2
1
0
14
19
Euthanasia Day

Figure 3.6 EAM in the Lewis rat show characteristics of a chronic model

A longitudinal EAM study in Lewis rats was conducted. EAM was actively induced using CFA + myosin 1052-1076 on day 0 and IFA + myosin 1052-1076 on day 7. Animals were euthanized on days 14, 21, 28, and 50. All hearts were placed in zinc fix for 1 week followed by paraffin embedding and staining with H&E. The longitudinal study revealed 3 rats had histology scores of 2, 3, and 4 on day 50.

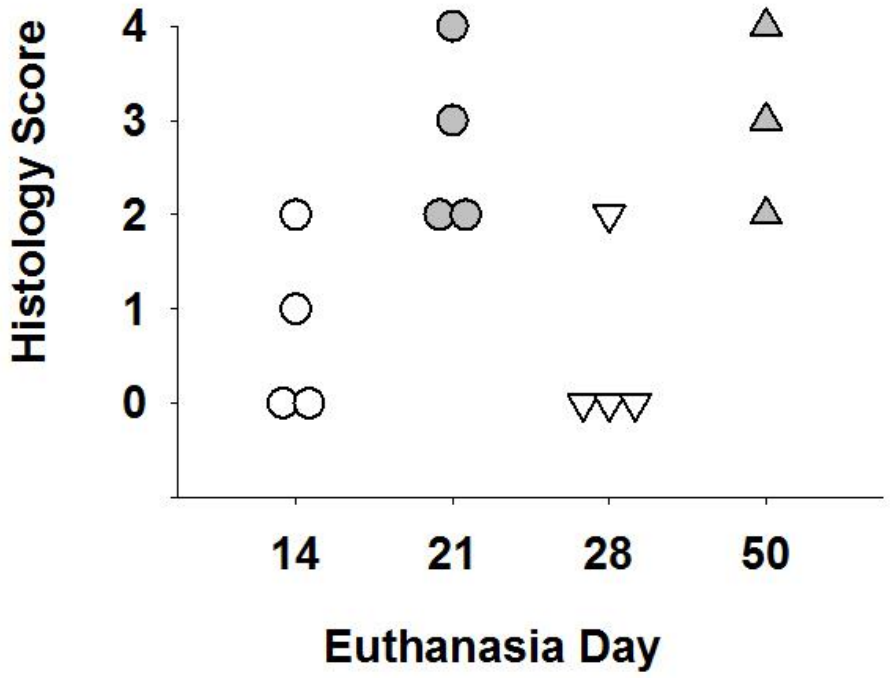
Histology Score
4
3
2
1
0
14
21
28
50
Euthanasia Day

Figure 3.7 Pretreatment with GMCSF-Myo1052

Figure 3.8 shows the level of myocardial inflammation at day 21 after pretreatment with saline, myosin 1052-1076, or GMCSF-Myo1052. Each symbol represents a single rat. Of animals pretreated with GMCSF-Myo1052, 10 of 14 had no myocardial inflammation, 3 of 14 had minimal inflammation, and only one animal had medium inflammation. The saline group had a stratification of histology scores, while the myosin 1052-1076 group did display a low level of tolerance; however there was no statistical significant difference between the saline and myosin 1052-1076 pretreatment groups. With the exception of a single animal, all rats in the GMCSF-Myo1052 pretreatment group had minimal to no infiltration, and pretreatment with the fusion protein provided statistically significant protection against EAM compared the PBS and Myosin 1052-1076 control groups. Shaded symbols represent animals with pericardial effusion which was observed during echocardiography and was confirmed at euthanasia. Pretreatment with the fusion protein completely prevented the occurrence of pericardial effusions.

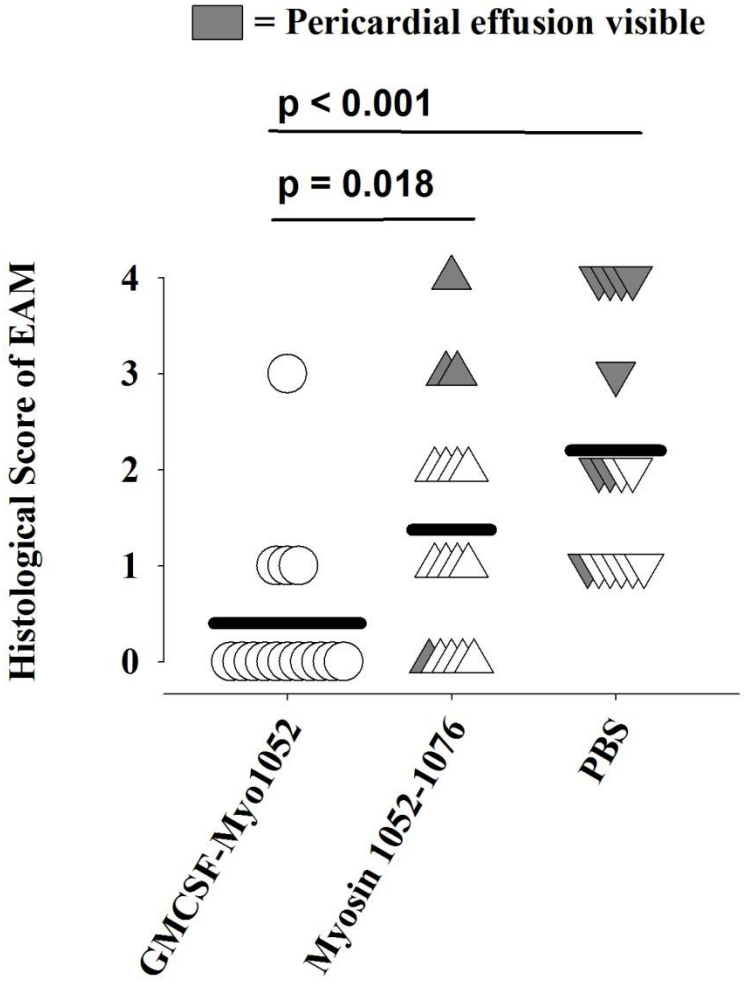
= Pericardial effusion visible
p < 0.001
p = 0.018
Histological Score of EAM
4
3
2
1
0
GMCSF-Myo1052
Myosin 1052-1076
PBS

Figure 3.8 Lewis rat GMCSF-Myo1052 Pretreatment Histology and Echocardiography

In (A and C) depict a healthy heart protected against myocarditis by pretreatment with GMCSF-Myo1052, while in (B) and (D) a heart from animal pretreated with only saline has developed severe infiltration and a pericardial effusion. In (A) a cross section of a healthy heart stained with H&E shows predominately Eosin staining with mostly pink tissue. In (B) a heart with severe EAM is evident as the infiltrating cells pick up the Hematoxylin staining resulting in more visible purple. In (C) echocardiography of a normal heart is shown in parasternal long axis view in M mode, while in (D) a heart in the same view with a pericardial effusion. Note the fluid between the pericardial membrane and the myocardium as denoted with red marks. Also notice the thicker walls of left ventricle due to edema. The green marks in (C) show the anterior and posterior walls of the left ventricle beating in phase. In (D) where an effusion is present the green marks show the walls of the left ventricle are not contracting in phase.

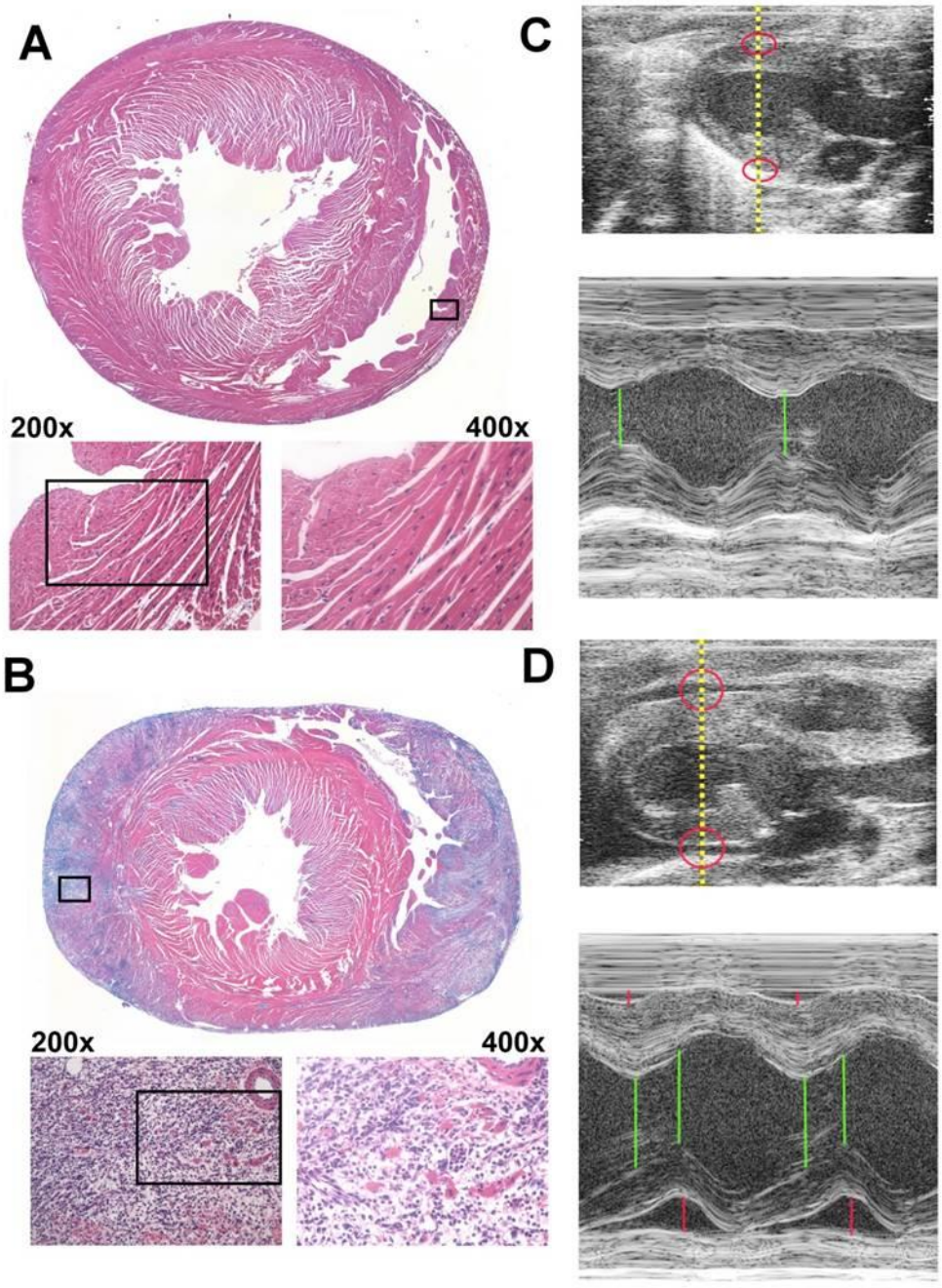
A
C
200x
400x
B
D
200x
400x

3.3 Generation, Expression, and Validation of GMCSF-Myosin fusion proteins for BALB/c and A/J mice

Previous experiments by Blanchfield et al and Abbott et al have revealed GM-CSF based cytokine-antigen fusion proteins are potent inhibitors of EAE in rat and mouse models. GM-CSF covalently linked to cardiac myosin was also found to attenuate myocarditis in a rat model of EAM. Given the previous success of GM-CSF based cytokine-antigen fusion proteins, GM-CSF/myosin based fusion proteins were created to study their potential efficacy and mechanisms in the treatment of murine EAM. At minimum, GMCSF-Myosin fusion proteins should provide protection against all epitopes represented by the attached myosin antigen domain. Therefore peptides capable of inducing EAM in a given rodent strain are prime candidates for testing GMCSF-Myosin fusion proteins. A literature search revealed myosin 614-629 and myosin 334-352 were capable of inducing EAM in BALB/c and A/J mice respectively. The original peptide discovered for BALB/c was 614-643 and this extended peptide was used in the BALB/c fusion protein to cover all possible epitopes. These two peptides were chosen to create two GM-CSF based fusion proteins. Both fusion proteins were designed with following sequence, N terminus-GMCSF-Myosin peptide-histidine tag-C terminus. The HEK 293F expression system was chosen instead of the SF-9 insect system to maximize post translation modification compatibility with the murine background. The pIRES2 vector was chosen for its compatibility with the HEK 293F cell line and because the vector contains a bicistronic reporter molecule, GFP, which can be assayed with flow cytometry to assess relative fusion protein production.

The basic plan to create fusion proteins for both the BALB/c and A/J strains involved expanding primer sets containing the appropriate myosin peptide with cytokine and vector

overlap which could then be used with an existing pIRES2 GMCSF-neuroantigen construct for extension and amplification. Primers were expanded via PCR in figure 3.9 (A) and (B) to generate a 178 bp sequence containing 5'-GMCSF overlap- myosin 614-643-histadine tag-vector overlap-3'. This 178 bp sequence was used with a pIRES2 vector containing GMCSF-PLP178 to generate GMCSF-Myo614 in figure 3.9 (C). For the A/J model of EAM a similar approach was used to expand primers in figure 3.10 (A) to generate a 146 bp sequence with 5'-GMCSF overlap-myosin 334-352-histadine tag-vector overlap-3'. This 146 bp sequence was then used with a pIRES2 vector containing GMCSF-PLP178 to generate GMCSF-Myo334 in figure 3.10 (B).

Building vectors containing GMCSF-Myo614 and GMCSF-Myo334

The products from both extension reactions were digested with Dpn I to destroy any methylated DNA and Afel I to destroy any GMSCF-PLP178. These vectors were then used to transform top10 E.coli using electroporation. The transformed bacteria were grown on agar plates with Kanamycin. Single colonies were picked from both plates and grown in 100 µl of LB containing Kanamycin for 1 hour. 1 µl of bacteria was harvested from each tube for whole cell polymerase chain reaction with vector specific primers. These products were digested with Afel I and Dpn I and run on an agarose gel in figure 13.11 to identify candidate colonies for sequencing. Because PLP178 contains a recognition site for Afel I, digestion of parent template vector produced a 535 bp fragment that migrated faster during agarose electrophoresis. In figure 3.11 (A) colonies in lanes 1, 3, 4, 5, 6, 8, and 12 were positive for GMCSF-PLP178 because they were migrating at the same rate as the 535 bp GMCSF-PLP178 control samples loaded in the flanking wells. In figure 3.12 (A) colonies 2, 7, 9, 10, and 11 were resistant to Afel I, and likely contained pIRES2 with GMCSF-Myo614, and were chosen for sequencing. In figure 3.11 (B),

colonies 1 and 5 contained GMCSF-Myo334 while colonies 2, 3, 4, 6 and 7 were positive for the template GMCSF-PLP 178. Sequencing results in table 13.12 showed clones 1 and 5 contain no errors in the region coding for GMCSF-Myo334, while clones 2, 7, 10, 11 contained no errors for GMCSF-Myo614. Ultimately GMCSF-Myo334 clone 1 and GMCSF-Myo614 clone 2 were chosen for plasmid midi preparations which were then used to transfect HEK 293F cells.

Transfection and selection of HEK 293 cells with GMCSF-Myo614 and GMCSF-Myo334

Naïve HEK 293 cells were transfected with plasmid preparations of either GMCSF-Myo614 clone 2 or GMCSF-Myo334 clone 1 using the Lipofectamine reagent (Life Technologies). The cells were cultured for 48 hours before starting antibiotic selection with Geneticin to select only those cells which were transfected with the pIRES2 vector. Because the pIRES2 vector is bicistronic, GFP and the inserted fusion protein are translated from a single mRNA transcript. Therefore GFP expression should mirror fusion protein expression on a cell by cell basis. This allows for the selection of HEK cells producing relatively high quantities of GMCSF-Myosin by sorting against GFP fluorescence. In figure 3.13 (A) and (C) a minimum fluorescence at 509 nm was set between 10^1 and 10^2 for HEK cells transfected with GMCSF-Myo614 and GMCSF-Myo334 respectively. Cells were then sorted according to this gate and checked for purity (the number of cells below the gate criteria after the sort). Post sort purity checks in figure 3.13 (B) and (D) revealed HEK cells transfected with GMCSF-Myo614 and GMCSF-Myo334 respectively were greater than 95% pure compared the original gates. These cells were carefully cultured for expansion, freezer stocks, and expression of fusion of protein.

Protein production and purification of GMCSF-Myo614 and GMCSF-Myo334

Protein production of GMCSF-Myo614 and GMCSF-Myo334 was performed by culturing transfected HEK 293F cells in serum free Freestyle Expression media (Invitrogen). After approximately 1 to 2 liters of supernatant was harvested from cell culture, the media was concentrated to a volume of 20-30 ml prior to nickel column purification. The histidine tag in both GMCSF-Myo614 and GMCSF-Myo334 allow the fusion proteins to bind to a nickel column and be eluted by using increasing concentrations of imidazole. A small amount of each elution fraction was run on SDS PAGE to identify purity and the fractions containing the fusion protein. In figure 3.14 (A) significant quantities of GMCSF-Myo614 is present in the fraction containing 250 mM imidazole while in (B) GMCSF-Myo334 is also eluting at 250 mM imidazole. Undesired proteins are shown eluting at 60 mM and 100 mM imidazole however these proteins are practically nonexistent in the 250 mM fractions. The 250 mM imidazole fractions for each fusion protein were pooled and washed multiple times to reduce the final imidazole concentration to less than 1mM. The washing was done to avoid any *in vivo* reactions from the imidazole.

Validation of the cytokine domain for GMCSF-Myo614 and GMCSF-Myo334

Bioactivity of cytokine domain for GMCSF-Myo614 and GMCSF-Myo334 was assessed by culturing bone marrow cells harvested from the femurs of BALB/c mice with increasing concentrations of fusion protein or control unconjugated GM-CSF. In figure 3.15 cellular proliferation of bone marrow cells as measured by [3H]thymidine incorporation shows the C terminal addition of myosin 614-643 or myosin 344-352 has no detrimental impact on the bioactivity of GM-CSF in the fusion proteins. These data indicate both fusion proteins should be fully capable of interacting with their cognate cytokine receptors *in vivo*.

Figure 3.9 GMCSF-Myo614 PCR extension reactions

For myosin 614-643 three pcr primer expansion reactions were required. The first reaction produced 90 bp fragment shown in (A) that encoded Myosin 614-643. A second pcr reaction expanded Myosin 614-643 (90 bp) to include GMCSF overlap on the 5 prime end and an 8 residue histidine tag on the 3 prime end (144 bp). The 144 bp fragment is shown in (B). The final expansion reaction for the BALB/c construction created a 178 bp fragment in (C).

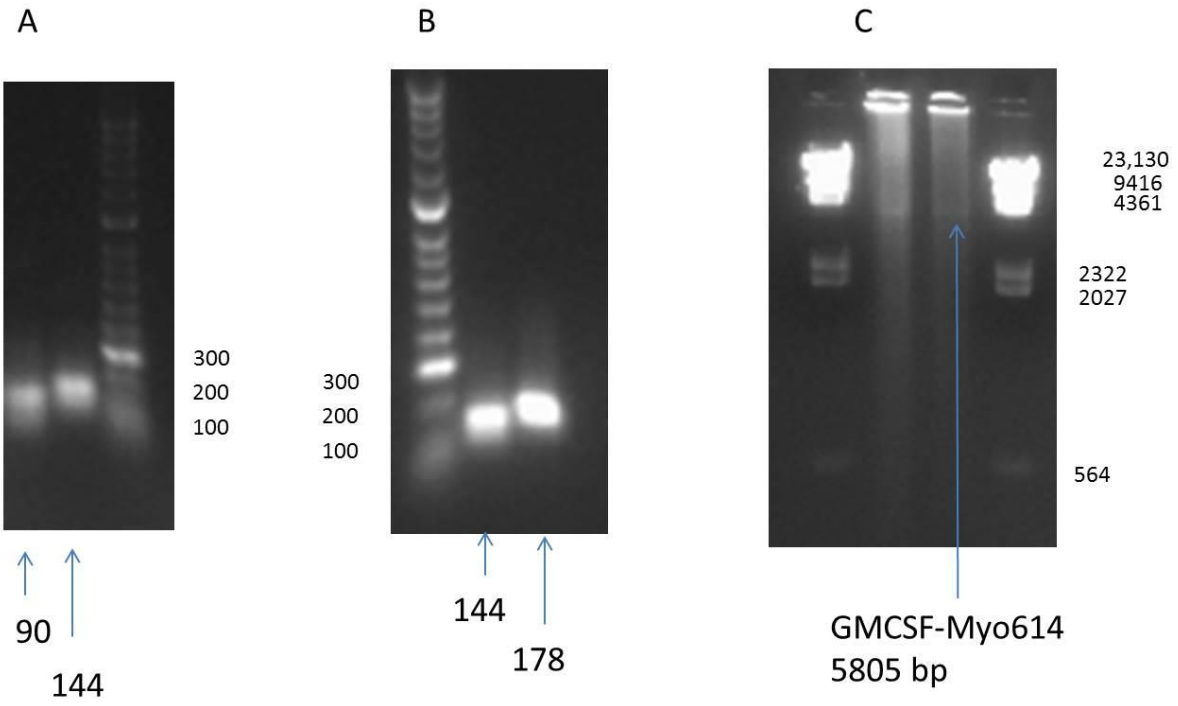
A
B
C
300
200
100
90
144
300
200
100
144
178
23,130
9416
4361
2322
2027
564
GMCSF-Myo614
5805 bp

Figure 3.10 GMCSF-Myo334 polymerase chain reaction extension reactions

For the A/J fusion protein the first polymerase chain reaction produced a 111 bp fragment, shown in (A), encoding the myosin 334-352 peptide with GM-CSF overlap on the 5 prime end and an 8 residue histidine tag on the 3 prime end. A second reaction expanded the 111 bp fragment to 146 bp, shown in (B).

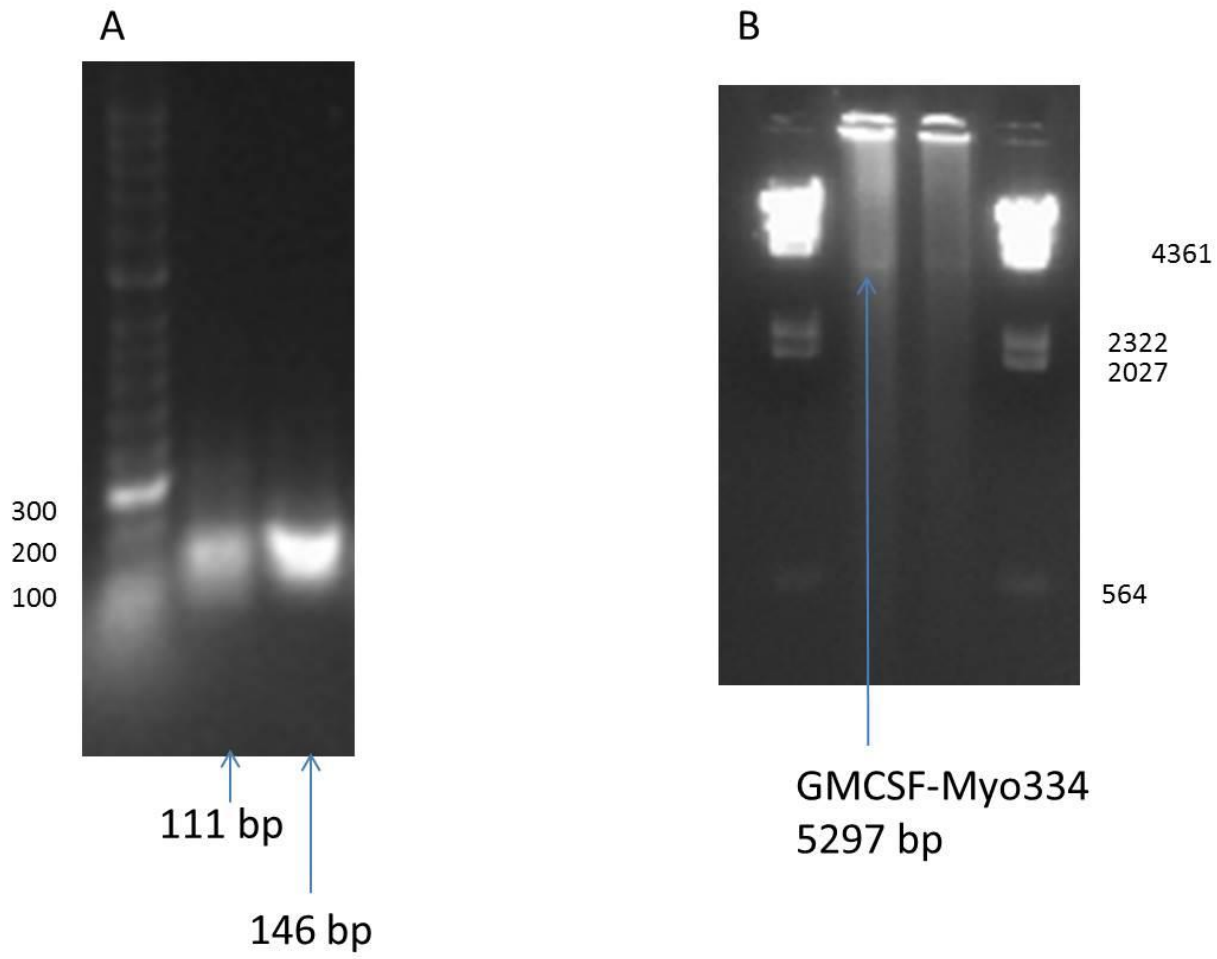
A
300
200
100
111 bp
146 bp
B
4361
2322
2027
564
GMCSF-Myo334
5297 bp

Figure 3.11 Identifying colonies with GMCSF-Myo614 and GMCSF-Myo334

Whole cell PCR reactions using pIRES2 vector specific primers were setup from single colonies on Kanamycin plates following electroporation. After whole cell PCR reactions were complete, digestion with Afel I was performed to discriminate between GMCSF-Myosin or GMCSF-PLP (template). Colonies containing GMCSF-PLP contain a recognition site for Afel I and are reduced to a 535 bp fragment that migrates faster in agarose gel compared to GMCF-Myosin. In (A) colonies 2, 7, 9, 10, and 11 were identified as containing GMCSF-Myo614. In (B) colonies 1 and 5 were identified with GMCSF-Myo334.

A

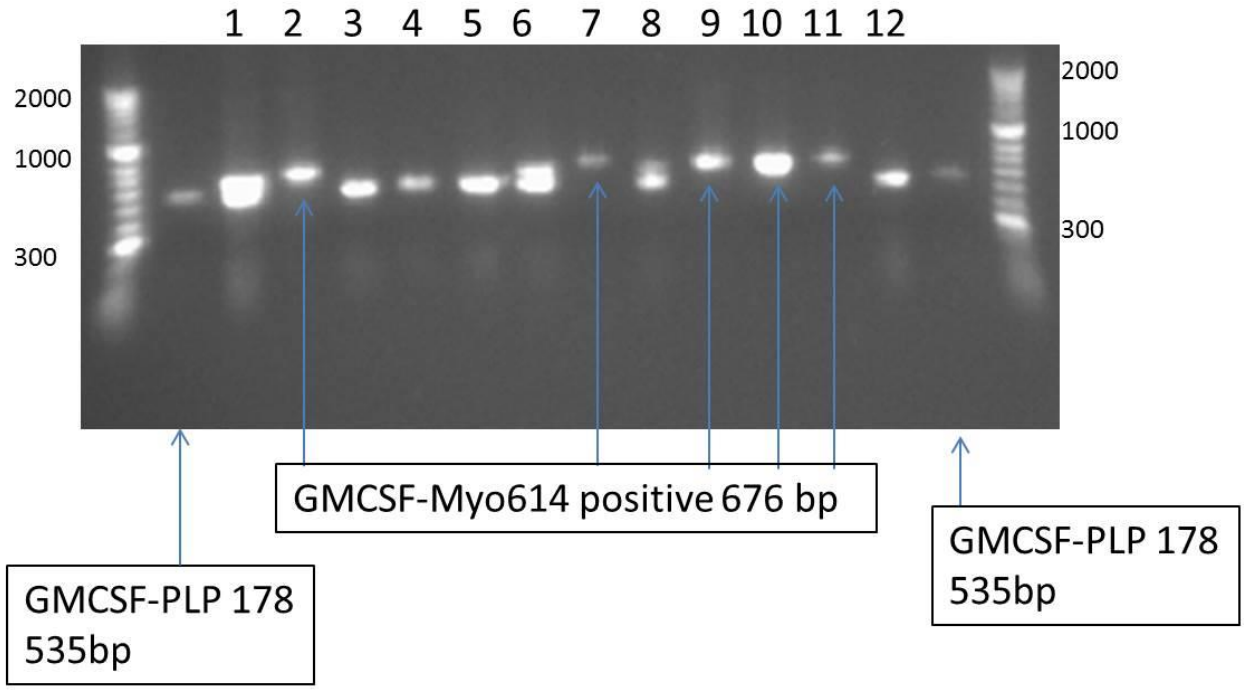
1 2 3 4 5 6 7 8 9 10 11 12
2000
1000
300
2000
1000
300
GMCSF-Myo614 positive 676 bp
GMCSF-PLP 178 535bp
GMCSF-PLP 178 535bp

B

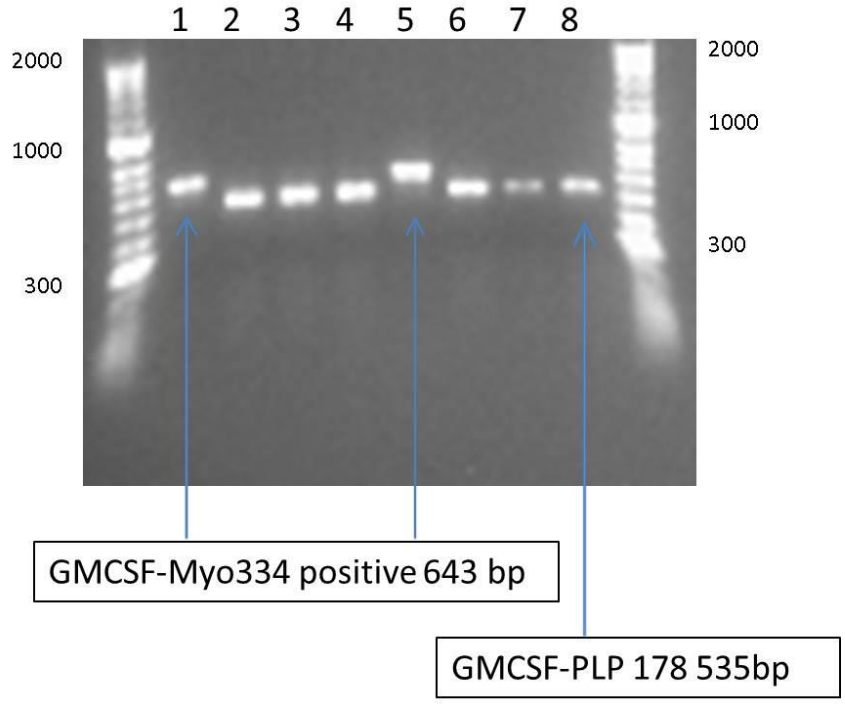
1 2 3 4 5 6 7 8
2000
1000
300
2000
1000
300
GMCSF-Myo334 positive 643 bp
GMCSF-PLP 178 535bp

Table 3.12 Sequence results for PIRES2 GMCSF-Myo614 and GMCSF-Myo334

Construct Name	Clone Number	Start codon	Stop codon	Perfect sequence (yes/no)
PIRES2 GMCSF-Myo 334	1	603	1112	yes
PIRES2 GMCSF-Myo 334	5	603	1112	yes
PIRES2 GMCSF-Myo 614	2	603	1143	yes
PIRES2 GMCSF-Myo 614	7	603	1143	yes
PIRES2 GMCSF-Myo 614	9	603	1143	no
PIRES2 GMCSF-Myo 614	10	603	1143	yes
PIRES2 GMCSF-Myo 614	11	603	1143	yes

Figure 3.13 Establishing gates for GFP high cells transfected with fusion proteins and checking post sort purity

HEK 293F cells transfected with either GMCSF-Myo614 or GMCSF-Myo334 were sorted to select cells producing relatively high amount of fusion protein. Using the 488 nm laser and measuring emission at 509 nm a gate was established in Figure 3.14 to select only cells with high GFP production. In figure 3.14, the boxes present in the upper half of (A) and (C) were established for cells transfected with GMCSF-Myo614 and GMCSF-Myo334 respectively. After sorting the cells, their fluorescent intensity at 509 nm was measured again, and confirmed that 95% of cells with GMCSF-Myo614 (B) and 96% of cells with GMCSF-Myo334 (D) had GFP fluorescence at or above the previous gates set in (A) and (C) respectively.

A

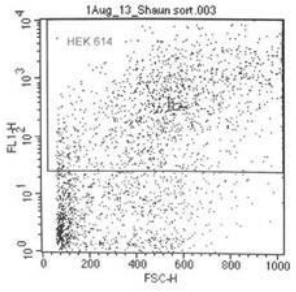

B

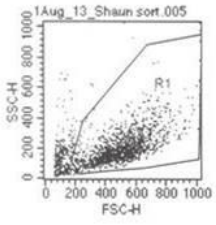

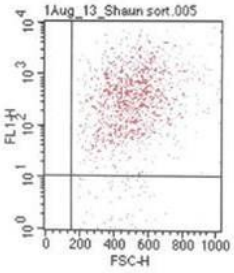

Quadrant Statistics

File: 1Aug_13_Shaun sort.005
Sample ID: sorted 614
Gate: G1

Quad	% Gated
UL	0.00
UR	95.58
LL	0.00
LR	4.42

C

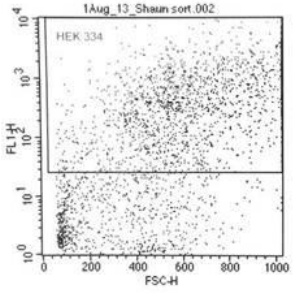

D

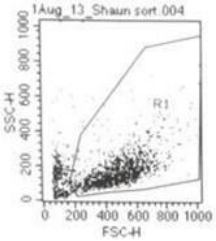

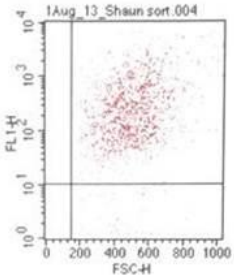

Quadrant Statistics

File: 1Aug_13_Shaun sort.004
Sample ID: sorted 334
Gate: G1

Quad	% Gated
UL	0.00
UR	96.06
LL	0.00
LR	3.94

Figure 3.14 Expression and Purification of GMCSF-Myosin fusion proteins for BALB/c and A/J mice

Figure 3.16 (A) shows the elution of GMCSF-Myo614 (20,355 kDa) at 100 mM and 250mM of imidazole while figure 3.16 (B) shows the elution of GMCSF-Myo334 (19,427 kDa) at 100mM and 250mM. The multiple bands of GMCSF-Myo334 are likely due to differences in post translation modification. The purity of each fusion protein preparation was estimated by comparing the intensity of contaminating bands to the intensity of the bands representing the fusion protein. Both preparations were assumed to be at least 90% pure.

A

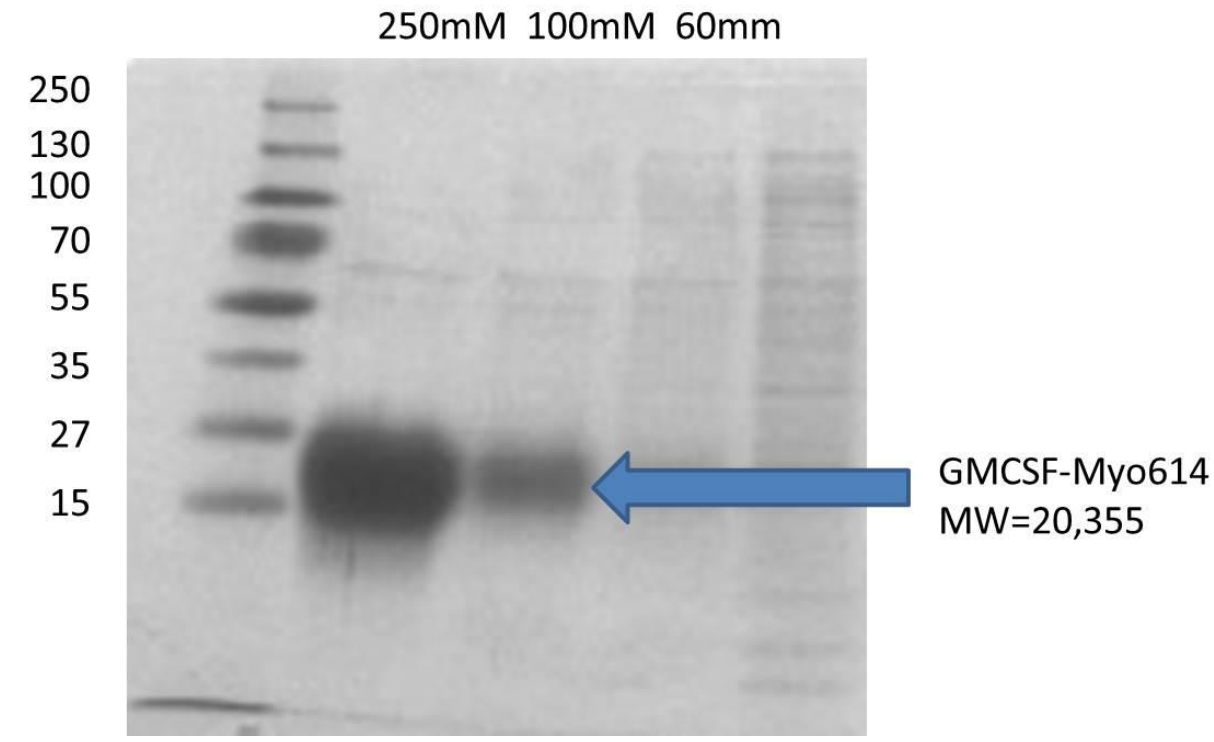
250mM 100mM 60mm
250
130
100
70
55
35
27
15
GMCSF-Myo614
MW=20,355

B

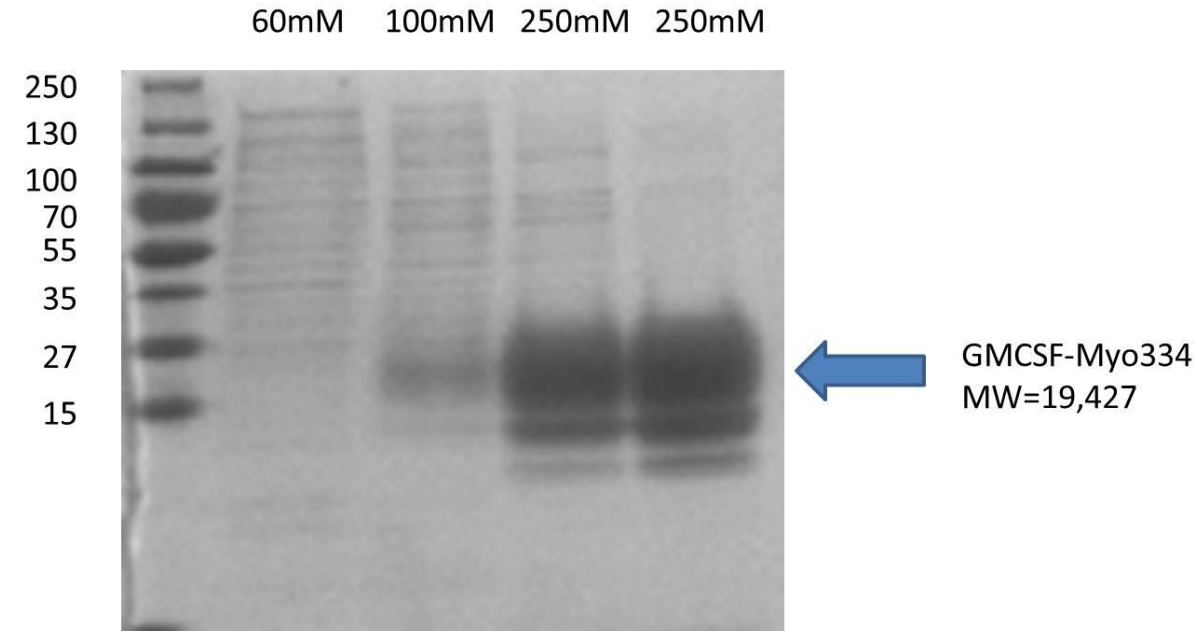
60mM 100mM 250mM 250mM
250
130
100
70
55
35
27
15
GMCSF-Myo334
MW=19,427

Figure 3.15 Validation of GMCSF-Myosin fusion proteins for BALB/c and A/J mice

Bioactivity of the cytokine domains of GMCSF-Myo614 and GMCSF-Myo334 were verified by culturing bone marrow cells with increasing concentrations of fusion protein or unconjugated GM-CSF. Bone marrow cells were cultured with GMCSF-Myo614, GMCSF-Myo334 or GM-CSF in full log dilutions from one femptomolar to one nanomolar. All concentrations were present in triplicate to assess variability. On day 2 all cells were pulsed with [3H]thymidine and on day 3 all cells were harvested for [3H]thymidine counts. Both fusion proteins as well as unconjugated GM-CSF induced a rapid increase in bone marrow proliferation from one picomolar to one nanomolar.

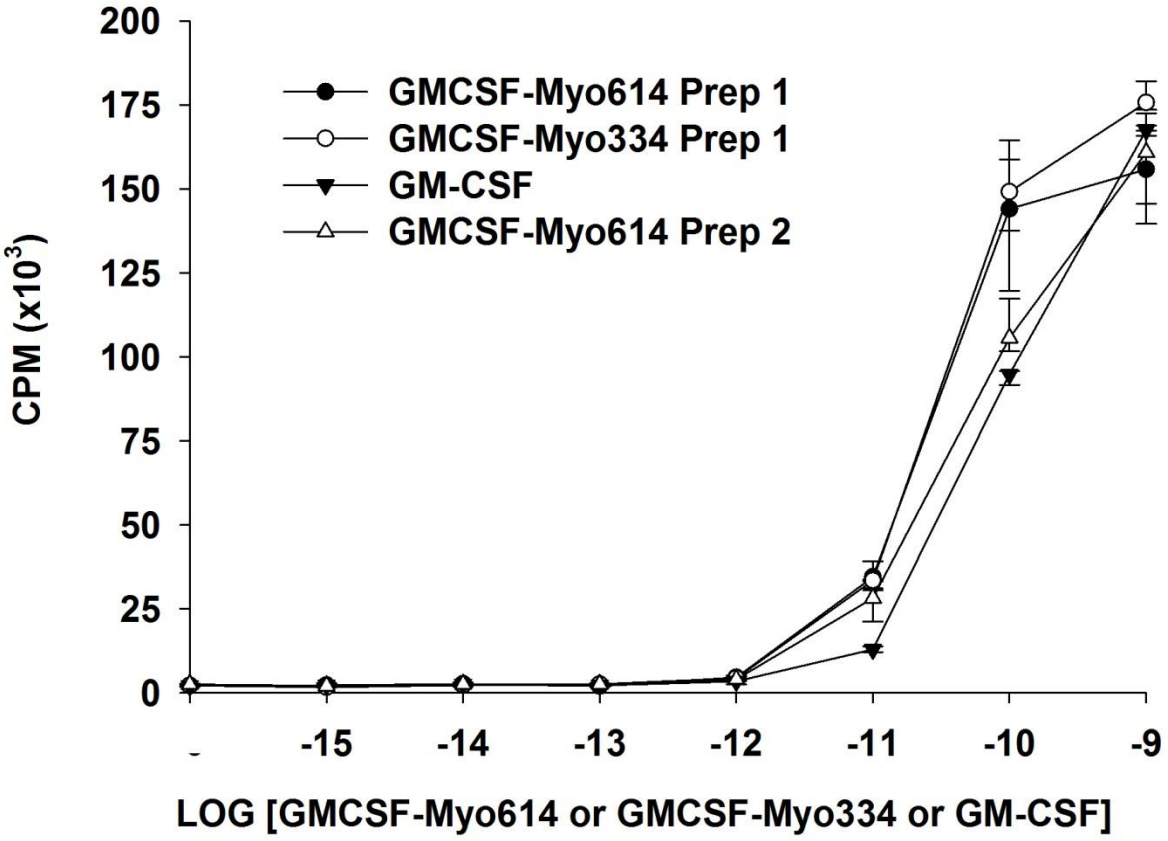
200
175
150
125
100
75
50
25
0
CPM (x10^3)
GMCSF-Myo614 Prep 1
GMCSF-Myo334 Prep 1
GM-CSF
GMCSF-Myo614 Prep 2
-15
-14
-13
-12
-11
-10
-9
LOG [GMCSF-Myo614 or GMCSF-Myo334 or GM-CSF]

3.4 Testing the Efficacy of GMCSF-Myo614 in the BALB/c model of EAM

Pretreatment and treatment experiments with GMCSF-Myo614 were conducted to explore the hypothesis that GMCSF-Myo614 could alter the myosin 614 $CD4^+$ T cell repertoire and prevent or inhibit EAM in BALB/c mice. In figure 3.16 two pretreatment experiments have been combined into one graph. Mice received either saline, myosin 614-629 or GMCSF-Myo614 on days -21, -14, and -7 prior to active EAM induction on day 0. The data in figure 3.18 demonstrate mice receiving GMCSF-Myo614 prior to EAM induction with myosin 614-629 are well protected against myocardial inflammation. A one way ANOVA analysis with a Bonferroni post hoc test revealed statistical significant differences between the fusion protein group and either control group. To further assess the ability of GMCSF-Myo614 to inhibit EAM, a treatment experiment was conducted and is shown in figure 3.17. Mice were subjected to active EAM induction on day 0 with myosin 614-629. Mice were assigned to one of four treatment groups receiving either saline, myosin 614-629, GMCSF-Myo334 or GMCSF-Myo614 on days 10, 12, 14 and 16. On day 28 all mice were euthanized and their hearts were collected for histological analysis as previously described. Statistical significance was not reached when comparing the severity of inflammation in the GMCSF-Myo614 group to the control groups. The pretreatment experiments demonstrate GMCSF-Myo614 has the ability to inhibit myosin 614 induced EAM in BALB/c mice. Table 3.18 shows summary statistics for all GMCSF-Myosin experiments in Lewis rats and BALB/c mice.

Figure 3.16 Pretreatment with GMCSF-Myo614 in the BALB/c model of EAM

BALB/c mice were given either PBS, 2 nanomoles of Myosin 614-629, or 2 nanomoles of GMCSF-Myo614 on days -21, -14 and -7 prior to EAM induction on day 0 and day 7 with CFA + Myosin 614-629. All animals were euthanized on day 21 to collect hearts for histological analysis with H&E staining. Animals pretreated with PBS, Myosin, or GMCSF- Myo614 had average histology scores of 2.0, 3.0, and 0.17 respectively. Pretreatment with GMCSF-Myo614 significantly blocked or attenuated myocardial infiltration when EAM was induced with Myosin 614-629.

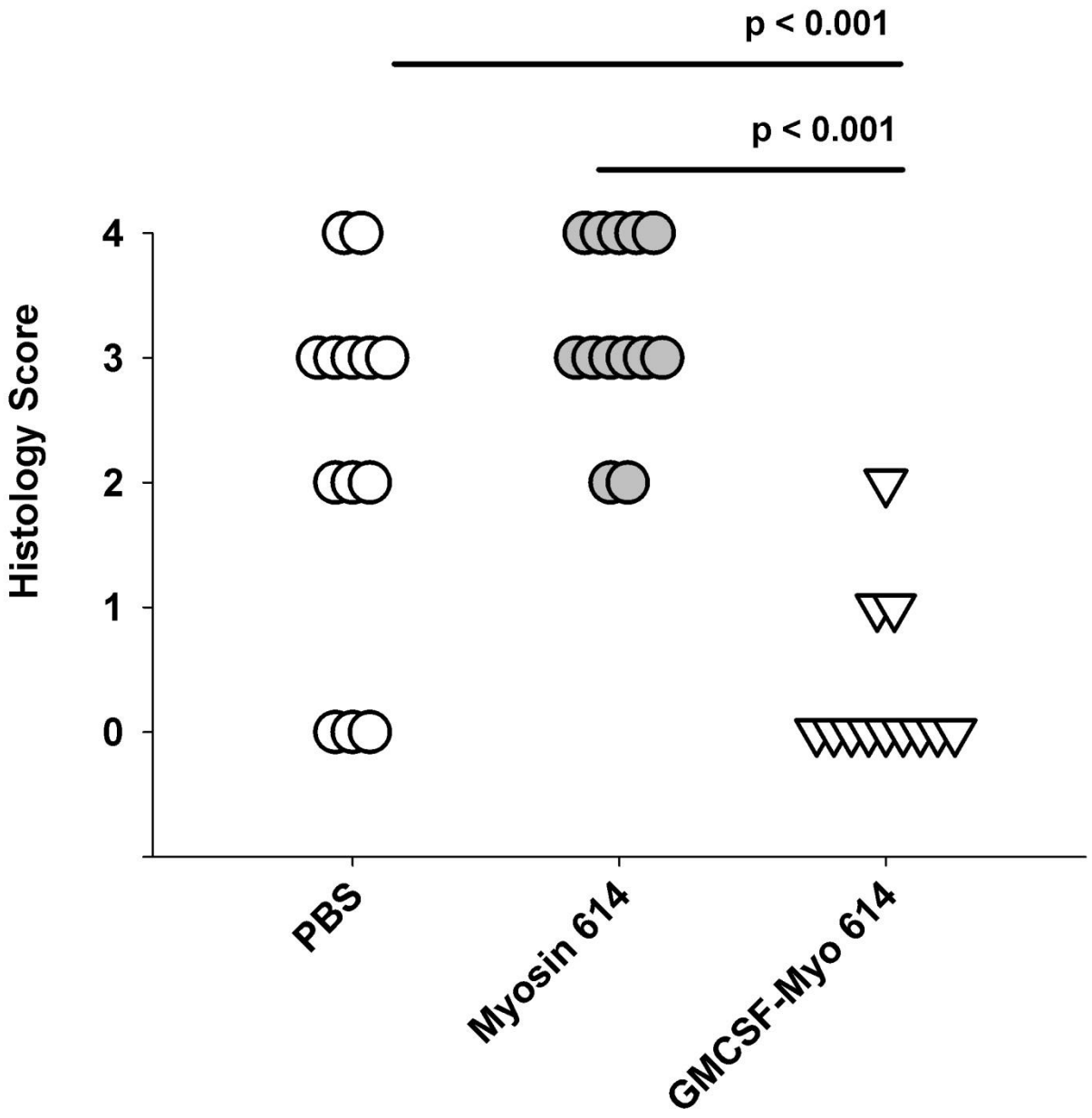
p < 0.001
p < 0.001
Histology Score
4
3
2
1
0
PBS
Myosin 614
GMCSF-Myo 614

Figure 3.17 GMCSF-Myo614 treatment after EAM induction

Previous experiments showed that GMCSF-Myo614 and GMCSF-Myo1052 inhibited EAM when given as a pretreatment before EAM induction. The current experiment was conducted to evaluate the efficacy of GMCSF-Myo614 when given after EAM induction. All animals received myosin 614-629 emulsified in CFA on days 0 and 7. On days 10, 12, 14, and 16 animals received either saline, myosin 614-629, GMCSF-Myo334 or GMCSF-Myo614 according to their respective group assignments. Upon euthanasia all hearts were placed in zinc fix. The hearts were paraffin embedded, stained with H&E, and scored for infiltration as previously described. The level of myocardial infiltration in the GMCSF-Myo614 treatment group was not statistically different compared to the level of myocardial infiltration in the control groups.

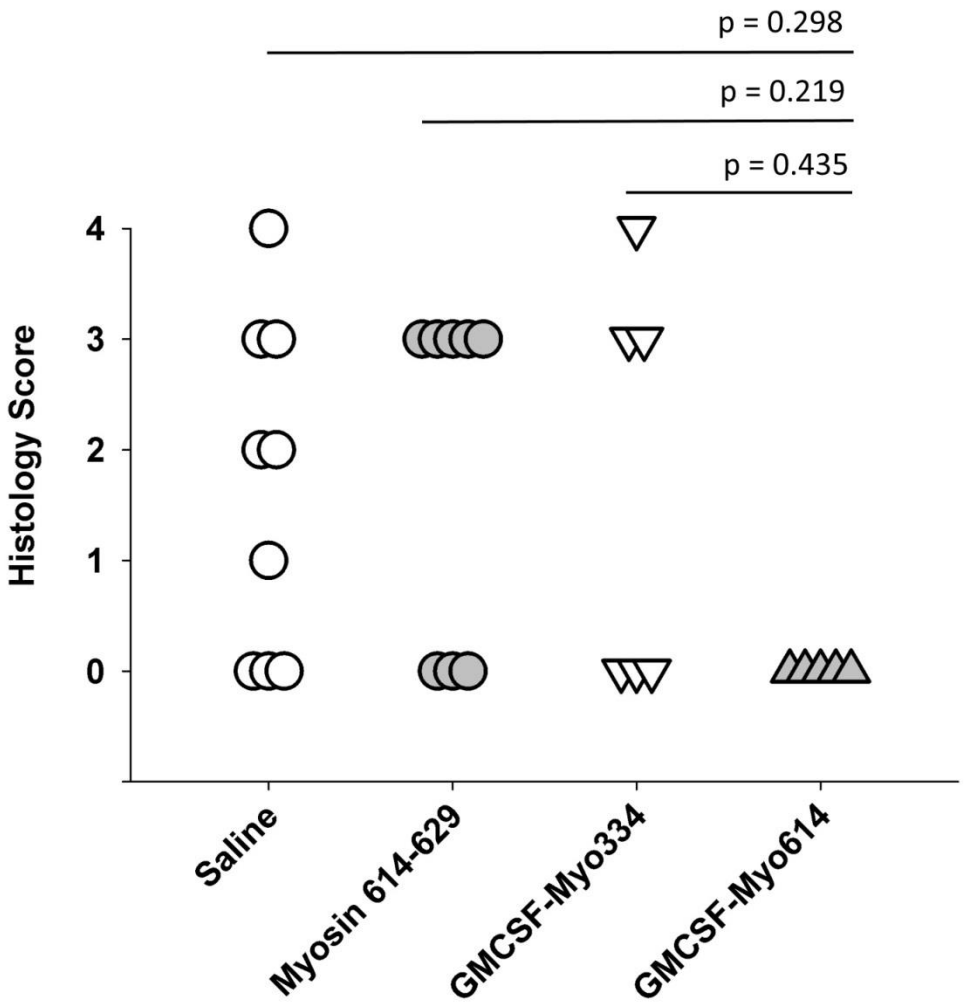
p = 0.298
p = 0.219
p = 0.435
Histology Score
4
3
2
1
0
Saline
Myosin 614-629
GMCSF-Myo334
GMCSF-Myo614

Table 3.18 Summary of GMCF-Myosin fusion protein inhibition of EAM in mice and rats

Treatment type	Group	Incidence of EAM	Mean histology score	Median histology score	Standard Deviation of histology score
Pretreatment	Saline	14 of 15	2.00	2.00	1.22
	Myosin 1052-1076	13 of 16	1.56	1.00	1.41
	GMCSF-Myo1052	7 of 15	0.60	0.00	0.83
Pretreatment	Saline	10 of 13	2.23	3.00	1.42
	Myosin 614-629	13 of 13	3.23	3.00	0.75
	GMCSF-Myo614	3 of 12	0.33	0.00	0.65
Treatment	Saline	6 of 9	1.67	2.00	1.50
	Myosin 614-629	5 of 8	1.88	3.00	1.55
	GMCSF-Myo334	3 of 6	1.67	1.50	1.86
	GMCSF-Myo614	0 of 5	0.00	0.00	0.00

3.5 EAM on the C57BL/6 Background

Current EAM studies in mice are not conducted in the C57BL/6 strain. Acute myocarditis can be induced in C67BL/6 mice with coxsackie virus, however this model does not appear to be a self-sustaining autoimmune version of myocarditis. Due to the majority of knockout mice being maintained on the C57BL/6 background, EAM studies exploring genetic mechanisms using knockout mice are time consuming and expensive. Normally the knockout of choice on the C57BL/6 background must be back crossed to an EAM susceptible background such as BALB/c or A/J mice. In an effort to discover a myosin peptide capable of inducing EAM in C57BL/6 mice, the cardiac alpha myosin heavy chain was queried against the H2-I-A^b haplotype, the murine MHC II equivalent allele found in C57BL/6 mice. The search produced a cluster of hits ranging from 718 to 737 in figure 3.19. Two candidate peptides were chosen, myosin 718-736 and myosin 721-735. Previous EAM experiments in BALB/c mice and previous EAE experiments in C57BL/6 mice have shown Interferon gamma knockout mice or Interferon gamma receptor knockout mice develop a much more severe form of their respective autoimmune diseases [61, 62]. Enhanced autoimmune disease has also been found in C57BL/6 which are void of B cells [63].

Because the C57BL/6 background is notoriously difficult to induce EAM, *Ifngr1* $^{-/-}$ mice and B cell deficient mice were included with wildtype mice for the first attempt to induce EAM with the new myosin candidates. Myosin 718-736 was emulsified in CFA and injected on day 0 and day 7. On day 0 the mice were also injected with pertussis toxin IP. On day 21 all animals were euthanized to collect hearts. Upon opening the chest, the hearts of the *Ifngr1* $^{-/-}$ mice displayed severe lesions over the entire heart. The lesions appeared to be similar to those

sometimes seen in the Lewis rat model of EAM. In figure 3.20 (A) and (B), histological analysis with H&E staining confirmed 9 of 11 *Ifngr1* $^{-/-}$ mice had severe level 4 (>25%) infiltration. C57BL/6 wild type mice in figure 3.20 (A) and B cell deficient mice in (B) were mostly resistant to EAM with myosin 718-736. Representative H&E images and echocardiography from *Ifngr1* $^{-/-}$ mice and wildtype C57BL/6 mice, immunized with myosin 718-736, are shown in figure 3.21. In figure 3.21 (B) greater than 75% of cross section of the heart is infiltrated with leukocytes. In figure 3.21 (D), the edema is so severe the lumen of the left ventricle has been significantly reduced which would affect cardiac output. Unaffected hearts from C57BL/6 wildtype mice are shown in figure 3.22 with histology (A) and echocardiography (C).

The second myosin peptide candidate, myosin 721-735 was tested using male and female *Ifngr1* $^{-/-}$ mice, B cell deficient mice, and C57BL/6 wild type mice. In figure 3.22 both B cell deficient mice and C57BL/6 wildtype mice are resistant to myosin 721-735 induced EAM. Severe disease was observed in the two male *Ifngr1* $^{-/-}$ mice, while little to no infiltration was found in the female *Ifngr1* $^{-/-}$ mice. Splenocyte activation data in figure 3.23 supports the hypothesis that myosin 718-736 is more potent for inducing EAM compared to myosin 721-735. In figure 3.23 splenocytes were collected from two *Ifngr1* $^{-/-}$ mice primed with CFA+ myosin 718-736. These splenocytes were subsequently activated in vitro with myosin 718-736 and myosin 721-735 as well as two additional control peptides. The data show myosin 721-735 cannot activate the full repertoire of T cells created from the myosin 718-736 priming compared to myosin 718-736.

An experiment was conducted to ascertain if Myosin 718-736 could induce EAM in mice deficient in inducible nitric oxide synthase 2 (*iNOS2* $^{-/-}$). Previous EAE experiments in C57BL/6 mice have indicated IFN-γ mediated nitric oxide is a critical signaling responsible for apoptotic

control of antigen specific activated T cells [64]. The working hypothesis was with inducible nitric oxide eliminated myosin specific T cells would experience less apoptosis and may survive long enough to cause EAM in C57BL/6 mice. The data in figure 3.24 indicate nitric oxide from inducible nitric oxide synthase 2 is not by itself responsible for the inhibition of myosin 718-736 induced EAM in C57BL/6 mice.

Figure 3.19 Selecting candidate peptides from the cardiac myosin heavy chain to induce EAM on the C57BL/6 background.

The alpha cardiac myosin heavy chain was selected to search for peptide epitopes capable of inducing EAM in mice on the C57BL/6 background. The website: http://tools.immuneepitope.org/mhcii/ was chosen. The murine alpha cardiac myosin heavy chain protein sequence was obtained from PubMed accession number: AAA37162. The algorithm selected a number of overlapping predicted sequences from the alpha cardiac myosin heavy chain predicted to have high affinity for the H2-I-A^b MHC II allele. The lower the percentile rank the more likely a peptide sequence is predicted to be displayed by the selected haplotype. Myosin 718-736 and myosin 721-735 were chosen as candidate peptides to induce EAM in mice on the C57BL/6 background.

Allele	#	Start	End	Peptide	Method used	Percentile rank
H2-IAb	1	720	734	FRQRYRILNPAAIPE	Consensus (smm/nn)	1.77
H2-IAb	1	721	735	RQRYRILNPAAIPEG	Consensus (smm/nn)	1.83
H2-IAb	1	719	733	DFRQRYRILNPAAIP	Consensus (smm/nn)	1.83
H2-IAb	1	718	732	GDFRQRYRILNPAAI	Consensus (smm/nn)	2.14
H2-IAb	1	722	736	QRYRILNPAAIPEGQ	Consensus (smm/nn)	2.15
H2-IAb	1	418	432	VQQVYYSIGALAKSV	Consensus (smm/nn)	3.06
H2-IAb	1	419	433	QQVYYSIGALAKSVY	Consensus (smm/nn)	3.24
H2-IAb	1	420	434	QVYYSIGALAKSVYE	Consensus (smm/nn)	3.50
H2-IAb	1	189	203	KRVIQYFASIAAIGD	Consensus (smm/nn)	4.16
H2-IAb	1	723	737	RYRILNPAAIPEGQF	Consensus (smm/nn)	4.32
H2-IAb	1	188	202	TKRVIQYFASIAAIG	Consensus (smm/nn)	4.36
H2-IAb	1	434	448	EKMFNWMVTRINATL	Consensus (smm/nn)	4.47

Figure 3.20 EAM in on the C57BL/6 background using Myosin 718-736

Two CFA + myosin 718-736 injections on days 0 and 7 resulted in severe EAM in *Ifngr1* $^{-/-}$ mice (A) and (B). Most *Ifngr1* $^{-/-}$ mice developed severe myocarditis with multiple lesions present on the outside of the heart and greater 50% infiltration in H&E cross sections. C57BL/6 wildtype mice (A) and B cell deficient mice (B) were generally resistant to myosin 718-736 induced EAM. In (B), groups labeled without 718 received emulsions containing saline and CFA without myosin 718-736. While groups labeled *Ifngr1*$^{-/-}$ and *Ighm*$^{-/-}$ received emulsions with myosin 718-736.

A

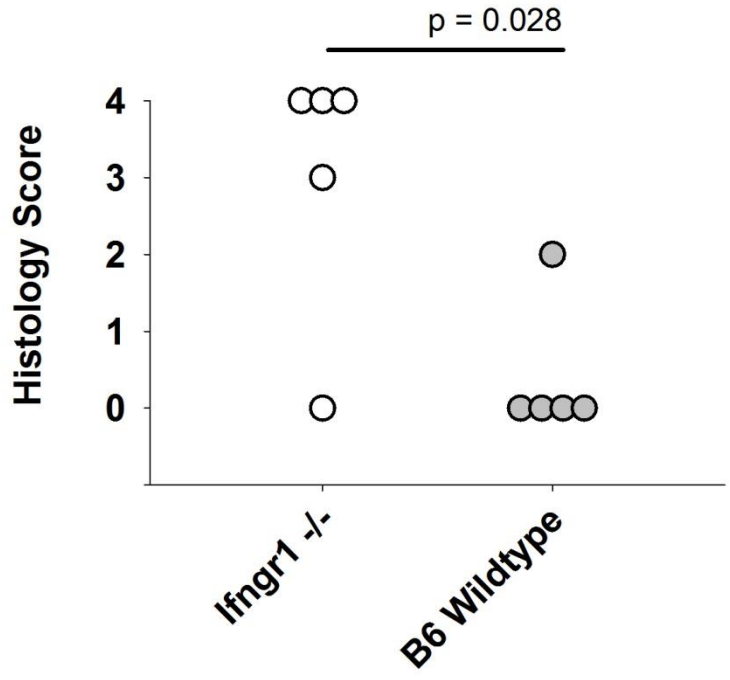
p = 0.028
Histology Score
4
3
2
1
0
Ifngr1 -/-
B6 Wildtype

B

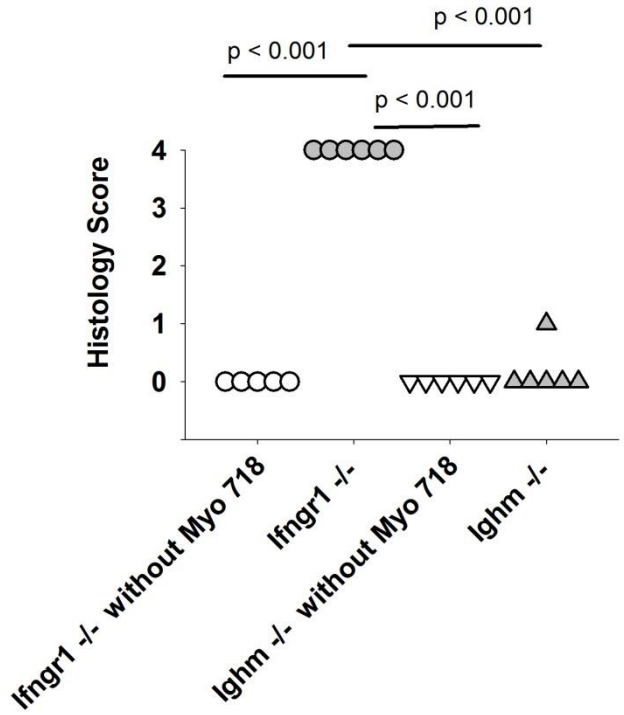
p < 0.001
p < 0.001
p < 0.001
Histology Score
4
3
2
1
0
Ifngr1 -/- without Myo 718
Ifngr1 -/-
Ighm -/- without Myo 718
Ighm -/-

Figure 3.21 Histology and echocardiography of EAM in *Ifngr1* $^{-/-}$ mice using myosin 718-736

H&E stained hearts from a wildtype C57BL/6 mouse (A) and an *Ifngr1* $^{-/-}$ mouse (B) after EAM induction with myosin 718-736. In (C) and (D) normal hearts and EAM affected hearts with severe edema respectively are shown using the parasternal long axis view with M mode during echocardiography. One would expect decreased cardiac output due to edema reducing the size of the left ventricular lumen. Indeed some *Ifngr1* $^{-/-}$ mice with severe EAM experienced increased recovery times following isoflurance induced anathesia during echocardiography.

A **B**

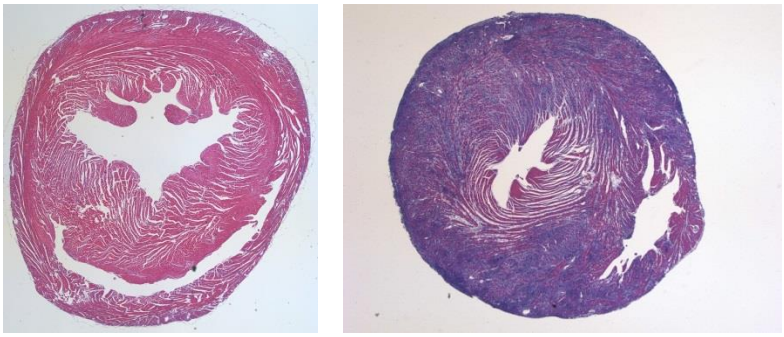

C **D**

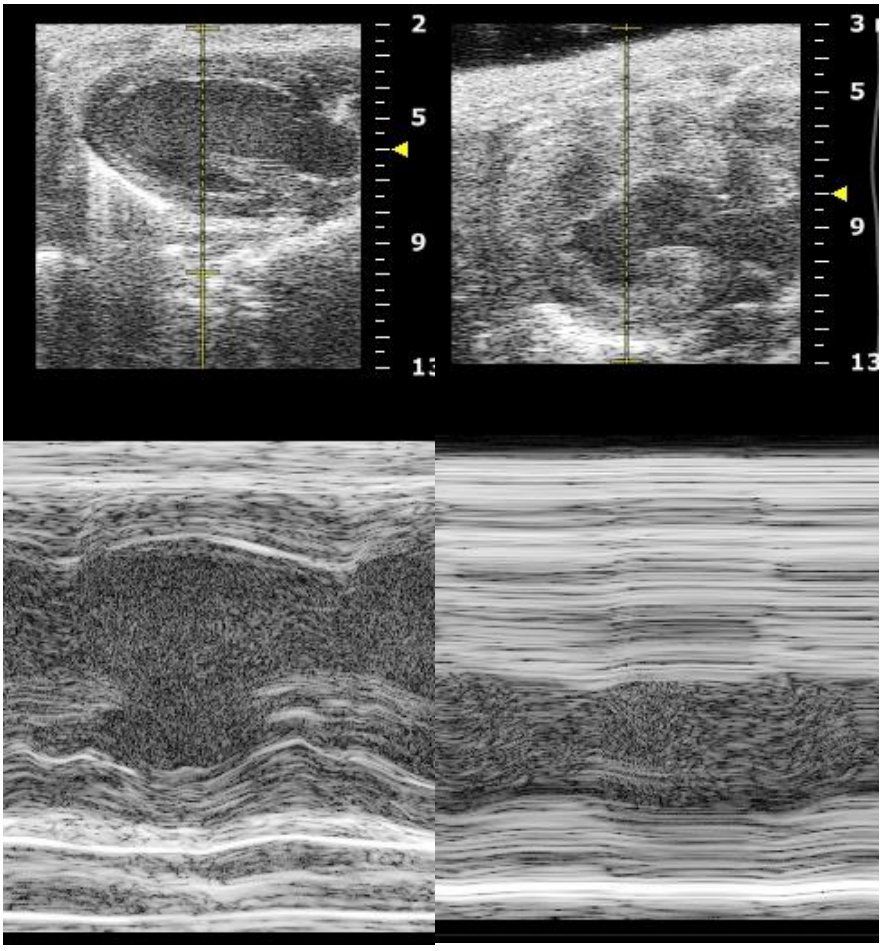

Figure 3.22 EAM using myosin 721-735

EAM induction using the shorter peptide candidate was also conducted on the C57BL/6 background using wildtype mice, *Ifngr1* $^{-/-}$ mice and *Ighm* $^{-/-}$ mice. The mice were injected with 200 µg of myosin 721-735 emulsifed in 50 µl of CFA and 50 µl of saline on days 0 and 7. The mice were also IP injected with pertussis toxin on day 0. All mice were euthanized on day 21 and hearts were placed in zinc fix for one week prior to paraffin embedding. Slides were stained with H&E and myocardtis was assessed on a scale of 0 to 4 as previously described. Wildtype and B cell knockout mice were resistant to myosin 721-735 induced EAM. *Ifngr1* $^{-/-}$ male mice developed full EAM to myosin 721-735 while female *Ifngr1* $^{-/-}$ mice displayed little to no inflammation.

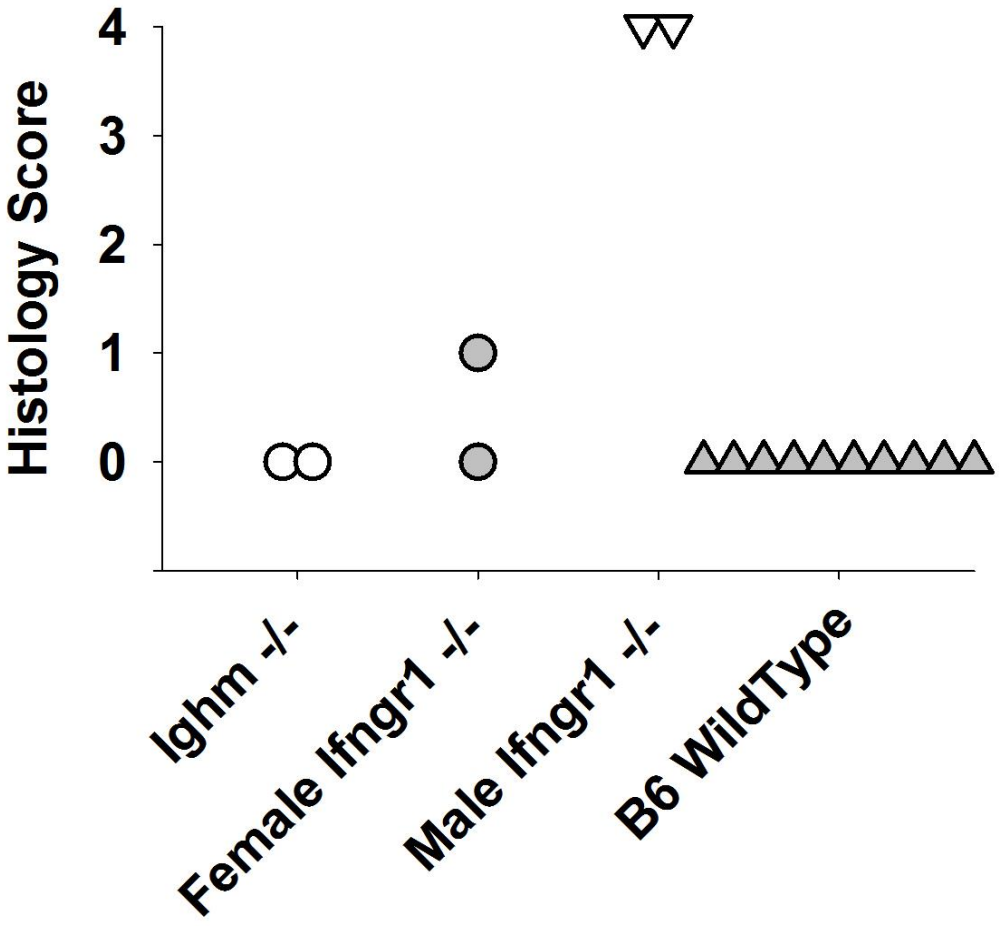
Histology Score
4
3
2
1
0
Ighm -/-
Female Ifngr1 -/-
Male Ifngr1 -/-
B6 WildType

Figure 3.23 Activation of splenocytes from animals primed with Myosin 718-736

Two female *Ifngr1* $^{-/-}$ mice were each injected with 200 µg of myosin 718-736 emulsified in 0.05 ml of saline and 0.05 ml of CFA on days 0 and 7. On day 14 the mice were euthanized and their spleens were harvested. The spleens were processed into a single cell suspension. Approximately 250,000 splenocytes were cultured in each well of a 96 well plate with various myosin peptides known to cause EAM in BALB/c mice, C57BL/6 mice and Lewis rats. Each concentration of each peptide was cultured in triplicate. The cells were pulsed with [3H]thymidine and harvested to assess T cell activation. The results show significant T cell activation in the presence of myosin 718-736 as expected. Myosin 721-735 displayed reduced T cell activation while the remaining control peptides, myosin 614-629 and myosin 1052-1076, induced no cell growth greater than background. The splenocyte activation data is consistent with reduced EAM from myosin 721-735 versus myosin 718-736.

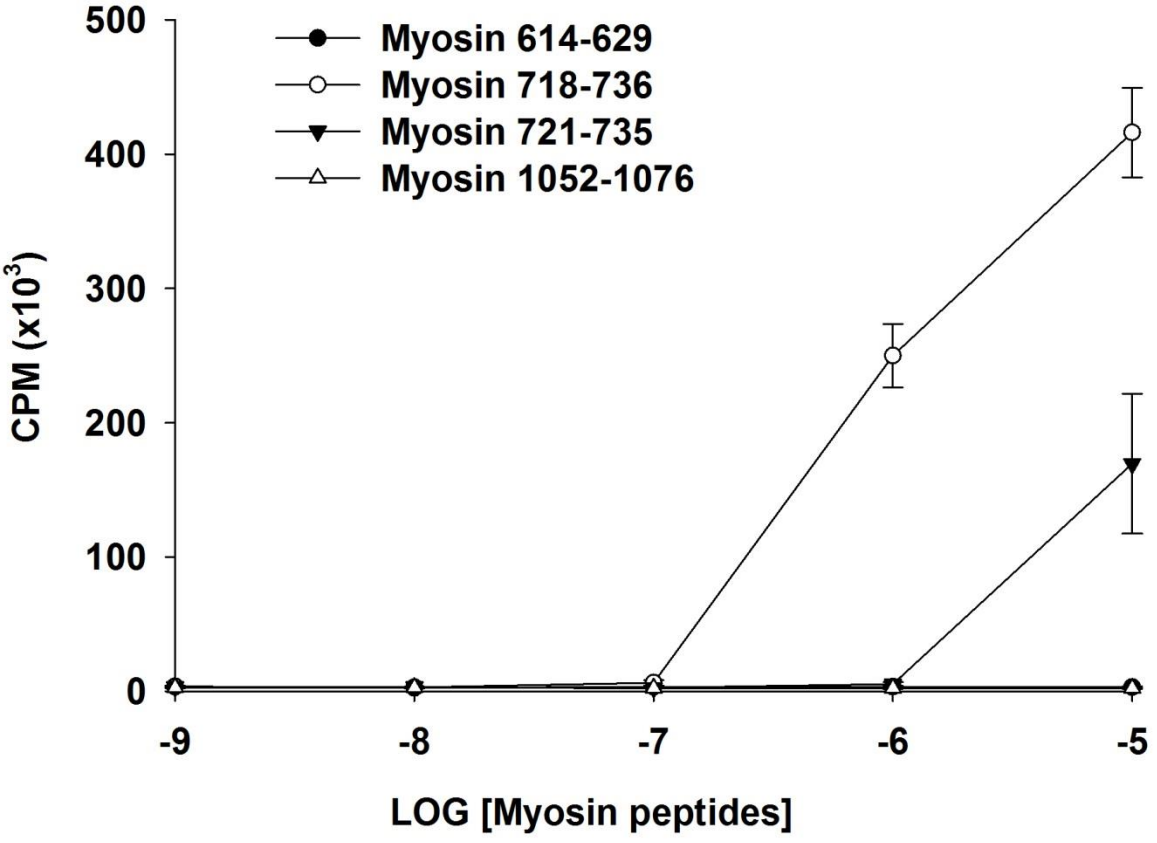
Myosin 614-629
Myosin 718-736
Myosin 721-735
Myosin 1052-1076
CPM (x10^3)
500
400
300
200
100
0
-9
-8
-7
-6
-5
LOG [Myosin peptides]

Figure 3.24 Exploring nitric oxide inhibition of EAM in C57BL/6 mice

Three *Ifngr1* $^{-/-}$ mice and four *iNOS2*$^{-/-}$ mice were injected with 200 µg of myosin 718-736 emulsified in 0.05 ml of saline and 0.05 ml of CFA on days 0 and 7. On day 21 all mice were euthanized to collect hearts for histological analysis. All hearts were zinc fixed, paraffin embedded, stained with H&E and scored from 0 to 4 as previously described. The positive control *Ifngr1* $^{-/-}$ mice displayed severe EAM while the *iNOS2*$^{-/-}$ mice had no myocardial infiltration. This experiment suggests nitric oxide by itself is not sufficient to inhibit antigen specific T cells and prevent EAM in C57BL/6 mice.

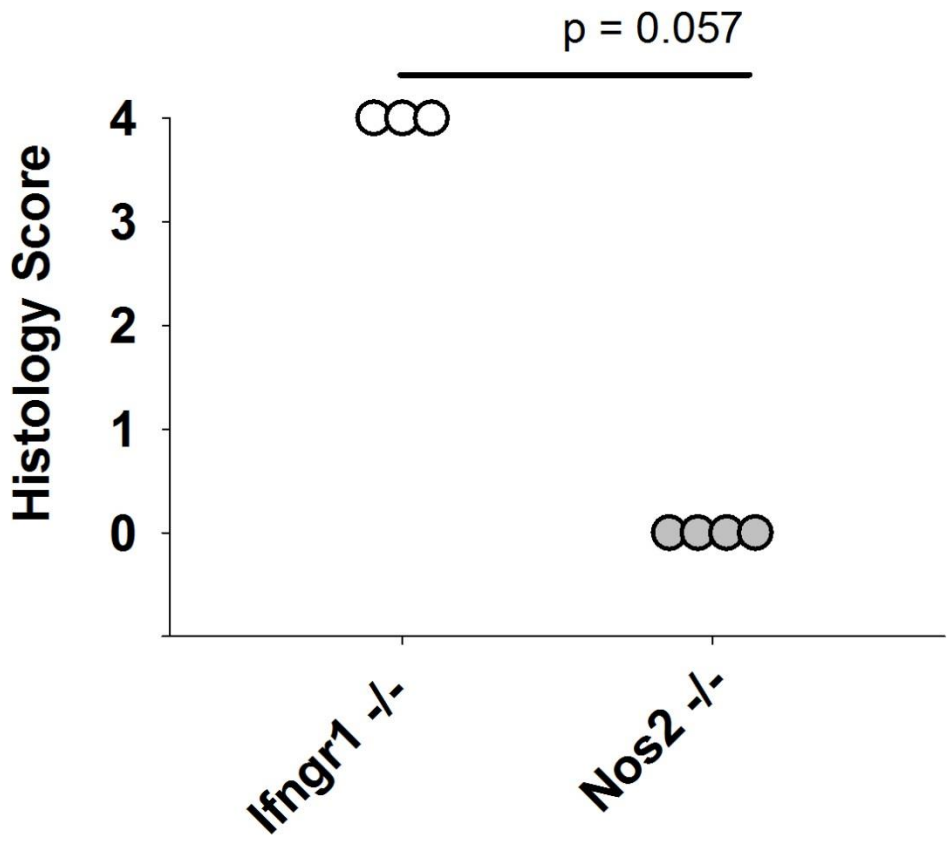
p = 0.057
Histology Score
4
3
2
1
0
Ifngr1 -/-
Nos2 -/-

Discussion

4.1 Significance of GMCSF-Myosin proteins

The primary purpose for creating GMCSF-Myosin fusion proteins was to assess their tolerogenic activity in the Lewis rat and BALB/c models of EAM. Previous studies have shown cytokine antigen fusion proteins using GM-CSF, Interferon-β, Interleukin (IL)-2, or IL-16 fused to a myelin autoantigen were capable of blocking progression of EAE [54-56, 58, 59]. GM-CSF based fusion proteins were found to be the most potent for inhibiting EAE compared to Interferon-β, Interleukin (IL)-2, or IL-16. It was therefore hypothesized GMCSF-Myosin based fusion proteins could achieve the significant tolerogenic activity in rodent models of EAM. The current study demonstrates for the first time that GM-CSF fused to a myocarditic antigen from the cardiac myosin heavy chain is capable of preventing myocarditis in the Lewis rat and BALB/c models of EAM, and provides evidence that GM-CSF fusion proteins can prevent autoimmune diseases other than EAE.

Several significant differences in EAE and EAM provide different challenges for tolerogenic vaccines. Previous GM-CSF fusion proteins have provided tolerance in rodent models of EAE to myelin basic protein, myelin oligodendrocyte glycoprotein, and proteolipid protein, all of which are proteins nervous system. The cardiac myosin heavy chain, in contrast, is contractile protein inside the membrane of cardiac muscle cells. Therefore, GMCSF-Myosin fusion proteins are the first GM-CSF fusion proteins in which the antigen domain is derived from a cardiac protein. Previous GMCSF-antigen fusion proteins have inhibited EAE, where significant inflammation occurs behind the blood brain barrier in the central nervous system. GMCSF-Myo1052 and GMCSF-614 are the first known fusion proteins to inhibit autoimmune

disease with a target organ in the periphery, not inside the blood brain barrier. Previous GMCSF-antigen fusion proteins have been used in mice on the C57BL/6 and SJL backgrounds due to their mainstream use in EAE models. Mice on the BALB/c and A/J background are the primary choice for EAM research, and GMCSF-Myo614 is first GMCSF-antigen fusion protein known to inhibit autoimmune disease in BALB/c mice.

Mechanistically GMCSF-Myosin fusion proteins appear to be targeting APCs through the cytokine domain. Figure 3.3 shows significantly higher proliferation of myosin 1052-1076 T cells from GMCSF-Myo1052 at lower concentrations compared to free peptide. This indicates the cytokine portion of the fusion protein is enhancing uptake through receptor mediated binding with subsequent presentation of the antigen domain. Choosing an appropriate peptide from the protein of interest is also crucial for successful tolerance. GMCSF-Myo334 is similar to GMCSF-Myo614 with exception of the antigen domain. Both fusion proteins have two n-linked glycosylation sites. In figure 3.14 (B) GMCSF-Myo334 has three distinct bands while in figure 3.14 (A) GMCSF-Myo614 has only one band. A possible explanation is that HEK cells producing GMCSF-Myo334 were overwhelmed with the amount of fusion protein being translated and could not glycosylate all the fusion protein before excretion. Like myosin 614-629, myosin 334-352 is derived from the alpha cardiac myosin heavy chain. However while myosin 334-352 can be presented in mice with the H2-I-A^a class II allele, such as A/J mice, myosin 334-352 cannot be presented in mice with the H2-I-A^d allele such as BALB/c mice. BALB/c mice possess the H2-I-A^d haplotype and can present myosin 614-629 but not myosin 334-352. Higher disease incidence in BALB/c mice pretreated with GMCSF-Myo334 compared to pretreatment with GMCSF-Myo614 indicates the antigen domain of the fusion

protein must not only be derived from the appropriate target organ but must also be presented on MHC II of the recipient. Reduced disease incidence in mice treated with GMCSF-Myo614 versus GMCSF-Myo334 also indicates antibodies against GM-CSF are not a likely mechanism for tolerance. If anti-GMCSF antibodies were responsible for the tolerance from GMCSF-Myosin one would expect similar results from GMCSF-Myo614 and GMCSF-Myo334.

It would be interesting to perform a longitudinal study with GMCSF-Myo1052 in Lewis rats given the chronic disease observed in figure 3.6. Historically EAM in the Lewis rats is referred to as a relatively acute model, with disease peaking at day 21 and a gradual decline thereafter. However, figure 3.6 clearly demonstrates some percentage of Lewis rats are capable of sustained myocardial inflammation at day 50 during EAM. Whether the decrease in disease severity at day 28 is indicative of relapsing disease or just reflects the small number of animals is a valid question.

4.2 GMCSF-ANTIGEN FUSION PROTEINS AND T CELL MEDIATED AUTOIMMUNE DISEASE

It is highly likely GMCSF-Myosin fusion proteins are providing tolerance against EAM by altering cardiac myosin specific $CD4^+$ T cells. Studies have demonstrated disease in both the Lewis rat and the BALB/c model of EAM are dependent on $CD4^+$ T cells for disease. In both the BALB/c and Lewis Rat models of EAM $CD4^+$ T cells that recognize the myosin 614-629 and myosin 1052-1076 epitopes respectively, have been shown capable and sufficient to induce EAM through adoptive transfer experiments. Previous adoptive transfer experiments have demonstrated myosin 1052-1076 specific $CD4^+$ T cells and myosin 614-629 specific $CD4^+$ T cells are sufficient for inducing autoimmune myocarditis in their respective models. Any successful inhibition of EAM in the BALB/c and Lewis rat models of EAM would logically have to inhibit these myosin specific $CD4^+$ T cells. Figure 3.3 demonstrates GMCSF-Myo1052 is capable of stimulating myosin specific T cells in the presence of antigen and irradiated APCs. Moreover, antibody inhibited proliferation of myosin 1052-1076 T specific cells through anti-MHC II or anti-CD4 in figure 3.4 provide evidence that GMCSF-Myo1052 is altering the $CD4^+$ T cell repertoire. The partial inhibition of myosin 1052-1076 T cells with anti CD4 is consistent with previous experiments demonstrating CD4 stabilizes and enhances the MHC II/peptide T cell receptor binding, but is not absolutely required for MHC II antigen presentation. The complete blockage of MHC II antigen presentation in the presence of anti MHC II indicates the antibody is directly preventing the T cell receptor of myosin 1052-1076 T cells from engaging with APCs. Figure 3.3 demonstrates GMCSF-Myo1052 has stimulatory effects *in vitro* on myosin specific $CD4^+$ T cells that are likely Th1 memory cells. However its effects *in vivo* appear to be

inhibitory as seen in pretreatment experiments in figures 3.7 and 3.16. This paradox might be explained by differences in APCs present in the subcutaneous compartment versus APCs derived from the spleen and maintained in culture. The OX6 and W3/25 antibody inhibition experiments suggest MHC II presentation is fundamental mechanism of GMCSF-Myo1052 whether it is providing stimulatory or inhibitory effects.

4.3 GMCSF-MYOSIN FUSION PROTEINS: TOLERANCE VERSUS IMMUNITY

Evidence for pro-inflammatory effects mediated by GMCSF-Myosin

GM-CSF is a key cytokine involved in the differentiation and maturation of myeloid leukocytes including macrophages and dendritic cells [65, 66]. Multiple studies in EAE and EAM indicate a pro-inflammatory role for GM-CSF in EAE and EAM. In the Lewis rat model of EAM, GM-CSF mRNA levels in heart lesions have been found to be elevated on days 14, 21, 28, 35, and 42 post EAM induction and correlated with disease severity [67]. GM-CSF $^{-/-}$ mice have been shown to be resistant to EAE and EAM induction [68, 69]. Moreover adoptive transfer experiments using GM-CSF$^{-/-}$ donor mice have demonstrated antigen specific CD4^{+} T cells to be the source of GM-CSF required for EAE and EAM [69-71].

In EAE and EAM, GM-CSF produced by antigen specific T cells has been shown to have a profound effect on antigen presenting cells, including dendritic cells and macrophages. GM-CSF produced by encephalitogenic T cells has been shown to increase cell surface expression of MHC II, CD80, and CD40 on microglial cells [71]. Furthermore EAE was restored in mice with GM-CSF $^{-/-}$ T cells by injecting LPS directly into the CNS, indicating GM-CSF plays a critical role in EAE by activating APCs [71]. Other data has shown GM-CSF dependent CD103+ dermal dendritic cells can induce severe EAE and stimulate naïve T cells to produce IFN-γ and IL-17 [72]. Given that IFN-γ and IL-17 have been notably increased in both models of EAE and EAM it is likely both Th subsets are contributing to disease.

It is conceivable that GMCSF-antigen fusion proteins are activating APCs which then increase IFN-γ to concentrations high enough for self-regulating effects. Several studies indicate that IFN-γ can mediate apoptosis of CD4+ T cells [62, 73, 74]. In EAE specifically it has been observed that IFN-γ mediated production of indoleamine 2,3 dioxygenase (IDO) by DCs lead to T cell apoptosis and suppression of disease [75, 76]. It also possible IDO produced by activated APCs can inhibit EAE by increasing regulatory T cells [77]. Another study found IFN-γ plays a critical role in the induction of T regulatory cells that limit EAE [78]. Other data suggests the Th1:Th17 ratio may play a role in number of neutrophils in the CNS during EAE and effect disease severity [74]. The studies above indicate numerous possible pathways for IFN-γ to regulate or inhibit EAE. Exacerbated disease observed in IFN-$\gamma^{-/-}$ mice in both EAE and EAM further indicate a regulatory role for IFN-γ [61, 79-82]. As GM-CSF activated APCs can produce IL-12 which then drive production of IFN-γ, it is possible GMCSF-antigen fusion proteins are accelerating this pathway and providing tolerance indirectly via IFN-γ.

Published data investigating the mechanisms of GMCSF-NAg fusion proteins support an IFN-γ mediated pro-inflammatory hypothesis. GMCSF-MOG_{35-55} has been shown to inhibit EAE when delivered adjacent to CFA-MOG_{35-55} emulsions and when added directly to CFA-MOG_{35-55} emulsions [50]. Furthermore it has been demonstrated *in vitro* that GMCSF-MOG_{35-55} can differentiate and expand inflammatory dendritic cells, which when stimulated with IFN-γ can inhibit MOG specific T cells through the secretion of nitric oxide [50]. It is therefore possible the inhibition of EAM observed in Figure 3.17, when GMCSF-Myo614 was administered after disease induction, was due in part to GMCSF-Myo614 derived inflammatory dendritic cells responding to IFN-γ by the secretion of nitric oxide thereby inhibiting myosin 614-629 specific T cells and preventing EAM.

Evidence for tolerance mediated by GMCSF-Myosin

Dendritic cells are considered professional antigen presenting cells due to their native ability to present antigens via MHC II. However, the context in which these antigens are presented can have a profound effect on how the immune system responds to the presented antigen in question. Dendritic cells in an immature state express low levels of MHC II and costimulatory molecules such CD80/86 [83]. Antigen presentation without co-stimulation by immature DCs can result in T cell anergy [84]. Studies have also shown semi-mature DCs can also support tolerance by increasing expression of MHC II, CD 80/86, and tolerogenic cytokines such IL-10 but not pro-inflammatory cytokines such IL-12 and IL-6 [83, 85]. In a non-inflammatory environment, GM-CSF and cytokines such as TGF-beta will result in immature and semi-mature DCs that favor tolerance.

Abundant evidence supports the concept that semi-mature DCs provide tolerance by increasing antigen specific $CD4^+$ $Foxp3^+$ T regulatory cells. $CD4^+$ $Foxp3^+$ T cells have been extensively studied and found capable of suppressing or inhibiting effector T cells through inhibitory cytokines, cytolysis, metabolic disruption, and by fostering tolerogenic phenotypes in APCs [86]. Multiple studies in models of experimental autoimmune thyroiditis, experimental autoimmune myasthenia gravis, and experimental type 1 diabetes have demonstrated treatment with GM-CSF before and after disease induction suppresses disease via semi-mature DCs that increase antigen specific IL-10 secreting T regulatory cells [87-92]. Experiments by Prabhakar et al. have specifically demonstrated dendritic cells of non-splenic origin ($CD11c^+$ $CD8^-$) are the subset of GM-CSF derived DCs responsible for tolerance [92, 93]. It has also been shown, that dendritic cells derived from bone marrow cells using GM-CSF are capable of expanding natural T regulatory cells and adaptive T regulatory cells *in vitro* by T cell receptor independent and T

cell receptor dependent mechanisms respectively [94]. Previous experiments, in which GM-CSF was injected *in vivo,* indicated tolerogenic DCs were providing efficacy by expanding antigen specific T regulatory cells. To further confirm this theory, multiple experiments were conducted in which *in vitro* derived tolerogenic DCs were pulsed with antigen, relevant to the disease model, prior to *in vivo* administration [95-97]. Specifically in EAE, MOG_{35-55} pulsed dendritic cells were shown to inhibit EAE in C57BL/6 mice while DCs not pulsed provided no protection [98]. In EAM, DCs pulsed with myosin 614-629 were found to inhibit disease while DCs pulsed with type II collagen provided no protection [99]. Given the abundant evidence that semi-mature DCs can induce tolerance through antigen specific T regulatory cells, and that this mechanism has been confirmed in same models of EAE and EAM with exact same antigens used in GMCSF-MOG_{35-55} and GMCSF-Myo614, is not unreasonable to speculate that GMCSF-myosin antigen fusion proteins are mediating protection in part, by binding to monocytes inducing their differentiation into semi-mature DCs while also providing the appropriate antigen for MHC II presentation and subsequent expansion of antigen specific T regulatory cells.

Although regulatory T cells specific for the antigen domain of GMCSF-Myosin are powerful in their own right, it is plausible their suppression is greatly amplified by infectious tolerance. Numerous studies provide evidence that T regulatory cells are key players in the phenomenon of infectious tolerance [100]. At its most simple definition, infectious tolerance occurs when a regulatory T cell specific to antigen "A" confers a regulatory phenotype to a naïve or effector T cell specific for different antigen "B". In this regard infectious tolerance is powerful immune modulator that is thought to play a major role in preventing autoimmunity. One model of infectious tolerance involves a regulatory T cell acting directly on a naïve or effector T cell. This interaction may occur when both cells are bound to a common APC that is

not directly responsible. Evidence for this model comes from experiments where TGF-β derived from T regulatory cells was found to convert effector T cells into suppressive $Foxp3^+$ T cells [101]. IL-10 produced by T regulatory cells has been shown to convert effector T cells into suppressive T cells [102, 103]. It has also been shown that $Foxp3^+$ T regulatory cells can respond to IL-10 by making more IL-10 in positive feedback loop [104]. A third cytokine produced by T regulatory cells that could mediate infectious tolerance is IL-35 [105]. It has been shown that IL-35 from T regulatory cells can convert effector $CD4^+$ T cells into class of suppressive T cells that do not express Foxp3 yet can still mediate tolerance through IL-35 [105]. It is therefore possible that if GMCSF-Myosin fusion proteins are creating tolerogenic APCs that express multiple antigens from cardiac proteins, they would create an environment where regulatory T cells, could convert nearby effector T cells, on the same APC, to a suppressive phenotype through TGF-β, IL-10, or IL-35.

In addition to providing an environment that fosters proximity between T regulatory cells and effector cells, APCs such as dendritic cells may play an active role in creating T cells with suppressive function. $CD8^+$ splenic DCs are potent inducers of T regulatory cells when TFG-β is available [106]. IL-10 producing DCs generated *in vitro* with GM-CSF, IL-4 and IL-10 have also been found capable of converting effector T cells into IL-10 secreting suppressive T cells [107, 108]. It is therefore conceivable during the pretreatment experiments GMCSF-Myosin was upregulating $IL\text{-}10^+$ DCs expressing the myosin domain. If these GMCSF-Myosin induced $IL\text{-}10^+$ DCs also expressed other cardiac antigens from normal turn-over they could in theory convert effector cardiac autoreactive T cells into T regulatory cells. If IL-10 is being produced by GMCSF-Myosin induced DCs as well as T regulatory cells that respond to IL-10 in a feed

forward loop, it is possible reciprocal exchange of cytokines such IL-10 may serve to amplify infectious tolerance to prevent autoimmune myocarditis.

Variables that could determine tolerance or immunity from GMCSF-Myosin

Evidence for micro environmental effects of GM-CSF on DCs in EAM come from two key studies. One study demonstrated that bone marrow derived dendritic cells, created using GM-CSF, LPS, and anti CD40 are capable of inducing EAM when pulsed with myosin 614-629 and adoptive transferred into naïve BALB/c recipient mice [10]. A seemingly contradictory study found bone marrow derived dendritic cells cultured with TNF-alpha, IL-4 and pulsed with cardiac myosin are capable of preventing EAM in BALB/c mice [99]. The important note here is the way in which the dendritic cells were created. The pro-inflammatory experiment used GM-CSF, LPS, and anti CD40 to induce the dendritic cells into a fully mature state and acquire an inflammatory phenotype capable of supporting Th1 effector cells. The tolerogenic experiment used GM-CSF, TNF-alpha, and IL-4 to create dendritic cells with relatively lower levels of MHC II, CD80, CD86, IL-12p70, and IL-23. GM-CSF is common to both experiments but other growth factors included in the generation of the dendritic cells had a profound effect on the outcome. It is therefore possible the inhibition of EAM observed during fusion protein pretreatment and treatment are due to different mechanisms in which tolerogenic or inflammatory DCs respectively, are modulating the antigen specific T cell repertoire via different but not mutually exclusive mechanisms.

GM-CSF concentration is a factor that could affect the balance between inflammatory versus tolerogenic responses. Lower levels of GM-CSF favor immature tolerogenic DCs while higher concentrations promote inflammatory DCs [109]. In EAM specifically it has been

observed that using 1 millon tolerogenic DCs pulsed with myosin can provide tolerance while 2 million cells actually enhanced disease [99]. This suggests the concentration of GM-CSF in addition to other stimuli present can impact tolerance versus inflammation. It is possible the dose of GMCSF-Myosin used could have a significant effect on tolerance versus inflammation. However EAE experiments have demonstrated higher doses of GMCSF-neuroantigen fusion proteins provide more tolerance. It is therefore likely higher doses of GMCSF-Myosin will provide more tolerance and not lead to myocarditis.

4.4 THE IMPLICATIONS OF GMCSF-ANTIGEN FUSION PROTEINS FOR CLINICAL MYOCARDITIS

GMCSF-Myosin and HLA alleles

GMCSF-Myosin fusion proteins have demonstrated repeatable success in murine models of experimental autoimmune myocarditis. These experiments were possible because specific myocarditic epitopes are known in Lewis rats and BALB/c mice. For successful treatment of autoimmune myocarditis with GMCSF-antigen fusion proteins, specific major myocarditic epitopes will need to be identified in the human population. The epitopes will depend on the MHC II haplotype of each individual. Because the MHC II genes are some of the most polymorphic in our genome, identifying myocarditic epitopes will be a significant task.

Preliminary studies have identified certain MHC II haplotypes with possible associations to myocarditis or inflammatory idiopathic cardiomyopathy. A significant association was found between HLA DQB1*0303 and patients with myocarditis. Other studies have found associations between idiopathic dilated cardiomyopathy and the following HLA alleles: HLA-DR4, HLA-DR5, HLA-DQA1∗0501, and HLA-DQB1∗0303. These haplotypes could serve as starting points for identifying myocarditic epitopes in the human population. The algorithm used at http://tools.immuneepitope.org/mhcii/ maybe of some help given the extensive list of human MHC II haplotypes it supports. If future studies confirm elevated $CD4^+$ T cells that recognize cardiac antigens when presented by APCs with the afore mentioned alleles or other HLA-DP, HLA-DQ, or HLA-DR alleles in patients with chronic myocarditis, it would provide critical information for developing GMCSF-antigen fusion proteins for clinical applications.

Progress towards a GMCSF-Myosin fusion protein to prevent myocarditis and cardiomyopathy in type 1 diabetic patients may be underway. Many type 1 diabetic patients have the HLA-DQ8 allele, and experience excessive morbidity due cardiovascular disease and complications following a myocardial infarction. Evidence for an autoimmune etiology to this excessive morbidity comes from a murine animal model. Transgenic non-obese diabetic mice were altered with murine CD4 and H2 genes knocked out, and human CD4 and HLA-DQ8 inserted. It was soon discovered HLA-DQ8 mice spontaneously developed myocarditis and cardiomyopathy. Additional experiments revealed the myocarditis was lymphocyte mediated and not humoral dependent. When HLA-DQ8 was queried against the murine cardiac alpha myosin heavy chain on http://tools.immuneepitope.org/mhcii/, three unique regions were identified with high affinity for HLA-DQ8. One of these epitopes was myosin 334-352. Interestingly, this is a known myocarditic epitope capable of inducing autoimmune disease in A/J mice which possess the murine H2-I-A^a. The cytokine bioactivity of GMCSF-Myo334 has already been confirmed figure 3.15. In figure 3.17, GMCSF-Myo334 was included as a control and failed to provide protection against EAM in BALB/c as expected due to differences in H2 alleles between BALB/c and A/J mice. It remains to be seen if myosin 334-352 is truly a myocarditic epitope in NOD HLA-DQ8 mice, and if so could treatment with GMCSF-Myo334 prevent the spontaneous myocarditis associated with this strain.

The Need for antigen specific therapy to treat myocarditis

To date this is first known example of a therapeutic that can affect progression of experimental autoimmune myocarditis via inhibition of the immune system in an antigen specific manner without using *in vitro* derived cells. The only previous known therapeutic approach

capable of inhibiting EAM in an antigen specific manner utilized bone marrow derived dendritic cells pulsed with myosin 614-629 [99]. While this approach is promising, therapeutics using clinical administration of *in vitro* cultured cells are more expensive and more difficult to standardize compared to traditional drugs and biologics including fusion proteins. In addition, GMCSF-Myosin fusion proteins may be providing inhibition of EAM through inflammatory and tolerogenic mechanisms. To date antigen pulsed DCs appear to be providing inhibition of EAM exclusively through tolerogenic mechanisms.

GMCSF-Myosin fusion proteins represent a major step forward towards the development of antigen specific therapy for clinical use. All know previous therapeutics in a clinical setting do not treat myocarditis with antigen specific inhibition of the immune system. For some patients supportive therapies that manage cardiac load are enough for a recovery, however, other patients spiral into progressive cardiac inflammation that culminates in cardiomyopathy and heart failure. Multiple types of clinical myocarditis including giant cell myocarditis and eosinophilic myocarditis have especially grim prognoses but do respond to general autoimmune inhibitors such as prednisone [28, 36, 37]. The response to prednisone is promising, and suggests if more precise and effective immuno-modulatory therapeutics, such GMCSF-Myosin fusion proteins, were developed for clinical application they could have a major positive impact on treatment and survival rates. In addition, multiple clinical trials studying the effects of immunosuppression on myocarditis found increased HLA expression, anti-cardiac antibodies, and presence of T cells were the best indicators for a positive response to immune suppression therapy [27, 39, 40]. These studies highlight the need for a more effective treatment with therapeutics, such as GMCSF-Myosin fusion proteins, that can permanently eliminate or inhibit

cardiac auto-reactive $CD4^{+}$T cells. Permanent inhibition of auto-reactive cardiac specific $CD4^{+}$T cells would prevent future cardiac insults from reigniting these antigen specific lymphocytes that could once again start the process towards dilated cardiomyopathy and death.

4.5 EAM on the C57BL/6 background

Previous experiments using whole cardiac myosin emulsified in CFA have found wild type C57BL/6 to be resistant to EAM [49]. A bioinformatics approach was used to identify specific epitopes from the cardiac myosin heavy chain that may have affinity for H2-I-A^b using the website: http://tools.immuneepitope.org/mhcii/ [110, 111]. To confirm the accuracy of the algorithm the murine cardiac myosin heavy chain was tested against H2-I-A^d and myelin oligodendrocyte glycoprotein was tested against H2-I-A^b. These tests were conducted due to known peptide sequences, myosin 614-629 and MOG 35-55, that are capable of inducing EAM and EAE, respectively. The algorithm successfully identified the peptide sequences already known to cause EAM and EAE and therefore was used to predict a peptide antigen from the cardiac myosin heavy chain capable of causing EAM in C57BL/6 (H2-I-A^b) mice.

The algorithm predicted myosin 718-736, a peptide derived from the alpha cardiac myosin heavy chain, would have high affinity for mice expressing the H2-I-A^b allele. Using specific epitopes versus and an entire protein increases the likelihood of expanding $CD4^+$ T cells that recognize a particular antigen. The disadvantage of this approach is if the peptide included is not a major antigen, autoimmune disease is less likely compared to using a total protein. To further increase the chance of myosin 718-736 induced EAM in mice on the C57BL/6 background IFN-γ receptor deficient mice were selected. Enhanced EAE has been observed in IFN-$\gamma^{-/-}$ mice and B cell deficient mice on the C57BL/6 background [52, 53]. Additionally enhanced EAM has been observed in *Ifng* $^{-/-}$ or *Ifngr1* $^{-/-}$ mice on the BALB/c background [61, 79-81]. Therefore in addition to testing the theoretical EAM peptide (myosin 718-736) in wild

type C57BL/6 mice, *Ifngr1* $^{-/-}$ mice and B cell deficient mice were used to explore EAM on the C57BL/6 background.

It was found myosin 718-736 is a potent antigen capable of inducing severe myocarditis in mice on the C57BL/6 background. Figure 3.20 demonstrates Myosin 718-736 can induce EAM in both genders of *Ifngr1* $^{-/-}$ mice. Figure 3.22 shows myosin 721-735 can induce EAM in male but not female *Ifngr1* $^{-/-}$mice. The loss of pathogenicity between myosin 718-735 and myosin 721-735 is reflected in figure 3.23 where myosin 721-735 is only able to activate a subset of Myosin 718-736 T cells from primed splenocytes compared to myosin 718-736. It is possible multiple epitopes are presented from a single peptide due to different anchor residues making contact with the variable regions of the MHC II pocket. Having a shorter peptide such as myosin 721-735 could possible reduce the number of anchor residues. Another theory for the loss of pathogenicity between the two peptides could relate to inefficient loading on MHC II due to the shorter length.

In an effort to explore the mechanisms responsible for EAM in *Ifngr1* $^{-/-}$ mice, a study was conducted with *iNOS2* $^{-/-}$ mice. Previous experiments have suggested IFN-γ dependent nitric oxide is responsible for increased apoptosis of activated antigen specific T cells in experimental autoimmune disease in C57BL/6 mice [80]. However other studies have shown inhibition of nitric oxide in BALB/c mice did not reproduce the severe EAM observed in IFN-γ deficient mice on this strain [82]. In figure 3.24, *iNOS2*$^{-/-}$ mice on the C57BL/6 background failed to develop EAM when challenged with myosin 718-736. It is therefore likely the severe EAM in *Ifngr1* $^{-/-}$ mice on the C57BL/6 background is not solely due to nitric oxide. Future experiments are need to confirm the exact signaling molecules downstream from IFN-γ, responsible for regulating apoptosis of myosin 718-736 specific T cells and thus controlling EAM in C57BL/6 mice.

Although EAM was shown to be possible in only one previously resistant H2 haplotype, it does raise the question of the incidence of auto reactive T cells in the human population. In C57BL/6 mice auto reactive T cells that recognize epitopes derived from cardiac myosin do exists in the periphery. The major reason for C57BL/6 wild type EAM resistance is probably due to antigen specific T regulatory cells and other unknown variables. Previous research has indicated cardiac myosin maybe weakly expressed in the thymus where elimination of self-reactive T cells occurs [14]. More research is needed to conclusively state cardiac myosin is indeed weakly expressed in the thymus. However if cardiac antigens are under expressed in the human thymus, a significant portion of the population may possess cardiac auto reactive T cells. These individuals may be more susceptible to developing autoimmune myocarditis in the future.

4.6 Conclusion

New therapies are urgently needed to treat autoimmune myocarditis and prevent progression to dilated cardiomyopathy and heart failure. Current therapies for managing autoimmune myocarditis are limited to global immunosuppressive treatment and supportive medication for cardiac output. Certain types of myocarditis including giant cell myocarditis and eosinophilic myocarditis have especially grim prognoses. Multiple factors are likely responsible for developing clinical autoimmune myocarditis. However cardiac auto reactive $CD4^+$ T cells are likely a major contributing factor to autoimmune myocarditis. Future treatments which can selectively manage the cardiac specific leukocytes are desperately needed for these patients. GMCSF-Myosin fusion proteins show promise as platform for drug development to selectively manage cardiac specific T cells. If GMCSF-Myosin fusion proteins are found to operate through T regulatory cells capable of infectious tolerance, they have the potential to provide immunological memory over multiple cardiac epitopes. While hurdles such as epitope identification and mechanism verification must be overcome for human application, GMCSF-antigen fusion proteins provide a novel exciting platform for autoimmune disease therapeutic development.

References

1. Passarino, G., et al., *Prevalence of myocarditis at autopsy in Turin, Italy.* Arch Pathol Lab Med, 1997. **121**(6): p. 619-22.
2. Rose, N.R., *Myocarditis: infection versus autoimmunity.* J Clin Immunol, 2009. **29**(6): p. 730-7.
3. Bowles, N.E., et al., *Detection of viruses in myocardial tissues by polymerase chain reaction. evidence of adenovirus as a common cause of myocarditis in children and adults.* J Am Coll Cardiol, 2003. **42**(3): p. 466-72.
4. Dale, J.B. and E.H. Beachey, *Epitopes of streptococcal M proteins shared with cardiac myosin.* J Exp Med, 1985. **162**(2): p. 583-91.
5. Hotez, P.J., et al., *An unfolding tragedy of Chagas disease in North America.* PLoS Negl Trop Dis, 2013. **7**(10): p. e2300.
6. Ferrari, I., et al., *Molecular mimicry between the immunodominant ribosomal protein P0 of Trypanosoma cruzi and a functional epitope on the human beta 1-adrenergic receptor.* J Exp Med, 1995. **182**(1): p. 59-65.
7. Abel, L.C., J. Kalil, and E. Cunha Neto, *Molecular mimicry between cardiac myosin and Trypanosoma cruzi antigen B13: identification of a B13-driven human T cell clone that recognizes cardiac myosin.* Braz J Med Biol Res, 1997. **30**(11): p. 1305-8.
8. Li, Y., et al., *Cryptic epitope identified in rat and human cardiac myosin S2 region induces myocarditis in the Lewis rat.* J Immunol, 2004. **172**(5): p. 3225-34.
9. Pummerer, C.L., et al., *Identification of cardiac myosin peptides capable of inducing autoimmune myocarditis in BALB/c mice.* J Clin Invest, 1996. **97**(9): p. 2057-62.
10. Eriksson, U., et al., *Dendritic cell-induced autoimmune heart failure requires cooperation between adaptive and innate immunity.* Nat Med, 2003. **9**(12): p. 1484-90.
11. Cooper, L.T., Jr., *Giant cell myocarditis: diagnosis and treatment.* Herz, 2000. **25**(3): p. 291-8.

12. Starr, T.K., S.C. Jameson, and K.A. Hogquist, *Positive and negative selection of T cells.* Annu Rev Immunol, 2003. **21**: p. 139-76.

13. Kim, J., et al., *Cutting edge: depletion of Foxp3+ cells leads to induction of autoimmunity by specific ablation of regulatory T cells in genetically targeted mice.* J Immunol, 2009. **183**(12): p. 7631-4.

14. Lv, H., et al., *Impaired thymic tolerance to alpha-myosin directs autoimmunity to the heart in mice and humans.* J Clin Invest, 2011. **121**(4): p. 1561-73.

15. Liu, W., W.M. Li, and N.L. Sun, *HLA-DQA1, -DQB1 polymorphism and genetic susceptibility to idiopathic dilated cardiomyopathy in Hans of northern China.* Ann Hum Genet, 2005. **69**(Pt 4): p. 382-8.

16. Portig, I., et al., *HLA-DQB1* polymorphism and associations with dilated cardiomyopathy, inflammatory dilated cardiomyopathy and myocarditis.* Autoimmunity, 2009. **42**(1): p. 33-40.

17. Jin, B., et al., *A meta-analysis of HLA-DR polymorphism and genetic susceptibility to idiopathic dilated cardiomyopathy.* Mol Biol Rep, 2012. **39**(1): p. 221-6.

18. Frangogiannis, N.G., C.W. Smith, and M.L. Entman, *The inflammatory response in myocardial infarction.* Cardiovasc Res, 2002. **53**(1): p. 31-47.

19. Yan, X., et al., *Temporal dynamics of cardiac immune cell accumulation following acute myocardial infarction.* J Mol Cell Cardiol, 2013. **62**: p. 24-35.

20. Maisel, A., et al., *Experimental autoimmune myocarditis produced by adoptive transfer of splenocytes after myocardial infarction.* Circ Res, 1998. **82**(4): p. 458-63.

21. Elliott, J.F., et al., *Autoimmune cardiomyopathy and heart block develop spontaneously in HLA-DQ8 transgenic IAbeta knockout NOD mice.* Proc Natl Acad Sci U S A, 2003. **100**(23): p. 13447-52.

22. Taylor, J.A., et al., *A spontaneous model for autoimmune myocarditis using the human MHC molecule HLA-DQ8.* J Immunol, 2004. **172**(4): p. 2651-8.

23. Orchard, T.J., et al., *Type 1 diabetes and coronary artery disease.* Diabetes Care, 2006. **29**(11): p. 2528-38.

24. van Lummel, M., et al., *Type 1 diabetes-associated HLA-DQ8 transdimer accommodates a unique peptide repertoire.* J Biol Chem, 2012. **287**(12): p. 9514-24.

25. Gottumukkala, R.V., et al., *Myocardial infarction triggers chronic cardiac autoimmunity in type 1 diabetes.* Sci Transl Med, 2012. **4**(138): p. 138ra80.

26. Feldman, A.M. and D. McNamara, *Myocarditis.* N Engl J Med, 2000. **343**(19): p. 1388-98.

27. Wojnicz, R., et al., *Randomized, placebo-controlled study for immunosuppressive treatment of inflammatory dilated cardiomyopathy: two-year follow-up results.* Circulation, 2001. **104**(1): p. 39-45.

28. Cooper, L.T., Jr., *Myocarditis.* N Engl J Med, 2009. **360**(15): p. 1526-38.

29. Shauer, A., et al., *Acute viral myocarditis: current concepts in diagnosis and treatment.* Isr Med Assoc J, 2013. **15**(3): p. 180-5.

30. Kuhl, U., et al., *High prevalence of viral genomes and multiple viral infections in the myocardium of adults with "idiopathic" left ventricular dysfunction.* Circulation, 2005. **111**(7): p. 887-93.

31. Why, H.J., et al., *Clinical and prognostic significance of detection of enteroviral RNA in the myocardium of patients with myocarditis or dilated cardiomyopathy*, in *Circulation*. 1994. p. 2582-9.

32. Pauschinger, M., et al., *Viral heart disease: molecular diagnosis, clinical prognosis, and treatment strategies.* Med Microbiol Immunol, 2004. **193**(2-3): p. 65-9.

33. Liu, P.P. and J.W. Mason, *Advances in the understanding of myocarditis.* Circulation, 2001. **104**(9): p. 1076-82.

34. Kuhl, U., *Antiviral treatment of myocarditis and acute dilated cardiomyopathy.* Heart Fail Clin, 2005. **1**(3): p. 467-74.

35. Sherry, B., *The role of interferon regulatory factors in the cardiac response to viral infection.* Viral Immunol, 2002. **15**(1): p. 17-28.

36. Kandolin, R., et al., *Diagnosis, treatment, and outcome of giant-cell myocarditis in the era of combined immunosuppression.* Circ Heart Fail, 2013. **6**(1): p. 15-22.

37. Cooper, L.T., Jr. and C. ElAmm, *Giant cell myocarditis. Diagnosis and treatment.* Herz, 2012. **37**(6): p. 632-6.

38. Mason, J.W., et al., *A clinical trial of immunosuppressive therapy for myocarditis. The Myocarditis Treatment Trial Investigators.* N Engl J Med, 1995. **333**(5): p. 269-75.

39. Frustaci, A., M.A. Russo, and C. Chimenti, *Randomized study on the efficacy of immunosuppressive therapy in patients with virus-negative inflammatory cardiomyopathy: the TIMIC study.* Eur Heart J, 2009. **30**(16): p. 1995-2002.

40. Frustaci, A., et al., *Immunosuppressive therapy for active lymphocytic myocarditis: virological and immunologic profile of responders versus nonresponders.* Circulation, 2003. **107**(6): p. 857-63.

41. Towbin, J.A., et al., *Incidence, causes, and outcomes of dilated cardiomyopathy in children.* JAMA, 2006. **296**(15): p. 1867-76.

42. Caforio, A.L., et al., *Circulating cardiac autoantibodies in dilated cardiomyopathy and myocarditis: pathogenetic and clinical significance.* Eur J Heart Fail, 2002. **4**(4): p. 411-7.

43. Wallukat, G., et al., *Autoantibodies against the beta-adrenergic receptor in human myocarditis and dilated cardiomyopathy: beta-adrenergic agonism without desensitization.* Eur Heart J, 1991. 12 Suppl D: p. 178-81.

44. Zhang, P., et al., *Cutting edge: cardiac myosin activates innate immune responses through TLRs.* J Immunol, 2009. **183**(1): p. 27-31.

45. Li, Y., et al., *Mimicry and antibody-mediated cell signaling in autoimmune myocarditis.* J Immunol, 2006. **177**(11): p. 8234-40.

46. Li, Y., et al., *Protection against experimental autoimmune myocarditis is mediated by interleukin-10-producing T cells that are controlled by dendritic cells.* Am J Pathol, 2005. **167**(1): p. 5-15.

47. Donermeyer, D.L., et al., *Myocarditis-inducing epitope of myosin binds constitutively and stably to I-Ak on antigen-presenting cells in the heart.* J Exp Med, 1995. **182**(5): p. 1291-300.

48. Cihakova, D. and N.R. Rose, *Pathogenesis of myocarditis and dilated cardiomyopathy.* Adv Immunol, 2008. **99**: p. 95-114.

49. Neu, N., et al., *Cardiac myosin induces myocarditis in genetically predisposed mice.* J Immunol, 1987. **139**(11): p. 3630-6.

50. Islam, S.M., et al., *GM-CSF-neuroantigen fusion proteins reverse experimental autoimmune encephalomyelitis and mediate tolerogenic activity in adjuvant-primed environments: association with inflammation-dependent, inhibitory antigen presentation.* J Immunol, 2014. **193**(5): p. 2317-29.

51. Curtis, A.D., 2nd, et al., *The extracellular domain of myelin oligodendrocyte glycoprotein elicits atypical experimental autoimmune encephalomyelitis in rat and Macaque species.* PLoS One, 2014. **9**(10): p. e110048.

52. Mannie, M.D. and A.D. Curtis, 2nd, *Tolerogenic vaccines for Multiple sclerosis.* Hum Vaccin Immunother, 2013. **9**(5): p. 1032-1038.

53. Mannie, M.D., et al., *Cytokine-neuroantigen fusion proteins as a new class of tolerogenic, therapeutic vaccines for treatment of inflammatory demyelinating disease in rodent models of multiple sclerosis.* Front Immunol, 2012. **3**: p. 255.

54. Abbott, D.J., et al., *Neuroantigen-specific, tolerogenic vaccines: GM-CSF is a fusion partner that facilitates tolerance rather than immunity to dominant self-epitopes of myelin in murine models of experimental autoimmune encephalomyelitis (EAE).* BMC Immunol, 2011. **12**: p. 72.

55. Blanchfield, J.L. and M.D. Mannie, *A GMCSF-neuroantigen fusion protein is a potent tolerogen in experimental autoimmune encephalomyelitis (EAE) that is associated with efficient targeting of neuroantigen to APC.* J Leukoc Biol, 2010. **87**(3): p. 509-21.

56. Mannie, M.D., D.J. Abbott, and J.L. Blanchfield, *Experimental autoimmune encephalomyelitis in Lewis rats: IFN-beta acts as a tolerogenic adjuvant for induction of neuroantigen-dependent tolerance.* J Immunol, 2009. **182**(9): p. 5331-41.

57. Mannie, M.D., et al., *Cytokine-neuroantigen fusion proteins: new tools for modulation of myelin basic protein (MBP)-specific T cell responses in experimental autoimmune encephalomyelitis.* J Immunol Methods, 2007. **319**(1-2): p. 118-32.

58. Mannie, M.D., et al., *IL-2/neuroantigen fusion proteins as antigen-specific tolerogens in experimental autoimmune encephalomyelitis (EAE): correlation of T cell-mediated antigen presentation and tolerance induction.* J Immunol, 2007. **178**(5): p. 2835-43.

59. Mannie, M.D. and D.J. Abbott, *A fusion protein consisting of IL-16 and the encephalitogenic peptide of myelin basic protein constitutes an antigen-specific tolerogenic vaccine that inhibits experimental autoimmune encephalomyelitis.* J Immunol, 2007. **179**(3): p. 1458-65.

60. Mannie, M.D. and M.S. Norris, *MHC class-II-restricted antigen presentation by myelin basic protein-specific CD4+ T cells causes prolonged desensitization and outgrowth of CD4- responders.* Cell Immunol, 2001. **212**(1): p. 51-62.

61. Eriksson, U., et al., *Lethal autoimmune myocarditis in interferon-gamma receptor-deficient mice: enhanced disease severity by impaired inducible nitric oxide synthase induction.* Circulation, 2001. **103**(1): p. 18-21.

62. Furlan, R., et al., *Intrathecal delivery of IFN-gamma protects C57BL/6 mice from chronic-progressive experimental autoimmune encephalomyelitis by increasing apoptosis of central nervous system-infiltrating lymphocytes.* J Immunol, 2001. **167**(3): p. 1821-9.

63. Hjelmstrom, P., et al., *B-cell-deficient mice develop experimental allergic encephalomyelitis with demyelination after myelin oligodendrocyte glycoprotein sensitization.* J Immunol, 1998. **161**(9): p. 4480-3.

64. Dalton, D.K. and S. Wittmer, *Nitric-oxide-dependent and independent mechanisms of protection from CNS inflammation during Th1-mediated autoimmunity: evidence from EAE in iNOS KO mice.* J Neuroimmunol, 2005. **160**(1-2): p. 110-21.

65. Li, B.Z., et al., *GM-CSF alters dendritic cells in autoimmune diseases.* Autoimmunity, 2013. **46**(7): p. 409-18.

66. Shi, Y., et al., *Granulocyte-macrophage colony-stimulating factor (GM-CSF) and T-cell responses: what we do and don't know.* Cell Res, 2006. **16**(2): p. 126-33.

67. Kobayashi, Y., et al., *Levels of MCP-1 and GM-CSF mRNA correlated with inflammatory cytokines mRNA levels in experimental autoimmune myocarditis in rats.* Autoimmunity, 2002. **35**(2): p. 97-104.

68. McQualter, J.L., et al., *Granulocyte macrophage colony-stimulating factor: a new putative therapeutic target in multiple sclerosis.* J Exp Med, 2001. **194**(7): p. 873-82.

69. Sonderegger, I., et al., *GM-CSF mediates autoimmunity by enhancing IL-6-dependent Th17 cell development and survival.* J Exp Med, 2008. **205**(10): p. 2281-94.

70. Marusic, S., et al., *Local delivery of granulocyte macrophage colony-stimulating factor by retrovirally transduced antigen-specific T cells leads to severe, chronic experimental autoimmune encephalomyelitis in mice.* Neurosci Lett, 2002. **332**(3): p. 185-9.

71. Ponomarev, E.D., et al., *GM-CSF production by autoreactive T cells is required for the activation of microglial cells and the onset of experimental autoimmune encephalomyelitis.* J Immunol, 2007. **178**(1): p. 39-48.

72. King, I.L., M.A. Kroenke, and B.M. Segal, *GM-CSF-dependent, CD103+ dermal dendritic cells play a critical role in Th effector cell differentiation after subcutaneous immunization.* J Exp Med, 2010. **207**(5): p. 953-61.

73. Chin, Y.E., et al., *Activation of the STAT signaling pathway can cause expression of caspase 1 and apoptosis.* Mol Cell Biol, 1997. **17**(9): p. 5328-37.

74. Miller, N.M., et al., *Anti-inflammatory mechanisms of IFN-gamma studied in experimental autoimmune encephalomyelitis reveal neutrophils as a potential target in multiple sclerosis.* Front Neurosci, 2015. **9**: p. 287.

75. Sakurai, K., et al., *Effect of indoleamine 2,3-dioxygenase on induction of experimental autoimmune encephalomyelitis.* J Neuroimmunol, 2002. **129**(1-2): p. 186-96.

76. Kwidzinski, E., et al., *IDO (indolamine 2,3-dioxygenase) expression and function in the CNS.* Adv Exp Med Biol, 2003. **527**: p. 113-8.

77. Yan, Y., et al., *IDO upregulates regulatory T cells via tryptophan catabolite and suppresses encephalitogenic T cell responses in experimental autoimmune encephalomyelitis.* J Immunol, 2010. **185**(10): p. 5953-61.

78. Wang, Z., et al., *Role of IFN-gamma in induction of Foxp3 and conversion of CD4+ CD25- T cells to CD4+ Tregs.* J Clin Invest, 2006. **116**(9): p. 2434-41.

79. Afanasyeva, M., et al., *Interleukin-12 receptor/STAT4 signaling is required for the development of autoimmune myocarditis in mice by an interferon-gamma-independent pathway.* Circulation, 2001. **104**(25): p. 3145-51.

80. Chu, C.Q., S. Wittmer, and D.K. Dalton, *Failure to suppress the expansion of the activated CD4 T cell population in interferon gamma-deficient mice leads to exacerbation of experimental autoimmune encephalomyelitis.* J Exp Med, 2000. **192**(1): p. 123-8.

81. Eriksson, U., et al., *Dual role of the IL-12/IFN-gamma axis in the development of autoimmune myocarditis: induction by IL-12 and protection by IFN-gamma.* J Immunol, 2001. **167**(9): p. 5464-9.

82. Barin, J.G., et al., *Mechanisms of IFNgamma regulation of autoimmune myocarditis.* Exp Mol Pathol, 2010. **89**(2): p. 83-91.

83. Rutella, S., S. Danese, and G. Leone, *Tolerogenic dendritic cells: cytokine modulation comes of age.* Blood, 2006. **108**(5): p. 1435-40.

84. Schwartz, R.H., *Models of T cell anergy: is there a common molecular mechanism?* J Exp Med, 1996. **184**(1): p. 1-8.

85. Lutz, M.B. and G. Schuler, *Immature, semi-mature and fully mature dendritic cells: which signals induce tolerance or immunity?* Trends Immunol, 2002. **23**(9): p. 445-9.

86. Vignali, D.A., L.W. Collison, and C.J. Workman, *How regulatory T cells work.* Nat Rev Immunol, 2008. **8**(7): p. 523-32.

87. Vasu, C., et al., *Selective induction of dendritic cells using granulocyte macrophage-colony stimulating factor, but not fms-like tyrosine kinase receptor 3-ligand, activates thyroglobulin-specific CD4+/CD25+ T cells and suppresses experimental autoimmune thyroiditis.* J Immunol, 2003. **170**(11): p. 5511-22.

88. Gangi, E., et al., *IL-10-producing CD4+CD25+ regulatory T cells play a critical role in granulocyte-macrophage colony-stimulating factor-induced suppression of experimental autoimmune thyroiditis.* J Immunol, 2005. **174**(11): p. 7006-13.

89. Sheng, J.R., et al., *Suppression of experimental autoimmune myasthenia gravis by granulocyte-macrophage colony-stimulating factor is associated with an expansion of FoxP3+ regulatory T cells.* J Immunol, 2006. **177**(8): p. 5296-306.

90. Gaudreau, S., et al., *Granulocyte-macrophage colony-stimulating factor prevents diabetes development in NOD mice by inducing tolerogenic dendritic cells that sustain the suppressive function of CD4+CD25+ regulatory T cells.* J Immunol, 2007. **179**(6): p. 3638-47.

91. Sheng, J.R., et al., *Regulatory T cells induced by GM-CSF suppress ongoing experimental myasthenia gravis.* Clin Immunol, 2008. **128**(2): p. 172-80.

92. Cheatem, D., et al., *Modulation of dendritic cells using granulocyte-macrophage colony-stimulating factor (GM-CSF) delays type 1 diabetes by enhancing CD4+CD25+ regulatory T cell function.* Clin Immunol, 2009. **131**(2): p. 260-70.

93. Ganesh, B.B., et al., *GM-CSF-induced CD11c+CD8a--dendritic cells facilitate Foxp3+ and IL-10+ regulatory T cell expansion resulting in suppression of autoimmune thyroiditis.* Int Immunol, 2009. **21**(3): p. 269-82.

94. Bhattacharya, P., et al., *GM-CSF-induced, bone-marrow-derived dendritic cells can expand natural Tregs and induce adaptive Tregs by different mechanisms.* J Leukoc Biol, 2011. **89**(2): p. 235-49.

95. Yang, J., et al., *A mouse model of adoptive immunotherapeutic targeting of autoimmune arthritis using allo-tolerogenic dendritic cells.* PLoS One, 2013. **8**(10): p. e77729.

96. Marin-Gallen, S., et al., *Dendritic cells pulsed with antigen-specific apoptotic bodies prevent experimental type 1 diabetes.* Clin Exp Immunol, 2010. **160**(2): p. 207-14.

97. Verginis, P., H.S. Li, and G. Carayanniotis, *Tolerogenic semimature dendritic cells suppress experimental autoimmune thyroiditis by activation of thyroglobulin-specific CD4+CD25+ T cells.* J Immunol, 2005. **174**(11): p. 7433-9.

98. Zhou, F., et al., *Immune tolerance induced by intravenous transfer of immature dendritic cells via up-regulating numbers of suppressive IL-10(+) IFN-gamma(+)-producing CD4(+) T cells.* Immunol Res, 2013. **56**(1): p. 1-8.

99. Lee, J.H., et al., *Myosin-primed tolerogenic dendritic cells ameliorate experimental autoimmune myocarditis.* Cardiovasc Res, 2014. **101**(2): p. 203-10.

100. Gravano, D.M. and D.A. Vignali, *The battle against immunopathology: infectious tolerance mediated by regulatory T cells.* Cell Mol Life Sci, 2012. **69**(12): p. 1997-2008.

101. Andersson, J., et al., *CD4+ FoxP3+ regulatory T cells confer infectious tolerance in a TGF-beta-dependent manner.* J Exp Med, 2008. **205**(9): p. 1975-81.

102. Stassen, M., et al., *Human CD25+ regulatory T cells: two subsets defined by the integrins alpha 4 beta 7 or alpha 4 beta 1 confer distinct suppressive properties upon CD4+ T helper cells.* Eur J Immunol, 2004. **34**(5): p. 1303-11.

103. Dieckmann, D., et al., *Human CD4(+)CD25(+) regulatory, contact-dependent T cells induce interleukin 10-producing, contact-independent type 1-like regulatory T cells [corrected].* J Exp Med, 2002. **196**(2): p. 247-53.

104. Chaudhry, A., et al., *Interleukin-10 signaling in regulatory T cells is required for suppression of Th17 cell-mediated inflammation.* Immunity, 2011. **34**(4): p. 566-78.

105. Collison, L.W., et al., *IL-35-mediated induction of a potent regulatory T cell population.* Nat Immunol, 2010. **11**(12): p. 1093-101.

106. Wang, L., et al., *Programmed death 1 ligand signaling regulates the generation of adaptive Foxp3+CD4+ regulatory T cells.* Proc Natl Acad Sci U S A, 2008. **105**(27): p. 9331-6.

107. Gregori, S., et al., *Differentiation of type 1 T regulatory cells (Tr1) by tolerogenic DC-10 requires the IL-10-dependent ILT4/HLA-G pathway.* Blood, 2010. **116**(6): p. 935-44.

108. Levings, M.K., et al., *Differentiation of Tr1 cells by immature dendritic cells requires IL-10 but not CD25+CD4+ Tr cells.* Blood, 2005. **105**(3): p. 1162-9.

109. Torres-Aguilar, H., et al., *Tolerogenic dendritic cells in autoimmune diseases: crucial players in induction and prevention of autoimmunity.* Autoimmun Rev, 2010. **10**(1): p. 8-17.

110. Wang, P., et al., *Peptide binding predictions for HLA DR, DP and DQ molecules.* BMC Bioinformatics, 2010. **11**: p. 568.

111. Wang, P., et al., *A systematic assessment of MHC class II peptide binding predictions and evaluation of a consensus approach.* PLoS Comput Biol, 2008. **4**(4): p. e1000048.

APPENDIX

East Carolina University

Animal Care and Use Commitee
212 Ed Warren Life Sciences Building
East Carolina University
Greenville, NC 27834

252-744-2436 office
252-744-2355 fax

January 31, 2011

Mark Mannie, Ph.D.
Department of Micro/Immuno
Brody 5E-106
ECU Brody School of Medicine

Dear Dr. Mannie:

Your Animal Use Protocol entitled, "Novel Anti-Inflammatory Treatments for Myocarditis (EAM)" (AUP #K150a) was reviewed by this institution's Animal Care and Use Committee on 1/31/11. The following action was taken by the Committee:

"Approved as submitted"

Please contact Dale Aycock at 744-2997 prior to hazard use

A copy is enclosed for your laboratory files. Please be reminded that all animal procedures must be conducted as described in the approved Animal Use Protocol. Modifications of these procedures cannot be performed without prior approval of the ACUC. The Animal Welfare Act and Public Health Service Guidelines require the ACUC to suspend activities not in accordance with approved procedures and report such activities to the responsible University Official (Vice Chancellor for Health Sciences or Vice Chancellor for Academic Affairs) and appropriate federal Agencies.

Sincerely yours,

Robert G. Carroll, Ph.D.
Chairman, Animal Care and Use Committee

RGC/jd

enclosure

East Carolina University

Animal Care and Use Commitee
212 Ed Warren Life Sciences Building
East Carolina University
Greenville, NC 27834

252-744-2436 office
252-744-2355 fax

December 22, 2011

Mark Mannie, Ph.D.
Department of Micro/Immuno
Brody 5E-106
ECU Brody School of Medicine

Dear Dr. Mannie:

Your Animal Use Protocol entitled, "Fusion Protein Therapy for a Model of Passively-Induced Experimental Autoimmune Myocarditis (EAM)" (AUP #K161) was reviewed by this institution's Animal Care and Use Committee on 12/22/11. The following action was taken by the Committee:

"Approved as submitted"

Please contact Dale Aycock at 744-2997 prior to hazard use

A copy is enclosed for your laboratory files. Please be reminded that all animal procedures must be conducted as described in the approved Animal Use Protocol. Modifications of these procedures cannot be performed without prior approval of the ACUC. The Animal Welfare Act and Public Health Service Guidelines require the ACUC to suspend activities not in accordance with approved procedures and report such activities to the responsible University Official (Vice Chancellor for Health Sciences or Vice Chancellor for Academic Affairs) and appropriate federal Agencies.

Sincerely yours,

Scott E. Gordon, Ph.D.
Chairman, Animal Care and Use Committee

SEG/jd

enclosure

East Carolina University

Animal Care and
Use Commitee
212 Ed Warren Life
Sciences Building
East Carolina University
Greenville, NC 27834

252-744-2436 office
252-744-2355 fax

October 30, 2012

Mark Mannie, Ph.D.
Department of Micro/Immuno
Brody 5E-106
ECU Brody School of Medicine

Dear Dr. Mannie:

Your Animal Use Protocol entitled, "Experimental Autoimmune Myocarditis (EAM) in Mice" (AUP #K165) was reviewed by this institution's Animal Care and Use Committee on 10/30/12. The following action was taken by the Committee:

"Approved as submitted"

Please contact Dale Aycock at 744-2997 prior to hazard use

A copy is enclosed for your laboratory files. Please be reminded that all animal procedures must be conducted as described in the approved Animal Use Protocol. Modifications of these procedures cannot be performed without prior approval of the ACUC. The Animal Welfare Act and Public Health Service Guidelines require the ACUC to suspend activities not in accordance with approved procedures and report such activities to the responsible University Official (Vice Chancellor for Health Sciences or Vice Chancellor for Academic Affairs) and appropriate federal Agencies.

Sincerely yours,

Susan McRae, Ph.D.
Chair, Animal Care and Use Committee

SM/jd

enclosure

East Carolina University

Animal Care and
Use Commitee
212 Ed Warren Life
Sciences Building
East Carolina University
Greenville, NC 27834

252-744-2436 office
252-744-2355 fax

May 16, 2014

Mark Mannie, Ph.D.
Department of Micro/Immuno
Brody 5E-106
ECU Brody School of Medicine

Dear Dr. Mannie:

The Amendment to your Animal Use Protocol entitled, "Experimental Autoimmune Myocarditis (EAM) in Mice", (AUP #K165) was reviewed by this institution's Animal Care and Use Committee on 5/16/14. The following action was taken by the Committee:

"Approved as amended"

****Please contact Dale Aycock prior to any hazard use**

A copy of the Amendment is enclosed for your laboratory files. Please be reminded that all animal procedures must be conducted as described in the approved Animal Use Protocol. Modifications of these procedures cannot be performed without prior approval of the ACUC. The Animal Welfare Act and Public Health Service Guidelines require the ACUC to suspend activities not in accordance with approved procedures and report such activities to the responsible University Official (Vice Chancellor for Health Sciences or Vice Chancellor for Academic Affairs) and appropriate federal Agencies. **Please ensure that all personnel associated with this protocol have access to this approved copy of the AUP/Amendment and are familiar with its contents.**

Sincerely yours,

Susan McRae, Ph.D.
Chair, Animal Care and Use Committee

SM/jd

enclosure